TOWARDS PRACTICAL APPLICATION OF METHANOTROPHIC METABOLISM IN CHLORINATED HYDROCARBON DEGRADATION, GREENHOUSE GAS REMOVAL, AND IMMOBILIZATION OF HEAVY METALS

by

Sukhwan Yoon

A dissertation submitted in partial fulfillment
of the requirements for the degree of
Doctor of Philosophy
(Environmental Engineering)
In The University of Michigan
2010

Doctoral Committee:

Associate Professor Jeremy D. Semrau, Chair
Professor Kim F. Hayes
Associate Professor Terese Olson
Assistant Professor Gregory Dick

ACKNOWLEDGEMENTS

I would like to thank Professor Jeremy D. Semrau for all his teaching, motivation and financial support, via Department of Energy and Carl Page Foundation. I would also like to appreciate the committee members, Professors Kim F. Hayes, Terese Olson, Gregory Dick for the teachings and comments they provided in my progress toward the doctoral degree. Outside the Unversity of Michigan, I would like to thank Prof. Alan A. Dispirito, Prof. Stefan Kraemer and Prof. J. Colin Murrell for providing priceless advices on development of manuscripts.

I would like to thank Professor Lutgarde Raskin for allowing the use of the real-time PCR apparatus and Giridhar Upadhyaya and Ameet Pinto for providing instructions. I would like to thank Thomas Yavaraski for all the help he provided with the analytical instruments.

I really appreciate help from my former labmates Dave Keeney and Sung-Woo Lee in helping me getting settled in the laboratory and learning experimental procedures and the present labmate, Jeongdae Im, for the fruitful discussions and all the help inside and outside the school. Also I would like to express thanks to my friends, Jim Lewis, Sung-Phil Hyun, Young-Soo Han, Dong-Hee Lim, Yongsub Jung, Yuntao Zhao, Mary Deneau Trin Tran, and Hoon-Young Jeong.

Last but not least, I would like to thank my fiancée, Jung Min Oh, and my family for all the emotional support they provided.

TABLE OF CONTENTS

LIST OF TABLES

LIST OF FIGURES

ABSTRACT

Methanotrophic bacteria, a group of microorganisms that utilize methane for energy and biomass, have long been studied for their practical applications. In this study, we have investigated the physiological properties of methanotrophs that are closely relevant to improvement of engineering practices or developmentment of biological engineering devices and processes *de novo*.

First, the degradation of chlorinated ethenes by methanotrophs was observed more closely. *Methylosinus trichosporium* OB3b was examined for the effectiveness of sMMO and pMMO in degradation of chlorinated ethenes at 20˚C. Congruent with the previous result at 30˚C, sMMO had much faster initial degradation kinetics towards TCE, *trans*-DCE, and VC than pMMO. In long-term batch degradation experiments with growth in consideration, however, pMMO-expressing cells were better in degrading the chlorinated ethenes at high concentrations due to the pronounced competition effect and more rapid exposure to the toxic intermediates in sMMO-expressing cells. The inhibition effect on sMMO-expressing cells, as estimated using Δ model, was more severe than when the temperature was 30˚C.

Second, *Methylocystis daltona* SB2, the first facultative methanotroph to be confirmed of constitutive pMMO expression, was examined for the expression of pMMO and degradation of chlorinated ethene compounds under growth on acetate in absence of methane. Real–time quantitative PCR and RT–PCR analyses confirmed the constitutive

expression of pMMO in *M. daltona* SB2 cells grown in acetate at two different stages of growth, mid-exponential and late-exponential growth phases, although the quantity of expression was found to be significantly reduced at the late-exponential phase. In the degradation experiment, significant degradation of *t*-DCE and VC was observed from the mixture of TCE, *t*-DCE and VC added to the batch cultures of *M. daltona* SB2. No degradation activity was observed upon addition of acetylene, supporting that active pMMO was present and responsible for the degradation.

Third, we have devised and modeled a methanotrophic biotrickling filtration system to promote methanotrophic activity in local methane "hotspots". Model results as well as economic analyses of these biofilters indicate that these biofilters may be feasible alternatives for the removal of methane, provided that pMMO expression conditions are maintained and a renewable energy source is used for the power supply.

Fourth, for better understanding of methanobactin, the biomolecule mediating interaction between methanotrophs and copper, we have devised a method for screening methanotrophs or any other cells for production of chalkophores, i.e., biological copper chelators, by adopting the CAS assay originally developed for siderophore production. Methanobactin production of four methanotrophic strains of diverse phylogenetic groups was assayed using this method. Interestingly, the methanotrophs had differing abilities to abstract copper from Cu-CAS, suggesting that the differential ability of these cells to abstract copper from environment might be a critical determinant in the distribution of methanotrophs in the environment.

CHAPTER I

Introduction

Microbial processes utilizing metabolic reactions and various cell products of different microorganisms have been employed in many different engineering practices. In the field of environmental engineering, biological processes for the removal of mixed organic waste has become the most widespread treatment method used in modern wastewater treatment systems. Further, decomposition of solid wastes deposited in landfills involves microbial degradation of organic compounds into simpler carbon molecules, e.g., carbon dioxide and methane. Recently, in anaerobic digesters in wastewater treatment plants and modernized landfill facilities, methane generated via methanogenesis is collected as biogas fuel to help meet regional energy requirements. Microbial processes are also widely used in bioremediation of sites contaminated with various organic and inorganic contaminants. In chemical engineering, a number of commercially available chemicals are produced via processes involving microbial reactions as well. Many pharmaceuticals including antibiotics and vaccines have been produced via microbial processes since discovery of penicillin (Bambini and Rappuoli, 2009; Demain and Sanchez, 2009). In fact, as of 1991, approximately half of commercial pharmaceuticals were manufactured from natural microbial products or chemically synthesized with these natural products. Siderophores are also examples of

biosynthesized peptides that have various practical and potential applications in medicine, agriculture, and bioremediation. Deferoxamine, for example, has been used since 1970s to treat iron storage disorders (Olivieri and Brittenham, 1997).

Methanotrophic bacteria are one of the groups of bacteria that have long been studied for their applications in environmental engineering. Methanotrophic bacteria, i.e., methanotrophs, are the group of bacteria that utilize methane as their sole carbon and energy source. Most known methanotrophs are found within the α-*Proteobacteria* and γ-*Proteobacteria* (Hanson and Hanson, 1996), as well as more recently within *Verrucomicrobia* (Dunfield et al., 2007; Islam et al., 2008; Semrau et al., 2008). Methanotrophic bacteria utilize the methane monooxygenase (MMO) to mediate the transformation of methane to methanol, the first step in methane metabolism. Two different MMOs exist in the nature that have significant differences. The membrane-bound form of the methane monooxygenase, or particulate methane monooxygenase (pMMO), is found in all but one known methanotrophic genera (Dedysh et al., 2005), and is an integral cytoplasmic membrane protein with enhanced activity in the presence of copper, whereas soluble methane monooxygenase (sMMO) is a cytoplasmic protein only expressed in the strict absence of copper, and only by a small subset of known methanotrophs. The active metal center of sMMO is a diiron center embedded in each of the protomers of the MMO hydroxylase dimer. The crystal structure of pMMO has revealed three metal centers, one of which is a putative diiron center analogous to the active center of sMMO, but its exact character is yet unknown (Lieberman and Rosenzweig, 2005; Martinho et al., 2007). Despite the differences in their loci and structures, pMMO and sMMO have strikingly similar functions. Since generation of

methanol from methane is regarded as one of the most difficult abiotic reactions to control due to the high carbon-hydrogen bond energy (Krylov, 1993), methanol is a common feedstock for many chemical processes (Cheng and Kung, 1994) and methane is a relatively inexpensive carbon source (Waki et al., 2008), MMOs, capable of mediating such a reaction, are considered to have significant industrial potential.

Both sMMO and pMMO have been found to be capable of degrading halogenated hydrocarbons, many of which have serious consequences to both environmental and human health (Bolt, 2005; Scott and Chiu, 2006). In contrast to other microorganisms that are known to degrade halogenated hydrocarbons via reductive pathways (Maymo-Gatell et al., 1999), biodegradation of chlorinated hydrocarbons via methanotropic pathway occurs in an oxidative manner (Fogel et al., 1986; Lontoh et al., 2000). Biodegradation by methane monooxygenases has drawn significant attention since the reductive dechlorination of chlorinated ethenes such as trichloroethylene and tetrachloroethylene often results in the accumulation of more toxic intermediates, e.g.,vinyl chloride, a known carcinogen (Maymo-Gatell et al., 1999), while no such accumulation has been observed in the oxidative reactions mediated by MMO (McCue et al., 2002). Thus, the applicability of methanotrophic degradation of halogenated hydrocarbons to *in situ* treatment of contaminated soil and groundwater system has been a major topic of study.

Although sMMO-expressing cells have been historically assumed to be the main players in degradation of chlorinated hydrocarbons *in situ* by methane oxidizing bacteria, as sMMO has much wider range of substrates than pMMO (Colby et al., 1977; Hanson and Hanson, 1996), recent evidence casts doubt on this assumption. In previous

laboratory experiments on whole-cell methanotrophic degradation of chlorinated hydrocarbons, cells incubated in the absence of copper indeed exhibited higher reactivity toward these compounds than those grown in presence of copper (Oldenhuis et al., 1991; Lontoh and Semrau, 1998; Lee et al., 2006). When long-term cell growth was considered, however, overall degradation was contrary to what was expected from whole-cell kinetics measured over shorter time frames (Lee et al., 2006). It was discovered that cell growth of *M. trichosporium* OB3b expressing sMMO is much more severely restricted than that of the same cells expressing pMMO, as the active site in sMMO is much more easily occupied by chlorinated ethenes, which act as competitive inhibitors for both MMOs. Also, due to the faster reaction rate, toxic transient intermediates are thought to be generated faster by sMMO-expressing cells. As a result, pMMO-expressing cells were found to degrade more chlorinated compounds when concentrations of these compounds were increased above 50 µM. This result indicated that pMMO-expressing cells could actually be the main player in *in situ* biodegradation.

Although this result raised an interesting objection to what was perceived to be an established theory, more needs to be investigated at conditions that better mimic *in situ* groundwater environments. One of the environmental factors considered most important is temperature. The optimal growth temperature of *M. trichosporium* OB3b, as most often used for laboratory degradation assays with these cells, is 30° C, while the temperature of groundwater *in situ* often is at or below 20° C (Wiedemeier et al., 1999). Since microbial reactions and growth are strongly affected by temperature, we hypothesized that both growth and chlorinated hydrocarbon degradation capability would be compromised differentially depending on the substrates and the type of and methane

monooxygenase the cells express. Thus, we decided to test this hypothesis by performing the degradation assays at 20°C for three chlorinated hydrocarbons commonly found at polluted sites, trichloroethylene (TCE), *trans*-dichloroethylene (*t*-DCE), and vinyl chloride (VC), using similar methods previously developed in the Semrau laboratory (Lee et al., 2006).

Methanotrophs have long been considered to be obligately methanotrophic, i.e., incapable of growth on multi-carbon substrates, until three facultatively methanotrophic strains, *Methylocella silvestris* BL2, *Methylocapsa aurea* KYG, and *Methylocystis daltona* SB2 were discovered to be able to grow on multi-carbon substrates including ethanol and acetate (Dunfield et al., 2003; Dedysh et al., 2005; Dunfield et al., 2010; Im et al., unpublished). The discovery of *M. daltona* SB2 was especially significant as it was the only mesophilic and neutrophilic facultative methanotroph with the fastest growth rate on methane among the three strains (Im et al., submitted). One interesting finding was that RT-PCR of *pmoA* found constitutive expression in the presence of actetate without methane (Im et al., submitted). As methane metabolism in facultative methanotrophs involving MMO is decoupled from acetate metabolism, this finding may have significant implications in bioremediation and atmospheric consumption of methane. We have verified the expression of pMMO upon growth on acetate and quantified the expression of pMMO in acetate-growth conditions as compared to the methane-growth conditions. We also examined the long-term degradation of mixtures of TCE, *trans*-DCE, and VC under acetate-growth conditions to verify the presence and activity of pMMO under acetate-growth conditions as well to determine the effectiveness of such conditions for bioremediation. After initial confirmation of degradation activity, a selective inhibitor

of pMMO, acetylene, was used to verify that pMMO was responsible for the observed degradation.

Recently, the capability of methanotrophs to consume methane and the utilization of this metabolic process in greenhouse gas reduction has been studied due to growing concerns over global warming. Although carbon dioxide is the single largest greenhouse gas in terms of global warming potential, methane is also a significant contributor to global warming as methane is known to have a ~25 times greate global warming potential than carbon dioxide of the same concentration (IPCC, 2007; Etheridge et al., 1998; Le Mer and Roger, 2001). Global population increase and consequent rise in consumption of energy and waste generation have led to a large increase in the anthropogenic contribution to atmospheric methane emissions, which now accounts for ~ 60% of 600 Tg CH_4 emitted each year to the atmosphere (Fung et al., 1991). The largest anthropogenic sources have been energy production, livestock feeding operations, landfills and rice cultivation, which have risen dramatically since the beginning of the industrial era. As a consequence, atmospheric methane concentration more than doubled from 695 ppb to 1.7 ppm in the period spanning from 1800 to 1981 (Etheridge et al., 1998). In response to this, many attempts have been made to reduce emission of methane from these major sources, e.g., installation of methane vents in modern sanitation landfills. Many of these devices have been successful in suppressing further increases in atmospheric methane concentration, but significant amounts of methane are still being emitted (IPCC, 2007). In response, recent research has considered methods to not only reduce methane emissions (Melse and van der Werf, 2005; Nikiema et al., 2005), but also to remove methane already in the atmosphere.

One such approach is the use of methanotrophs. Unfortunately, the average methane concentration in the atmosphere is too low to allow growth of most isolated laboratory methanotrophic strains. Most cultured methanotrophs have whole-cell half saturation constants (K_s) for methane of ~1- 10 μM (750 – 7500 ppmv assuming equilibrium between aqueous and gas phases at 30℃), and thus, the atmospheric methane concentration, 1.7 ppmv, results in negligible methane consumption rates. This is one of the reasons why past approaches for atmospheric methane removal have focused mainly on source reduction where methane is in very high concentrations (>7000 ppm) (Melse and Van der Werf, 2005; Nikiema et al., 2005). Here, we evaluated the feasibility of using biofiltration systems to accommodate methanotrophic activity to remove methane from lower concentrations of methane (i.e., < 6000 ppm).

Biofiltration is an engineered biological treatment process that utilizes the metabolic activity of microorganisms attached onto a variety of packing materials to treat a wide range of organic and inorganic contaminants (Cohen, 2001). In a biofilter, contaminants in the gas phase diffuse into biofilms, a thin layer of a microbial consortium on the packing material, to be consumed by microorganisms therein. Biofilters are filled with a variety of packing materials made of natural and synthetic materials to provide the surface area for establishment of biofilms. In order to commercially apply this treatment system to removal of methane utilizing methane-degrading capability of methanotrophs, it is essential that both engineering and economic feasibilities are examined using model and pilot tests. Conditions that are specific to methanotrophs, e.g., copper concentration controlling expression of pMMO and sMMO, must also be considered in the model. Here, we have designed and performed a model analysis to evaluate the feasibility of methane

biofiltration as part of a initial step in a multi-faceted approach to reduce the atmospheric concentration of this greenhouse gas.

Methanotrophs, like most microorganisms, excrete substances for many different purposes. One of these substances, named methanobactin, is a metal-chelating organic molecule that is produced and excreted by a number of known methanotrophs. Although methanobactin is analogous to siderophores in its function, i.e., uptake of a metal necessary for utilization in cellular functions, it is different from siderophores in several aspects. Siderophores are synthesized and emitted only when insufficient iron is available for growth, whereas methanobactin is constitutively synthesized even when the copper concentration is relatively abundant, i.e., 5 μM (DiSpirito et al., 1998). The association and interaction of the copper-bound form of methanobactin molecules with active pMMO as suggested by Dispirito and coworkers (Zahn and DiSpirito, 1996; Choi et al., 2003; Choi et al., 2005) has not been evidenced for cells synthesizing siderophores previously. Coordination of the metal ion was also found to be unique among the metal chelators, in that Cu (I) is bound by two nitrogen atoms and two sulfur atoms (Kim et al., 2004; Behling et al., 2008). Recent research has revealed the structure of methanobactin and efforts are ongoing to verify its properties and functions ((Kim et al., 2004; Choi et al., 2005; Kim et al., 2005; Choi et al., 2006a; Choi et al., 2006b; Behling et al., 2008; Choi et al., 2008). Despite these efforts, however, little is known about the precise role of methanobactin in methanotrophy other than that it has a high binding affinity for copper.

For further analyses on methanobactin, it is important that the genetics of methanobactin synthesis be examined in more detail. Currently, nothing has been confirmed about the gene(s) involved in the synthesis of methanobactin, although it is

hypothesized that methanobactin may be synthesized by non-ribosomal peptide synthase (NRPS), based on its similarity to siderophores (Ward et al., 2004; Balasubramanian and Rosenzweig, 2008). Without more information on its genetics, molecular quantification techniques, such as quantitative RT-PCR or competitive RT-PCR, cannot be used to acquire further information on the interaction between methanotrophs and metals in the environment. Also, with the limited genetic information available, the low yield of methanobactin (~10 mg per liter), has hindered methanobactin research and its practical application. It is hoped that this obstacle can be overcome through heterologous expression of methanobactin. According to (Choi et al., 2008), the reported maximum methanobactin yields for three laboratory strains, *M. trichosporium* OB3b, *M. album* BG8, and *M. capsulatus* (Bath) were lower than 60 mg l^{-1}. Thus, heterologous expression in a faster-growing and less fastidious hosts, e.g., *Escherichia coli*, is thought to be necessary.

For these reasons, work is ongoing to mutate putative NRPS genes to determine if any are involved in methanobactin synthesis. The lack of sufficient information on methanobactin, however, makes the screening process for these mutants extremely difficult. Up until now, the only way to characterize putative methanobactin-minus mutants was to isolate and characterize any methanobactin that is synthesized using large batch fermentations, a time-consuming and relatively challenging process. To facilitate genetic analyses of methanobactin synthesis, we have devised a plate method to determine production of methanobactin by modifying the popular chromo-azurol S (CAS) assay, originally developed for detection of siderophores (Schwyn and Neilands, 1987). This modified CAS assay will help screen putative mutants of methanobactin synthesis,

thereby facilitating the search for methanobactin synthesis genes. We expect that this will enhance understanding of methanobactin, which, in turn, will eventually allow for practical application of this fascinating molecule for clinical and engineering purposes.

As such, we performed multiple studies to consider the use of methanotrophs in various applications, i.e., *in situ* bioremediation, removal of atmospheric methane, and methanobactin production. From these analyses, the following was discovered regarding practical application of methanotrophs: (1) temperature is a significant factor controlling bioremediation of chlorinated ethenes using methanotrophs expressing either pMMO or sMMO; (2) some facultative methanotrophs, including *Methylocystis* sp. SB2 examined here, express pMMO and degrade chlorinated ethenes in absence of methane when an alternate substrate is available; (3) methanotrophic biofiltration is a technically feasible option for removing greenhouse gas from the atmosphere but is not economically feasible considering the current price of CO_2, and; (4) the Cu-CAS assay was successful in screening methanotrophs for production of methanobactin and may be able to screen other cells for production of equivalent chalkaphores. We expect that these results will serve as the basis for further research to develop more efficient methods for utilizing methanotrophs in various potential applications including those dealt with in this study.

CHAPTER II

Literature Review on Methanotrophs and Their Applications

II.1 Methanotrophs

II.1.1 Physiology

Methanotrophs are a group of bacteria that utilize methane for energy and carbon (Semrau et al., 2010). All known methanotrophs under α- and γ- *Proteobacteria* phyla oxidize methane ultimately to carbon dioxide via the general pathway shown in Figure II.1, although the initial hydroxylation step and carbon assimilation pathways vary for different types of methanotrophs. In the general methanotrophic pathway, methane is initially hydroxylated to methanol by pMMO or sMMO, which is further oxidized to formaldehyde by periplasmic methanol dehydrogenase (MDH). In the catabolic pathway, formaldehyde is oxidized to CO_2 via formate by formaldehyde dehydrogenase (FalDH) and formate dehydrogenase (FDH), yielding reducing equivalents as either quinol or NADH. In the anabolic pathway, formaldehyde is incorporated into cell biomass via incorporation into either ribulose monophosphate (RuMP) or serine pathway, depending on the type of methanotroph.

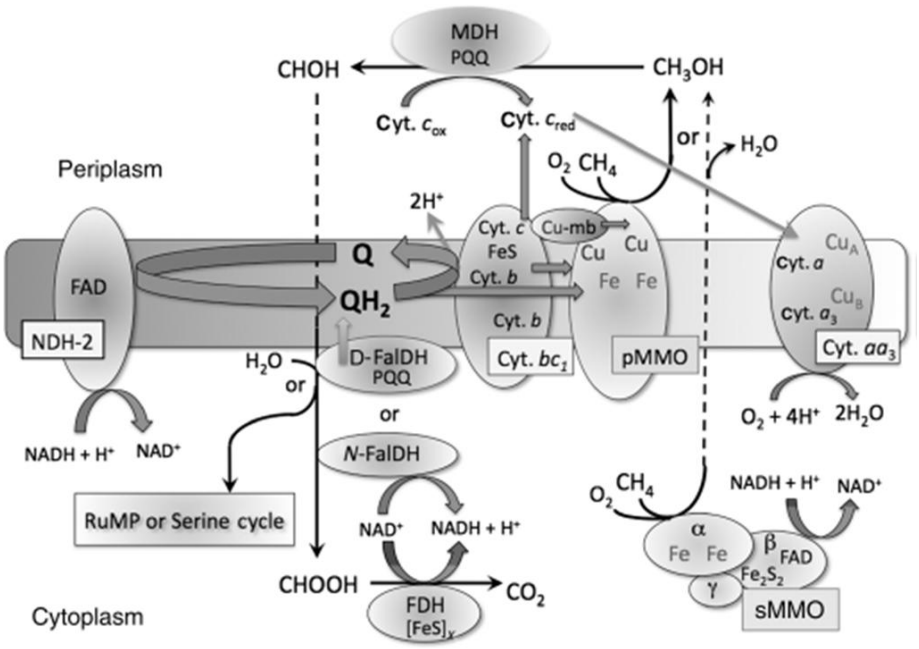

Figure II.1 Pathway of methane metabolism by methanotrophic bacteria. pMMO: particulate methane monoxygenase, sMMO: soluble methane monooxygenase, MDH: methanol dehydrogenase, FalDH: formaldehyde dehydrogenase, FDH: formate dehydrogenase

Newly discovered acidophilic methanotrophs under *Verrucomicrobia* phylum lack some of the key genes in the above pathways including *mxaI* that encodes for the small subunit of the methanol dehydrogenase (Dunfield et al., 2007; Pol et al., 2007; Hou et al., 2008). Neverthless, these cells are thought to have methanol dehydrogenase activity that oxidizes methanol either from methane turnover by pMMO, the only methane monooxygenase these bacteria possess, or from external sources. Formaldehyde dehydrogenase genes are found in some *Verrucomicrobia* species but formaldehyde oxidation to formate is thought to also occur via the tetrahydrofolate (THF) cycle. Formate dehydrogenase is commonly found in this group of microorganisms. The assimilatory pathway for these bacteria is thought to be the serine pathway analogous to that of type II methanotrophs or a novel pathway that has not yet been observed in methanotrophs (Semrau et al., 2008).

II.1.2 Phylogeny

Methanotrophic bacteria are classified into one of two major groups, type I and type II methanotrophs, save for a group of acidophilic bacteria classified under *Verrucomicrobia*. The major distinction between the two types is the pathway via which formaldehyde is incorporated into cell biomass. Type I methanotrophs assimilate biomass via ribulose monophosphate (RuMP) pathway, while type II methanotrophs use serine pathway for the same operation. Also, there are other notable differences that are used to distinguish these groups of methanotrophs other than biomass assimilation pathway such as cell morphology, composition of phospholipid fatty acids, and membrane arrangements as listed in Table II.1

Table II.1 Differential biochemical and physiological characteristics of type I, and II methanotrophic bacteria (Hanson and Hanson, 1996)

Characteristic	Type I	Type II
Cell morphology	Short rods, usually occur singly; some cocci or ellipsoids	Crescent-shaped rods, rods, pear-shaped cells, sometimes occur in rosettes
G+C content of DNA (mol%)	49-60	62-67
Membrane arrangement		
Bundles of vesicular disks	Yes	No
Paired membranes aligned to periphery of cells	No	Yes
Nitrogen fixation	No	Yes
Resting stages formed		
Exospores	No	Some strains
Cysts	Some strains	Some strains
RuMP pathway present	Yes	No
Serine pathway present	No	Yes
Major PLFAs	14:0, 16:1ω7c, 16:1ω5t	18:1ω8c
Proteobacterial subdivision	γ	α

From phylogenetic studies on 16S rRNA, type I and II methanotrophs are found to group with γ- and α- proteobacteria, respectively (Figure II.2). Type I methanotrophs include genera *Methylobacter*, *Methylomicrobium*, *Methylomonas*, *Methylocaldum*, *Methylococcus*, *Methylosoma*, *Methylosarcina*, *Methylothermus*, *Crenothrix*, *Clonothrix*, and *Methylosphaera* and type II methanotrophs include genera *Methylocapsa*, *Methylocella*, *Methylosinus*, and *Methylocystis*. Recently, acidophilic methanotrophs have been isolated, which are not classified into either *α*- or *γ*- *Proteobacteria*, but are phylogenetically located under *Verrucomicrobia* phylum. Although not fully characterized yet, these bacteria were found to have striking dissimilarities with other methanotrophic bacteria (Dunfield et al., 2007; Hou et al., 2008)).

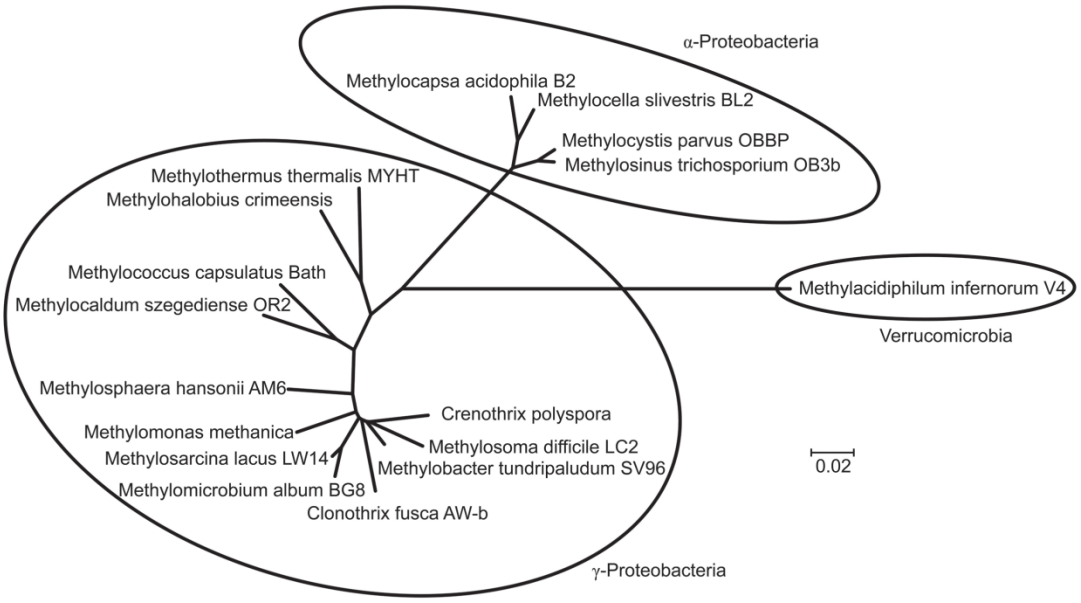

Figure II.2 Phylogenetic relationships between known methanotrophs based on 16S rRNA gene sequences using MEGA4 (Tamura et al., 2007). The tree was constructed using the neighbor-joining method with 1304 positions of 16S rRNA genes

II.1.3 Physiological diversity of methanotrophs

II.1.3.1 Extremophilic methanotrophs

Most cultured methanotrophs are mesophilic and neutrophilic, favoring moderate temperature (~ 25℃) and pH conditions (pH 6-7). There are, however, strains that favor extreme environmental conditions. Some type I strains, i.e., *M. capsulatus* (Bath) and related strains, are known to be thermophilic or thermotolerant (Foster and Davis, 1966; Malashenko et al., 1975). Relatively recently, a new thermophilic group of methanotrophs, *Methylocaldum*, have also been isolated (Bodrossy et al., 1997). The methanotroph with highest growth temperature, up to 72℃, was found in hot spring in Hungary and was tentatively named *Methylothermus* sp. HB. (Bodrossy et al., 1999). Interestingly, these thermophilic or thermotolerant methanotrophs share certain features, such as type I intracellular membranes and RuMP assimilation pathway (Hanson and Hanson, 1996). Psychrophilic methanotrophs have also been isolated, mostly from Siberian tundra and Antarctic environments (Omelchenko et al., 1993; Bowman et al., 1997; Wartiainen et al., 2006). These methanotrophs tolerate temperatures as low as 3.5℃ (Omelchenko et al., 1993) and usually have optimum growth temperature between 10℃ and 20℃. Identified and cultured psychrophilic bacteria comprise strains from genera *Methylobacter*, *Methylococcus, and Methylosphaera*, all of which incorporate biomass via the RuMP pathway (Omelchenko et al., 1993; Bowman et al., 1997; Trotsenko and Khmelenina, 2002; Wartiainen et al., 2006).

As for pH conditions, methanotrophs generally favor a neutral pH range, with optimum growth typically observed around pH 6 (Hanson and Hanson, 1996, Semrau et al., 2010). Instances of acidophilic/ tolerant and alkaliphilic/ tolerant methanotrophs,

however, have been observed. Strains phylogenetically under *Methylocella* and *Methylocapsa* genera have been isolated with moderate acidophilicity, i.e., with optimum pH at ~5.0-5.5 (Dedysh et al., 2000; Dedysh et al., 2002). Although these bacteria are classified as type II methanotrophs, they have many unique characteristics that are found in neither type I nor type II methanotrophs. For example, intracytoplasmic membranes of these genera have a morphology different from either type I or type II methanotrophs and they contain fatty acids unique to both types of methanotrophic *Proteobacteria*. Recently, extreme acidophiles that exhibit optimum activity at pH 2.0 – 2.5 have been isolated (Dunfield et al., 2007). These bacteria were classified under *Verrucomicrobia* phylum based on 16s rRNA analysis (Figure II.2). Several interesting observations have been made on *Methylacidiphilum infernorum* V4, including that the enzymes necessary for either RuMP and serine pathway for formaldehyde assimilation are absent and that this strain is the first thermoacidophilic methanotroph ever isolated (Hou et al., 2008). Alkaliphilic methanotrophs have also been isolated with optimum growth between pH 9.0 and 10.0 (Khmelenina et al., 1997; Sorokin et al., 2000; Reshetnikov et al., 2005). These alkaliphiles have been phylogenetically placed under type I methanotroph genera, *Methylomicrobium* and *Methylobacter*.

II.1.3.2 Facultative methanotrophs

Methanotrophs have long been considered to be obligately methanotrophic, i.e., incapable of growth on multi-carbon substrates, until the first facultatively methanotrophic strain, *Methylocella silvestris* BL2, was discovered to be able to grow on multi-carbon substrates including ethanol and acetate (Dunfield et al., 2003; Dedysh et al.,

2005). As described above this cell exhibits a number of characteristics that are deemed unusual for methanotrophs, e.g., absence of intracytoplasmic membrane, acidophilicity, and tolerance to low temperature (Dunfield et al., 2003). No *pmo* operon, which was found in every other isolated methanotroph, was found in the genome of *M. silvestris* BL2 and these cells exhibited higher specific growth rate upon growth on acetate than on methane (Dedysh et al., 2005). Transcriptional analysis on these cells grown under fed-batch fermentation revealed that expression of sMMO was repressed upon acetate addition (Theisen et al., 2005).

More recently, two more newly isolated methanotrophs in the α-*Proteobacteria*, *Methylocapsa aurea* KYG and *Methylocystis daltona* SB2, were found to maintain viability and growth under the presence of acetate as the sole carbon source (Dunfield et al., 2010; Im et al., unpublished). Unlike *M. silvestris* BL2, these cells were found to express only *pmoA* and possess intracytoplasmic membranes. Both *M. aurea* KYG and *M. daltona* SB2 are phylogenetically closest to the obligate methanotrophs, *Methylocapsa acidiphilia* B2 (98.1 % identity in partial 16S rRNA sequence) and *Methylocystis rosea* SV96 (98.1 % identity in partial 16S rRNA sequence), respectively. *M. aurea* KYG, like *M. silvestris* BL2 is in the *Beijerinckia* family, but *M. daltona* SB2 is phylogenetically grouped with the *Methylocystaceae* family. Interestingly, this methanotroph exhibited specific growth comparable to that of fast-growing methanotrophs, e.g., *M. trichosporium* OB3b, under optimum growth conditions in the presence of methane. The growth rate of these cells in methane-rich conditions was at least three times as high as the other two facultative methanotrophs. Most significantly, RT-PCR of *pmoA* found constitutive expression in the presence of actetate without methane.

This diversity in physiological properties indicate that methanotrophs might indeed be present in much more diverse forms than anticipated from information on isolated laboratory strains.

II.2 Methane monooxygenases

II.2.1 General Information

The first step in methane oxidation by methanotrophs, substitution of a hydrogen atom with a hydroxyl to yield methanol, is considered to be one of the most difficult reaction to biologically mediate, as oxidation of methane normally is rapidly converted to carbon dioxide and water. This step is catalyzed by two groups of enzymes found exclusively in methanotrophs, i.e., the particulate and soluble methane monooxygenases (pMMO and sMMO, respectively). Although these two groups of monooxygenases catalyze the same reaction via putatively similar mechanisms involving metal radicals, they are very different in many aspects, e.g., their distribution among methanotrophic strains, activity, loci in the cell, structure, and regulation. Particulate methane monooxygenases (pMMO) are found in all isolated methanotrophic strains comprising type I, type II and the *Verrucomicrobia* group of methanotrophs with the only exception of *Methylocella* species, which are, in fact, facultative bacteria able to use multi-carbon substrate for biomass (Dedysh et al., 2005). Soluble methane monooxygenases, however, are only found in small number of type I and type II methanotrophs including the genera *Methylococcus*, *Methylomonas*, *Methylocella*, *Methylocystis*, and *Methylosinus* (Hanson and Hanson, 1996; McDonald et al., 2006). No evidence of sMMO has been found in acidophilic methanotrophs in the *Verrucomicribia* phylum (Dunfield et al., 2007; Hou et

al., 2008; Islam et al., 2008). Since obvious similiarites in sMMO genes are observed throughout a wide range of phylogenetic groups of methanotrophs, it is hypothesized that sMMO genes have been transferred between strains by lateral gene transfer (Leahy et al., 2003). In contrast, pMMO is thought to have evolved vertically from a common ancestor species as suggested by the similarity of phylogenetic relationships based on *pmoA* to the one based on 16S rRNA with exception of the case for *Crenothrix polyspora* (Figure II.3). pMMO is also thought to have a common ancestor with the ammonia monooxygenase (AMO), as conserved residues are found throughout the entire length of PmoA and AmoA amino acid sequences, implying their structural similarities (Holmes et al., 1995).

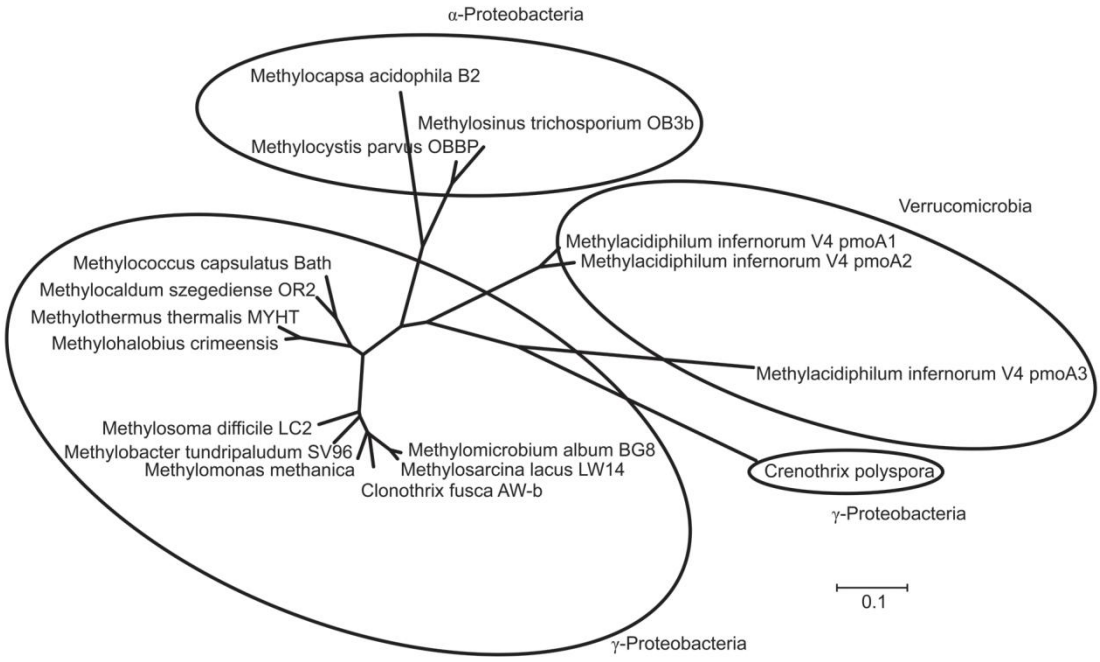

Figure II.3 Phylogenetic relationships between known methanotrophs based on *pmoA* gene sequences using MEGA4 (Tamura et al., 2007). The tree was constructed using the neighbor-joining method with 101 amino acid positions

II.2.2 Structure of methane monooxygenases

II.2.2.1 Soluble methane monooxygenase

sMMO is a cytoplasmic enzyme that exists as a cluster of three components, the hydroxylase (MMOH), reductase (MMOR), and regulatory protein (MMOB), all of which are essential for coupling NADH oxidation with methane hydroxylation (Colby and Dalton, 1978; Fox et al., 1989). MMOH, the 245 kDa hydroxylase component containing a di-iron active site, has a dimeric form, with each protomer consisting of three dissimilar subunits, α, β, and γ (Rosenzweig et al., 1993; Elango et al., 1997). The overall structure of MMOH is characterized by its extensively helical structure (Figure II.4).

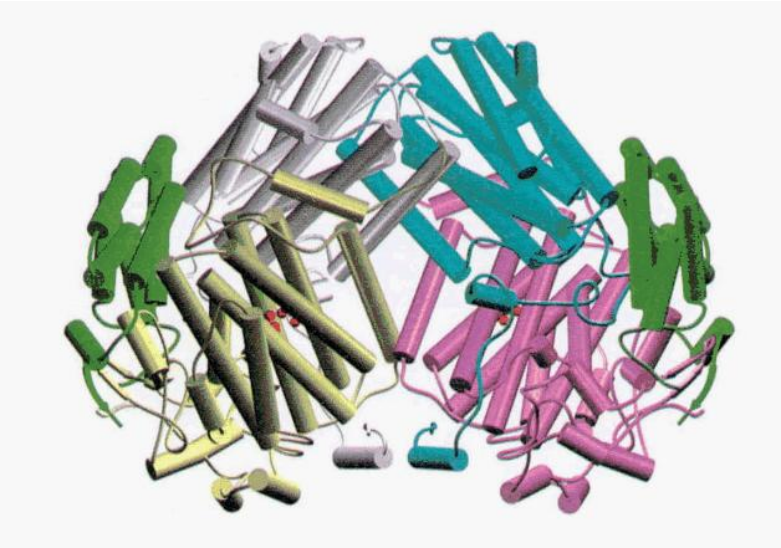

Figure II.4 The crystal structure of MMOH dimer with cylinders representing helices and arrows representing β-strands. α-chains are colored yellow and pink, β-chains are colored gray and cyan, and γ-chains are colored green (Elango et al., 1997)

The active center of MMOH, as mentioned above, is a di-iron center embedded in the center of each protomer of the MMOH dimer coordinated by side chains of helices of

subunit α. As can be seen in Figure II.5, two iron atoms are ligated to side chains of Glu α114, His α147, Glu α209, and His α246, that are coplanar with the two iron atoms, and water and Glu α243 above the plane. These iron atoms are bridged by two hydroxides on the plane and Glu α144 below the plane (numbering is based on *Methylococcus capsulatus* (Bath)). Near the diiron center, a hydrophobic pocket cavity is formed that confers specificity of the enzyme towards hydrophobic substrates including its main substrate, methane. Coordination of the diiron center was found to be significantly altered upon change in the oxidation state as seen in Figure II.5 (Rosenzweig et al., 1995). Coordination of Glu243 was changed from monodentate coordination with Fe2 to bidentate coordination with Fe2 and one of the bridging oxygens. In addition, Fe-O distances in the reduced form were found to be longer, which is indicative of weak binding between Fe atoms and bridging H_2O. The structures of the diiron active sites are conserved between *Methylococcus capsulatus* (Bath) and *Methylosinus trichosporium* OB3b (Rosenzweig et al., 1993; Elango et al., 1997).

A. B.

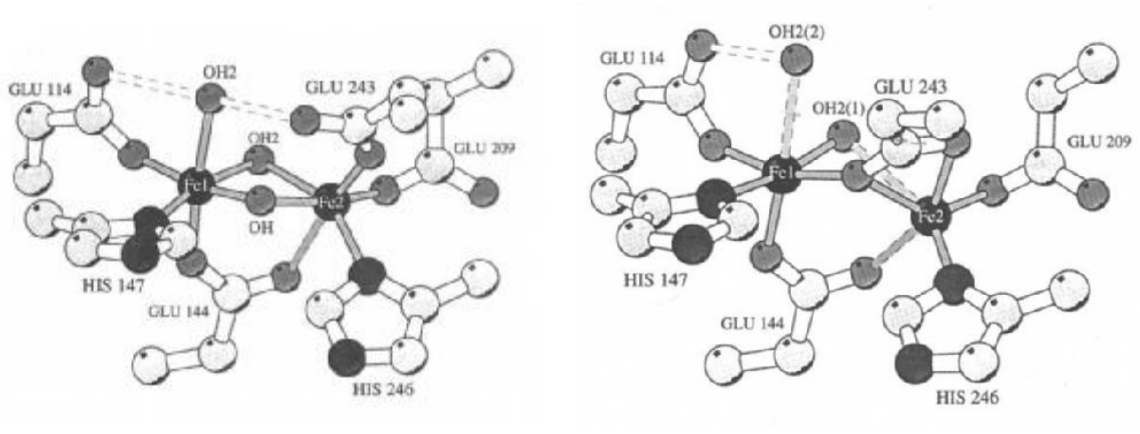

Figure II.5 Structure of the diiron center in (A) oxydized [Fe(III) – Fe(III)] form and (B) reduced [Fe(II) – Fe(II)] form of the hydroxylase component of sMMO (Rosenzweig et al., 1995)

MMOB, the regulatory component of sMMO, of *Methylococcus capsulatus* (Bath) is a 16-kDa protein that has a unique fold composed of alternation of α-helices and β-sheets (Walters et al., 1999). As seen in Figure II.6, residues 35-131 form the core with two β-sheets composed of three and four β-strands each and three α-helices bridging these β-strands. The structural core is stabilized by long-range hydrophobic interactions between side chains of the α-helices and β-sheets. Neither the N-terminus nor C-terminus has specific secondary structure. The interface between MMOH component and MMOB component is thought to be hydrophobic and the putative binding site is the gap between α and β subunit of MMOH.

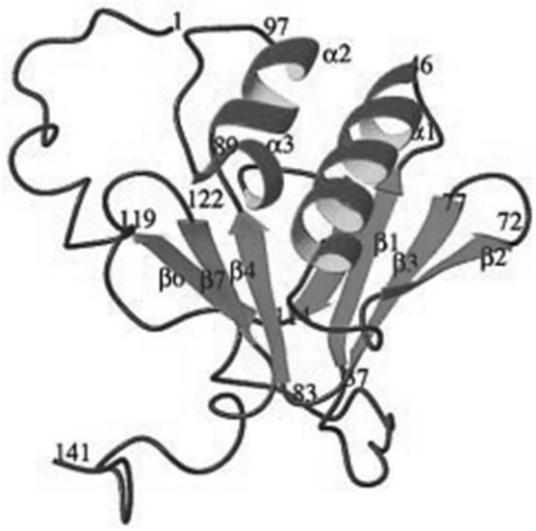

Figure II.6 NMR structure of MMOB component in ribbon diagrams with undetermined structure for C-terminus (Walters et al., 1999)

The 38.5-kDa reductase component of sMMO, MMOR, is classified as a modular flavoprotein electron transferase (Blazyk and Lippard, 2002; 2004). MMOR is composed of three domains, i.e., [2Fe-2S], FAD, and NAD domains, that retain most biochemical properties upon separate expression. MMOR-Fd ([2Fe-2S] ferredoxin domain) and

MMOR-FAD (a complex of FAD- and NADH- binding domains) expressed separately in *Escherichia coli* cells were analyzed by Müller et al. (2002) and Chatwood et al. (2004), respectively. MMOR-Fd is composed of three short α-helices and six β-strands (Figure II.7A). Three of four cysteine residues that constitute coordination of [2Fe-2S] cluster are located in the loop between α_1 and β_3 and the fourth cysteine residue is located in the loop connecting β_5 and β_6. The tertiary structure of the ferredoxin domain is stabilized via two inter-secondary-structure hydrogen bonds, one between Gln34 and Glu20 and the other between Ser65 and Gly45. MMOR-Fd was found to bind MMOH by both electrostatic and hydrophobic interactions, and α_2 in the unique helix-proline-helix motif is thought to be essential in this interaction between MMOR-Fd and MMOH.

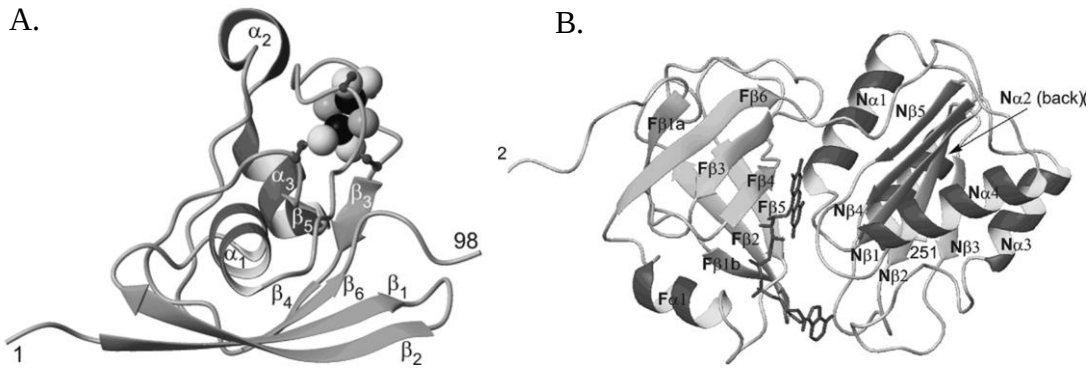

Figure II.7 NMR structure of (A) the reduced form of MMOR-Fd (Müller et al., 2002) with [2Fe-2S] cluster and (B) FAD- and NADH binding domain with FAD cofactor (Chatwood et al., 2004). α-helices and β-strands are shown in red and cyan, respectively

MMOR-FAD has a multi-domain structure consisting of FAD-binding domain and NADH-binding domain, as commonly observed in proteins in the flavoprotein electron transferase family. FAD-binding domain has a β-barrel that consists of six anti-parallel β-strands with an α-helix on one side of the β-barrel structure (Figure II.7B).

FAD-cofactor was found to bind to this protein in a unique extended conformation, so that intra-molecular interaction between AMP moiety and isoalloxazine moiety is neutralized and interaction of these moieties with the FAD-binding domain is maximized via charge neutralization, hydrogen bonding, and hydrophobic stacking. The NADH-binding domain consists of four α-helices and five β-strands that alternate to form a five-stranded parallel β-sheet (Figure II.7B). Since this NMR-structure was resolved in fully reduced form, NADH binding site was not observed.

II.2.2.2 Particulate methane monooxygenase

As pMMO is an integral membrane protein, information on the structure of pMMO has been very limited as compared that of sMMO. Its crystal structure was not revealed until recently, when Lieberman and Rosenzweig (2005) reported 2.8Å resolution structure of this membrane protein from *M. trichosporium* OB3b. Like sMMO, pMMO is composed of three subunits, PmoA, PmoB and PmoC, ~27 kDa, ~47 kDa, and ~25 kDa in size, respectively (Zahn and DiSpirito, 1996). pMMO exists as a trimer of identical protomers, each consisting of these three subunits (Figure II.8). Each protomer is composed of transmembrane helices and hydrophilic β-barrels. N-terminus and C-terminus of PmoB subunit form 7-stranded and 8-stranded anti-parallel β-barrels, respectively, and two helices in between form the transmembrane region. PmoA and PmoC are composed mostly of membrane-spanning helices. PmoA has seven trans-membrane helices slanted with respect to each other with a short helix and β-hairpin protruding out of the membrane and interacting with the C-terminus β-barrel of PmoB of

neighboring protomer. Five trans-membrane helices of PmoC, however, are more or less parallel to each other and normal to the membrane surface.

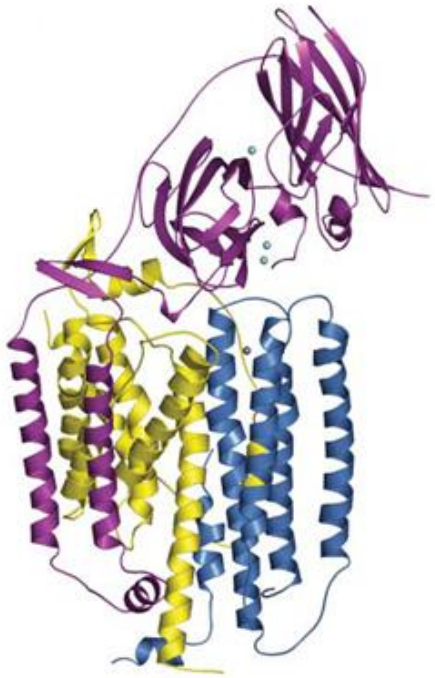

Figure II.8 Crystal structure of a single protomer of pMMO. PmoA, PmoB, and PmoC are shown in magenta, yellow, and blue, respectively (Lieberman and Rosenzweig, 2005)

The character and locus of the active redox center of pMMO has been under serious debate for decades. Widely varying hypotheses have been reached from electron paramagnetic resonance (EPR) and Mössbauer spectroscopy performed by different research groups regarding the amount of metal ions, copper, zinc, and iron, and their involvement in methane oxidation (Zahn and DiSpirito, 1996; Lemos et al., 2000; Miyaji et al., 2002; Lieberman et al., 2003; Chan et al., 2004; Lieberman and Rosenzweig, 2005; Lieberman et al., 2006; Martinho et al., 2007; Hakemian et al., 2008). The number of

copper ions has converged to 2-3 copper ions per protomer of both *Methylococcus capsulatus* (Bath) and *Methylosinus trichosporium* OB3b pMMO (Lemos et al., 2000; Miyaji et al., 2002; Hakemian et al., 2008), but the Chan research group reports a very differing amount, 15-20 copper ions per protomer (Nguyen et al., 1998; Chan et al., 2004). Zahn and Dispirito (1996) came up with a similar number, 14.5 Cu ions per 99,000 kDa, but they argued that only two of the type II copper atoms are embedded in each protomer of pMMO complex with rest of copper ions bound to copper-binding ligands attached to pMMO. The Chan research group has proposed trinuclear Cu (II) complexes identified from EPR signal as the active sites (Nguyen et al., 1994; Chan et al., 2004). This hypothesis differs greatly from what has been proposed by Zahn and Dispirito (1996) and Martinho et al. (2007) stressing the involvement of iron in the catalysis activity of pMMO along with copper ions.

The crystal structure of pMMO resolved by Lieberman et al. identified three metal centers (Lieberman and Rosenzweig, 2005). The first metal site, identified in hydrophilic portion of PmoB ~25 Å apart from the membrane, is thought to be occupied by a single copper ion, which is coordinated by nitrogen atoms of two histidine residues, His 48 and His 72. The second copper site, also located within the hydrophilic domain of PmoB, was proposed to contain two copper ions based on the shape of copper anomalous Fourier map and duplicity of peaks in zinc anomalous Fourier map. This dinuclear copper site is coordinated by N-terminal amino nitrogen and side chain of His 33 and side chain nitrogens of His 137 and His 139. One or both of copper ions in this dinuclear copper site is thought to exist in Cu (I) oxidation state. The third metal site, located within the lipid bilayer, was found to be occupied by a single zinc ion in the crystallized pMMO.

However, it is more likely to be occupied by copper or iron before addition of crystallization buffer, since inductively coupled plasma atomic emission spectroscopy (ICP-AES) could not detect significant amounts of zinc in either pMMO-enriched membrane fraction or the purified enzyme (Yu et al., 2003; Lieberman and Rosenzweig, 2005). This metal site is coordinated by Asp 156, His 160, and His 173 of PmoC and Glu195 of PmoA (Figure II.9). Martinho et al.(2007) related this metal site to a di-iron active site analogous to that of sMMO, based on Mössbauer spectra similar to that exhibited by sMMO. Conservation of the coordinating residues of PmoA and PmoC in pMMO gene sequences of all known methanotrophs further corroborates their argument.

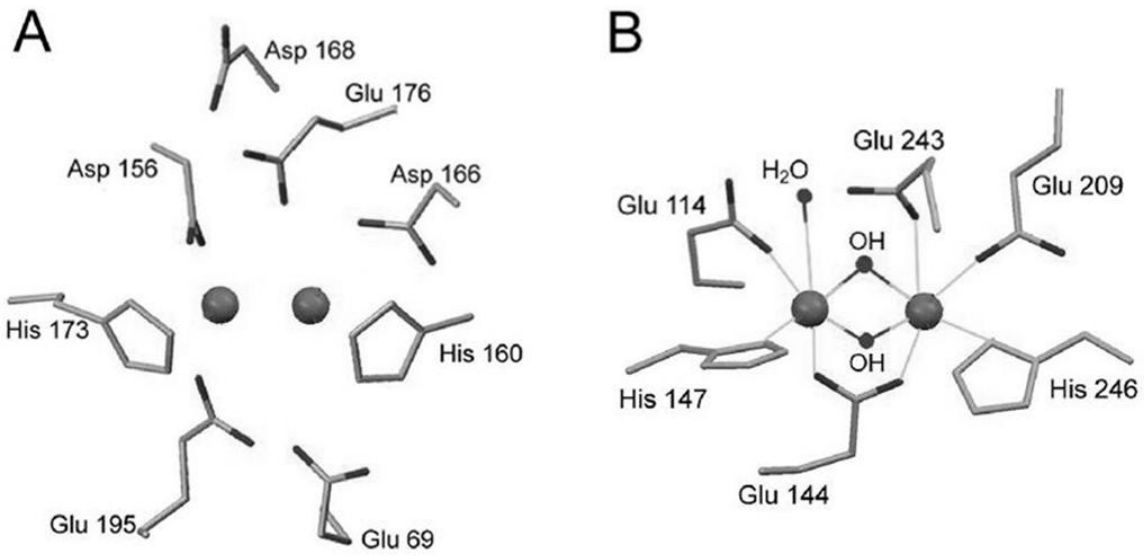

Figure II.9 Analogy between the compositions of (A) putative diiron site in pMMO and (B) diiron active site in sMMO (Martinho et al., 2007)

II.2.3 Mechanism of methane oxidation by soluble methane monooxygenase

The two different forms of methane monooxygenase, as they differ greatly in structure, were initially believed to utilize disparate mechanisms for methane

hydroxylation. Although the exact mechanism of the more prevalent form, pMMO, is still unknown, largely due to the difficulty in isolation of this enzyme with high activity, kinetics studies on purified sMMO have been carried out for many years.

A mechanism involving the MMOH cycle was proposed and supported by a series of experiments on steady-state and transient kinetics, spectroscopy, kinetic isotopic effects and enzyme structure (Green and Dalton, 1986; Lee et al., 1993; Lipscomb, 1994; Liu et al., 1994; Liu et al., 1995; Brazeau and Lipscomb, 1999; Lee and Lipscomb, 1999; Brazeau and Lipscomb, 2000). The proposed mechanism involves the hydroxylase component of sMMO going through a catalytic cycle (Figure II.10) from the fully reduced state ([Fe(II)-Fe(II)]) to a stable [Fe(III)-Fe(III)] state, substituting a hydrogen atom of the substrate with a hydroxyl group. Several intermediates of this reaction have been identified to date, including compounds **O**, **P***, **P** (or **L**), **Q**, **R**, and **T**(Lee et al., 1993; Liu et al., 1994; Liu et al., 1995; Lee and Lipscomb, 1999). **P*, P**, and **Q** are hypothesized to be a mixed valent (III-IV) superoxo adduct, symmetrical diiron-(III) peroxide complex, and dioxo-bridged $Fe^{IV}Fe^{IV}$ cluster, respectively, based on the character of Mössbauer spectra and g=16 EPR signal loss (Lee et al., 1993; Liu et al., 1995). Intermediates **O** and **T** are the oxygen- and methane-bound forms of intermediates, respectively (Lee et al., 1993; Liu et al., 1995). MMOB component was found to have a crucial role in the catalytic cycle as no detectable amount of **P** or **Q** was found in absence of MMOB (Liu et al., 1995). According to this mechanism, the product release step of the reaction was found to be the rate limiting step in the presence of MMOB (Lee et al., 1993).

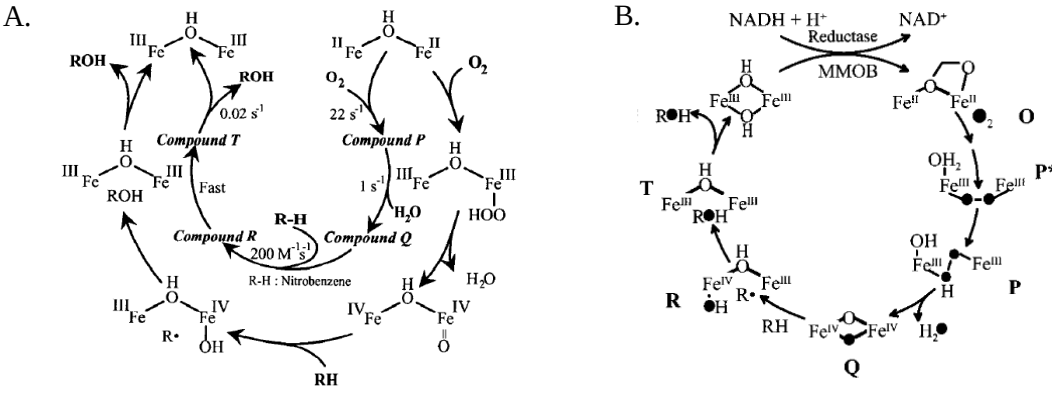

Figure II.10 The Catalytic cycle of sMMO (A) as proposed by Lipscomb (1994) and (B) later ammended with additional intermediates (Brazeau and Lipscomb, 2000)

II.2.4 Molecular biology of methane monooxygenases: genes and regulation

II.2.4.1 Soluble methane monooxygenase

The molecular biology of soluble and particulate methane monooxygenase has long been an intriguing topic in molecular biology primarily due to their unique regulation mediated by copper concentration.

The gene clusters of soluble methane monooxygenases from *Methylococcus capsulatus* (Bath) and *M. trichosporium* OB3b were cloned, sequenced, and analyzed for the first time by Stainthorpe et al. (1989) and Cardy et al. (1991), respectively. sMMO clusters of both strains comprise six operons, *mmoX*, *mmoY*, *mmoB*, *mmoZ*, *mmoC*, and *orfY*, which were later renamed as *mmoD* by Merkx and Lippard (2002). The six ORFs are arranged as seen in Figure II.11 and have a cumulative size of ~5.5 kb. *mmoX* (~1580 bp), *mmoY* (~1180 bp), and *mmoZ* (~510 bp) encode α, β, and γ subunits of MMOH, respectively. *mmoB* (~420 bp) and *mmoC* (~1340 bp) encode Protein B (regulatory protein) and Protein C (reductase), respectively. The function of *orfY*, or *mmoD*, is still unclear, although its expression *in vivo* and association with MMOH have been

confirmed by Merkx and Lippard (2002).

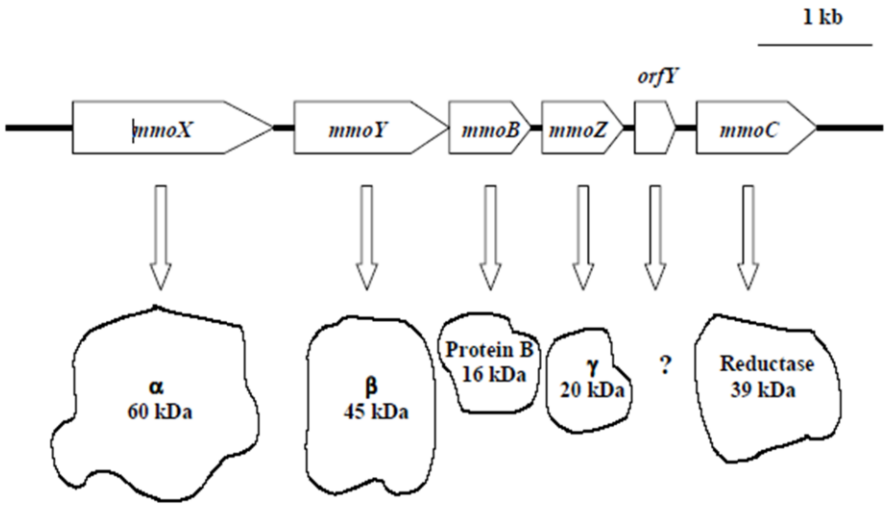

Figure II.11 Orientation of soluble monooxygenase gene clusters (Murrell et al., 2000a)

One of the most intriguing aspects of sMMO genes is their negative regulation by copper. Expression of the sMMO genes was found to be inhibited at copper concentrations as low as 0.25 µM (Murrell et al., 2000a). sMMO gene expression was thus extensively studied to identify this sensitivity toward copper (Nielsen et al., 1996; Nielsen et al., 1997; Csáki et al., 2003). From Northern blot experiments performed with *M. capsulatus* Bath, three transcripts with different sizes were identified with one of them being 5.5 kb long, putatively containing all six genes of this operon. Primer extension analyses of these genes revealed the only putative promoter sequence found at 5' end of *mmoX* gene, which is analogus to *E. coli* -35 and -10 consensus sequences (Nielsen et al., 1996). Later analyses on sMMO genes from *M. trichosporium* OB3b detected three transcripts of different sizes: ~3.3 kb fragment containing *mmoX*, ~4.0 kb fragment

containing *mmo Y, mmoB,* and *mmoZ,* and ~2.2 kb fragment containing *mmoY, mmoB,* and *mmoZ*. Unlike *M. capsulatus* (Bath), multiple promoter-region-like sequences were identified for *M. trichosporium* OB3b, two of which, σ^{70}- and σ^{54}- recognition sequences, are located upstream of *mmoX*. Another was found in an intergenic region between *mmoX* and *mmoY,* which might be the promoter region for two fragments without *mmoX*. Experimental results using either cell revealed that expression of all these mRNA fragments were suppressed upon addition of copper.

Later, Csáki et al. (2003) located the activator binding site upstream of *mmoX* gene in *M. Capsulatus* (Bath), identifying the σ^{N}-type promoter as the region responsible for copper regulation of sMMO expression. Four ORFs downstream of *mmoXYBDC, mmoG, mmoQ, mmoS,* and *mmoR* were also identified to contribute to copper regulation of sMMO genes in the same study. *mmoG* and *mmoR,* also found in *M. trichosporium* OB3b (Stafford et al., 2003), are hypothesized to be a GroEL-like chaperonin and a σ^{N}-dependent transcription activator, respectively, both of which were found to be indispensible for expression of sMMO. *mmoS* and *mmoQ* were hypothesized to form a two-component signal transduction system that responds to the copper stress, in which *mmoS* is thought to be the signal receptor and *mmoQ* is the downstream effecter. However, no gene corresponding to *mmoS* or *mmoQ* was found in the vicinity of *mmo* operon in the draft genome of *M. trichosporium* OB3b.

II.2.4.2 Particulate methane monooxygenase

The genes that encode pMMO were first cloned and sequenced by Semrau et al. (1995). In their study, genes encoding 45 kDa- and 27 kDa- sized components of pMMO

were identified from hybridization with DNA sequence derived from N-terminal amino acid sequences of PmoA and AmoA. The gene for the remaining component of pMMO, *pmoC*, was located in later research by Stolyar et al (1999). Juxtaposition of these three pMMO genes, as well as duplicity of the gene cluster, was observed in *M. capsulatus* (Bath), *M. trichosporium* OB3b, and *Methylocystis* sp. Strain M (Stolyar et al., 1999; Gilbert et al., 2000). *pmo* genes are arranged with *pmoC* located upstream of *pmoA* followed downstream by *pmoB* (Figure II.12). In *M. trichosporium* OB3b DNA, p*moC*, *pmoA*, and *pmoB* are 771 bp, 756 bp, and 1296 bp in size, respectively, with intergenic spaces, *pmoC-pmoA* and *pmoA-pmoB*, 244 bp and 174 bp in size, respectively (Gilbert et al., 2000). Duplicate copies of *pmoCAB* clusters were identified in all three strains with high degree of similarity between the copies (Semrau et al., 1995; Stolyar et al., 1999; Gilbert et al., 2000). Moreover, a third *pmoC* gene, not as a part of *pmoCAB* operon, was found in *M. capsulatus* (Bath) genome (Stolyar et al., 1999), *Methylokorus infernorum* V4 genome (Hou et al., 2008) and the draft genome of *M. trichosporium* OB3b. It was, however, not yet identified in the other type I methanotrophs. *pmoCAB* operon of two type II strains, *M. trichosporium* OB3b and *Methylocystis* sp. Strain M, have >80% identity while identity of *pmoCAB* of these genes to that of *M. capsulatus* (Bath) is around 70%. *pmoC* tends to have higher identity across species than *pmoA* and *pmoB*.

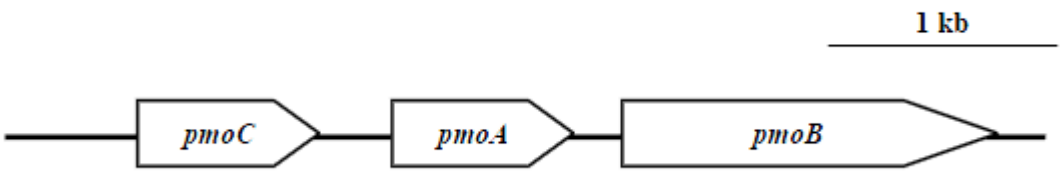

Figure II.12 A schematic map of *pmo* gene arrangement in *M. trichosporium* OB3b. The second copies of *pmo* genes are almost identical to these genes in sizes and sequences (Murrell et al., 2000a)

Primer extension studies on *pmoC* genes of *Methylocystis* sp. Strain M identified two possible transcription start sites with -35 σ^{70} consensus sequences (Gilbert et al., 2000). Both of these transcription start sites were located ~300 bp upstream of 5' end of *pmoC*, 12 base pairs apart from each other. Primer extension studies on *M. trichosporium* OB3b in the same study, however, failed to identify any analogous transcription start site upstream of *pmoC*, except for an evidence of a similar consensus sequence ~500 bp upstream. Expression of pMMO was found to be controlled by concentration of copper in a reciprocal manner to expression of sMMO. Increased transcription of mRNA upon addition of copper was evidenced in Northern blot analyses on total transcribed mRNA, competitive reverse transcriptase polymerase chain reaction (RT-PCR) and real-time RT-PCR (Nielsen et al., 1997; Choi et al., 2003; Knapp et al., 2007). Experimental results from Knapp et al. (2007) indicate that copper control on expression of pMMO, as well as that of sMMO, might be more complicated with engagement of the methanobactin, the copper binding biochelator, which will be discussed later.

II.3 Degradation of methane and halogenated hydrocarbon by methanotrophs

II.3.1 Significance of methane and halogenated hydrocarbon degradation

The capability of methanotrophs to degrade a wide variety of potential pollutants, including methane and halogenated hydrocarbons, has been studied for applications in climate change control and bioremediation (Colby et al., 1977; Fogel et al., 1986; Oldenhuis et al., 1989; Fox et al., 1990; Alvarez-Cohen and McCarty, 1991; Chang and Alvarez-Cohen, 1996; Lontoh and Semrau, 1998; Lontoh et al., 2000; Melse and van der Werf, 2005; Nikiema et al., 2005; Lee et al., 2006).

II.3.1.1 Methane

Methane is an important greenhouse gas contributing to global climate change. Although present in relatively small concentrations in the atmosphere, ~1.7 ppmv, methane is approximately 25 times as efficient as carbon dioxide at absorbing infrared radiation (Etheridge et al., 1998; Le Mer and Roger, 2001), and the atmospheric methane concentration has risen rapidly since the industrial revolution. The increase in atmospheric methane concentration is attributed to increased anthropogenic methane emissions, which have led to a disruption of global methane cycling (Etheridge et al., 1998). A significant portion of natural and anthropogenic methane generation occurs via biological methanogenesis. Strictly anaerobic environments such as wetlands and landfills promote microbial methanogenesis and thus, are major sources of the atmospheric methane. It is known, however, that significant amounts of methane are also emitted from upland forest soils, ruminant animals, and fossil fuel combustion (Blaha et al., 1999).

Degradation of atmospheric methane occurs via two general pathways: (1) photochemical elimination and (2) microbial oxidation (Bousquet et al., 2006). In photochemical elimination processes, atmospheric methane is primarily degraded through reactions in the stratosphere with either the hydroxyl radical (OH•) or electronically excited singlet oxygen (O1D) (Le Texier et al., 1988). It is estimated that methanotrophic consumption of methane accounts for 1–15% of the combined amount of biotic and abiotic methane removal (Wahlen, 1993). In natural environments, e.g., wetlands, methanotrophs are known to oxidize a significant portion of methane generated in anaerobic zones with reported methane oxidation potentials of up to 0.29 μmol CH_4/g wet

peat-h (Sundh et al., 1995). It is also known that methanotrophs in landfill cover soils significantly reduce the amount of methane released from landfills. Methane oxidation potentials up to 10.8 μmol CH_4/g dry weight of soil-h were reported in *in vitro* experiments performed with landfill cover soils (Börjesson et al., 1998).

II.3.1.2 Chlorinated hydrocarbons

Chlorinated ethenes are synthetic compounds with no identified natural sources and are commonly used in various industrial practices including degreasing operations, dry cleaning, dying, and textile production (Bakke et al., 2007). Despite their widely perceived carcinogenicity (Bolt, 2005; Scott and Chiu, 2006), there have been significant historical releases to the environment and as a result, these compounds are often detected in substantial concentrations in subsurface soils and groundwater (Westrick et al., 1984). The reductive anaerobic biodechlorination of these compounds, for example tetrachloroethylene to ethene through trichloroethylene (TCE), dichloroethylene (DCE), and vinyl chloride (VC) as intermediates, has been known for some time (Freedman and Gossett, 1989; Maymo-Gatell et al., 1999). However, *in situ* application of anaerobic biodechlorination has been limited as this process does not result in complete dechlorination in the presence of sulfate due to the competition with the sulfate reducing bacteria for hydrogen and thus, can lead to accumulation of TCE, *cis*-dichloroethylene (*c*-DCE), *trans*-dichloroethylene (*t*-DCE), and VC (Maymo-Gatell et al., 1999).

Aerobic biodegradation of chlorinated compounds has been widely examined as an alternative to anaerobic degradation. There have been several reports of aerobic bacterial strains that can utilize chlorinated ethenes as growth substrates (Verce et al.,

2000; Coleman et al., 2002), as well as many strains that cooxidize these compounds (Futamata et al., 2001). Methanotrophs are one of those groups of microorganisms capable of degrading these pollutants via cooxidation and due to their omnipresence in various environment, these cells have been widely applied to decontamination of sites polluted with chlorinated ethenes (Hanson and Hanson, 1996; Semrau et al., 2010).

II.3.2 Kinetics of methane and hydrocarbon degradation by purified sMMO

As mentioned above, the steady-state kinetics of methane degradation by isolated soluble methane monooyxgenase has been studied by Green and Dalton (1986). In the presence of excess oxygen and NADH, K_m and V_{max} for oxidation of methane were found to be 3 μM and 56.0 nmol/min per mg of protein A, respectively, for sMMO extracted from *M. capsulatus* (Bath). This enzyme degraded other alkane substrates as well but generally with much higher K_m values. V_{max} values remained at the same order of magnitude for alkanes with up to five carbons, as can be seen on Table II.2. In later research (Fox et al., 1990), the kinetics of chlorinated hydrocarbon degradation by purified sMMO from *M. trichosporium* OB3b were measured (Table II.2). Ethylene and chlorinated ethylene exhibited similar V_{max} and K_m values, indicating similar oxidation mechanisms for these different compounds. Unlike in oxidation of methane, the intermediates of chlorinated hydrocarbon degradation were found to have an adverse effect on the activity of the sMMO. By tracking incorporation of ^{14}C into the purified soluble monooxygenases, it was found that all three components of sMMO are affected by the intermediates that act as diffusible modifying reagents (Fox et al., 1990).

Table II.2 Kinetic data for oxidation of chlorinated ethylenes by the soluble methane monooxygenase from *M. trichosporium* OB3b

Substrate	V_{max} (nmol · min^{-1} · mg protein A^{-1})	K_s (μM)	Reference
Methane	56.0	3.0	Green and Dalton, 1986
Ethane	83.3	60.6	Green and Dalton, 1986
Propane	34.5	12.5	Green and Dalton, 1986
Butane	90.9	500.0	Green and Dalton, 1986
Pentane	10.3	392.0	Green and Dalton, 1986
Ethylene	858	32	Fox et al, 1990
Vinyl Chloride	748	33	Fox et al, 1990
cis - DCE	935	28	Fox et al, 1990
trans – DCE	888	38	Fox et al, 1990
Vinylidene chloride	648	18	Fox et al, 1990
TCE	682	35	Fox et al, 1990

II.3.3 Whole-cell kinetics of of methane and chlorinated hydrocarbon degradation by pMMO and sMMO

As anticipated from their differences in structure, sMMO and pMMO are known to have widely differing kinetic properties. Direct comparison of the enzymes, however, has not yet been made possible, due to the difficulty in purifying pMMO with full activity. Thus, comparison of kinetics of the two enzymes has relied on measurement of whole-cell enzyme activities (Sipkema et al., 1998; Lee et al., 2006). Steady-state kinetic parameters fitted from the experiments carried out with *M. trichosporium* OB3b at 30℃ showed that sMMO- and pMMO- expressing cells have comparable maximum oxidation rates (V_{max}) while sMMO expressing cells have half saturation constant (K_s) value that is ~30 times higher, indicating more effective methane oxidation by pMMO at lower concentration of methane.

Unlike in methane oxidation, whole-cell oxidation of chlorinated hydrocarbons reactions by sMMO- and pMMO- expressing cells exhibit a stark difference in kinetics. While sMMO have long been proven to effectively degrade various halogenated hydrocarbons, pMMO were thought to be exclusively specific to methane, being unable to catalyze dehalogenation reaction (Oldenhuis et al., 1989; Tsien et al., 1989). *M. trichosporium* OB3b cells expressing sMMO degraded compounds such as *t*-DCE and TCE with kinetics comparable to methane degradation as shown in Table II.3 (Oldenhuis et al., 1991). Later, however, *M. trichosporium* OB3b cells and *M. parvus* BG8 cells expressing pMMO, grown in presence of sufficient copper to elicit pMMO expression, were also able to degrade halogenated hydrocarbons, although with less favorable kinetics (Lontoh and Semrau, 1998; Han et al., 1999; Lee et al., 2006).

Table II.3 Comparison of whole cell kinetics data from *M. trichosporium* OB3b expressing pMMO and the same cells expressing sMMO (Lee et al., 2006)

Enzyme	Substrate	V_{max} (nmol · min^{-1} · mg $protein^{-1}$)	K_s (μM)	Reference
pMMO	CH_4	82	8.3	Lontoh and Semrau, 1998
	VC	42	26	Lee et al., 2006
	t-DCE	61	42	Lee et al., 2006
	TCE	4.1	7.9	Lontoh and Semrau, 1998
sMMO	CH_4	726	92	Oldenhuis et al., 1991
	VC	2100	160	Lee et al., 2006
	t-DCE	662	148	Oldenhuis et al., 1991
	TCE	580	145	Oldenhuis et al., 1991

The higher reactivity of sMMO toward these co-substrates, however, does not guarantee higher effectiveness in *in situ* remediation. In fact, in the presence of high concentrations of chlorinated solvents (≥50 μM), growth of *M. trichosporium* OB3b in

sMMO-expressing condition was found to be significantly impaired in a set of experiments performed by Lee et al. (2006). Thus, the ability to co-oxidize chlorinated hydrocarbons in the long term was reduced to levels less than that of pMMO-expressing cells (Lee et al., 2006). It is premature to conclude that this particular experiment represented *in situ* bioremediation conditions since optimal laboratory conditions were used for the assay. Nevertheless, these results imply that the common perception about methanotrophic degradation might prove not to be true, in that pMMO, not sMMO, might in fact be the key player in *in situ* methanotrophic bioremediation.

II.4 Methanobactin

II.4.1 Structure and properties

Many bacteria and fungi excrete iron chelators, i.e., siderophores, mostly when iron availability is limited, to facilitate iron uptake (Ratledge and Dover, 2000; Haas, 2003). Methanotrophs have also been found also to produce metal chelators (Zahn and DiSpirito, 1996; Tellez et al., 1998; Kim et al., 2004; Choi et al., 2005). These organic chelators, however, are involved in copper uptake instead of iron uptake. The existence of these copper binding biochelators was first suggested by the Georgiou research group in experiments with *M. trichosporium* OB3b mutants created via dichloromethane mutagenesis that had constitutive expression of sMMO regardless of copper concentration (Phelps et al., 1992; Fitch et al., 1993). In these experiments, abnormal copper localization was observed as copper was added to the mutants grown in the absence of copper (Fitch et al., 1993). In contrast to wildtype cells in which copper was concentrated in the particulate, or membrane cell fraction, these mutants had low-levels

of copper evenly distributed, leading to the hypothesis that there is a copper uptake system that helps transport of copper to pMMO, where copper is needed in the largest amount. The copper binding ligand was isolated and was estimated to have a copper binding constant on the order of 10^{16} M^{-1}, when 1:1 stoichiometry was assumed (Tellez et al., 1998). Later a conditioned copper binding constant of log K=10.3 was suggested by Morton et al. (2000a) from copper titration results, and the discrepancy with previous estimate was attributed to the pH effect on the competing chelating agents. In their work, Morton et al. also emphasized the capability of methanobactin to alter metal speciation in both culture media and soil to increase bioavailability of copper originally bound to other chelating agents or adsorbed to soil constituents (Morton et al., 2000a, b). Copper-induced repression of sMMO activity, as measured with quantitative naphthalene assay, was less pronounced in the presence of strong chelating agents (log K>16) or soil constituents with high surface hydroxyl concentration.

Several different methods were developed to isolate this ligand from the growth medium, involving column separation and HPLC methods (DiSpirito et al., 1998; Kim et al., 2005). Investigation on properties of methanobactin has been carried out with methanobactin isolated from *M. trichosporium* OB3b. The molecular weight of methanobactin was determined to be 1153 (without copper bound) and 1215 (with copper bound) from mass spectroscopy (Kim et al., 2005), consistent with previous estimates from the elution profile (DiSpirito et al., 1998). The first proposed structure of this peptide, as determined by a combination of crystallographic and mass spectroscopic analyses, is shown in Figure II.13A (Kim et al., 2004). According to this structure, a single copper ion in Cu^{+} state is coordinated by two nitrogen atoms from imidazole

moieties and two sulfur atoms from cysteine residues. This structure was recently slightly modified based on experimental NMR analysis (Behling et al., 2008). The modified structure of methanobactin on Figure II.13B has two alkylidene oxazolone rings in position previously thought to be occupied by two imidazole rings.

A.

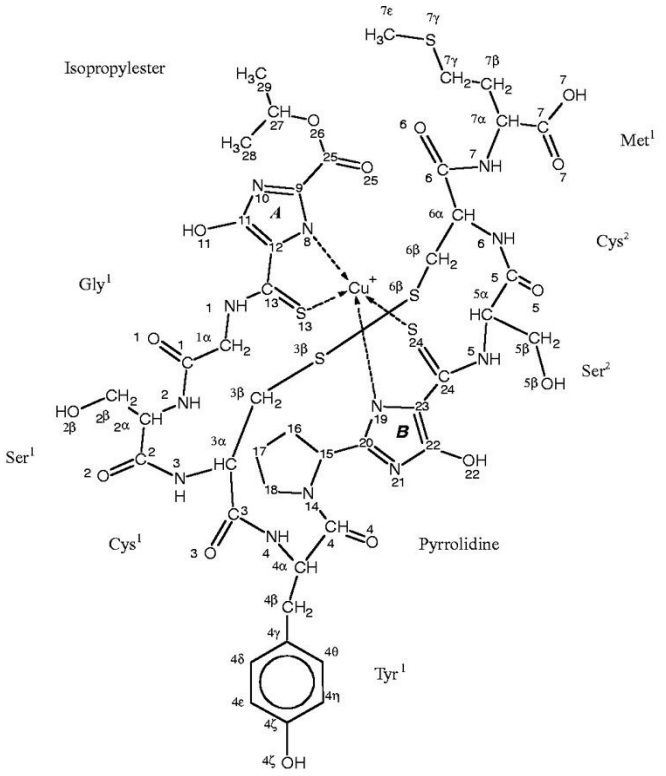

B.

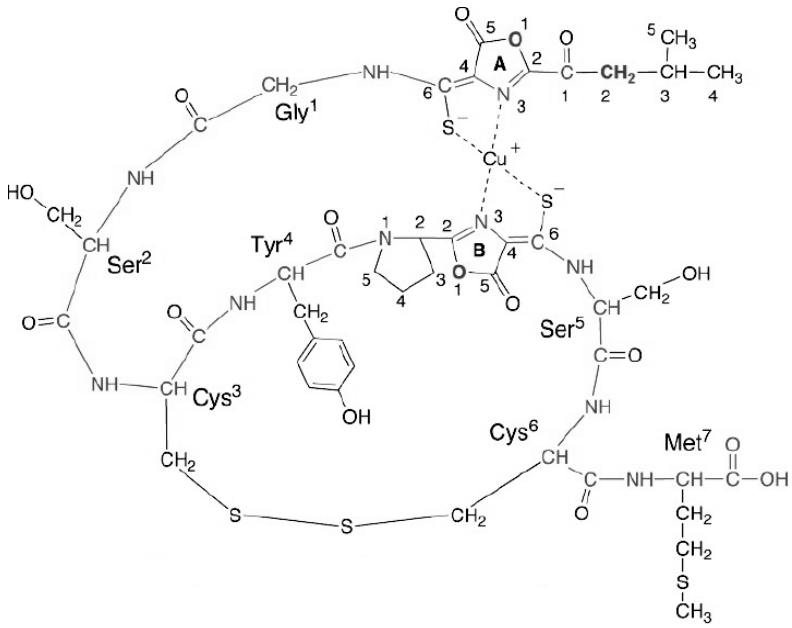

Figure II.13 (A) Molecular structure of methanobactin as proposed by Kim et al. (2004) (B) Modified structure of methanobactin (Behling et al., 2008)

Binding of Cu(I) or Cu(II) to methanobactin is hypothesized to be a multi-step reaction involving initial dimerization and eventual monomerization, based on spectroscopic, kinetics, and thermodynamics studies (Choi et al., 2006a). As shown in Figure II.14, experimental results indicate that Cu(II) is initially coordinated by immidazole N atoms and thiocarbonyl S atoms from two 4-hydroxy-5-thiocarbonyl imidazolate (HTI; according to the structure proposed by Kim et al. (2005)) from two methanobactin molecules. After reduction, gradual coordination change was observed with addition of another Cu (II) atom, eventually yielding two monomeric Cu-Mb complexes with copper ion intramolecularly coordinated to immidazole N atoms and thiocarbonyl S of HTI and 4-thiocarbonyl-5-hydroxy imidazolate (THI). This proposed mechanism had marked difference with the mechanism previously proposed by Kim et al (2005), perhaps owing to the method of isolation and consequential disparity in chemical properties of the isolated methanobactin.

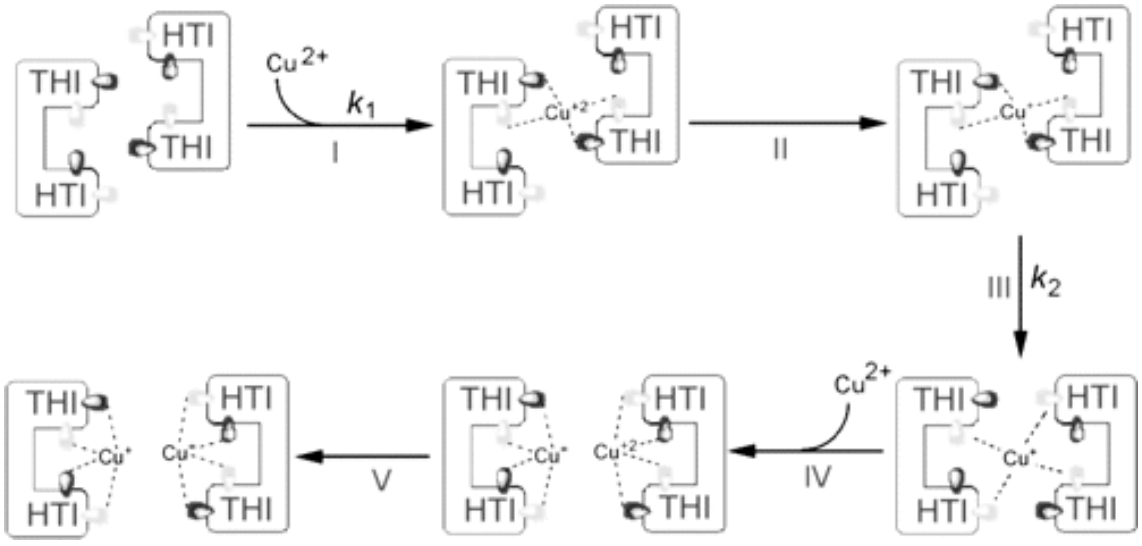

Figure II.14 A schematic of Cu(II) binding by mb. yellow: thiocarbonyl group, blue: imidazole N (Choi et al., 2006a)

Methanobactin has been known to bind metal ions other than copper, e.g., iron, since its discovery. Choi et al. (2006b) categorized transition metal ions according to the character of their interactions with methanobactin based on UV-sbsorption spectroscopy. The metal ions that exhibit similar binding mechanism with methanobactin, i.e., Ag(I), Au(III), Hg(II), Pb(II), and U(VI), were classified as group A, and the metal ions that are bound to methanobactin but via different coordination and dimerization, i.e., Cd(II), Co(II), Fe(III), Mn(ii), Ni(II), and Zn(II), are classified as Group B. Ba(II), Cr(VI), La(III), Mg(II), and Sr(II) were found not to be bound by methanobactin.

II.4.2 Two peptide synthesis pathways – ribosomal and non-ribosomal

There are several different pathways known to be involved in synthesis of secondary metabolites, including ribosomal peptide synthesis, non-ribosomal peptide synthesis, non-ribosomal independent siderophore (NIS) biosynthesis pathway, and polyketide biosynthesis pathway (Staunton and Weissman, 2001; Challis, 2005; Walsh and Nolan, 2008; McIntosh et al., 2009). In rarer occasions, hybrids of these pathways are used as well, as is the case for bleomycin synthesis (Shen et al., 2001; Shen et al., 2002; Pfeifer et al., 2003). Since methanobactin is a secondary metabolite with a modified peptide backbone, these possibilities are narrowed down to ribosomal and non-ribosomal peptide synthesis. As NIS and polyketide biosynthesis do not involve peptide linkage between monomeric units they can be eliminated from consideration.

Ribosomal peptides (RP) such as lantibiotics and microcins are ribosomally synthesized and posttranslationally modified. In most of the cases, RPs are expressed as precursor peptides with leader peptides, which are then removed via proteolysis

(McIntosh et al., 2009). This proteolysis reaction is mediated by various proteases including serine proteases, cysteine proteases attached to ABC transporters, and metal proteases. Another generally observed feature in RPs is the heterocyclic motif, usually in form of oxazoline/oxazole or thiazoline/thiazole, which is the posttranslational modification of Cys, Ser, or Thr (Figure II.15). In general, enzymes involved in heterocyclization are a zinc binding protein, a probable docking protein with ATPase/GTPase activity, and an oxidase, as are McbB, McbD, and McbC, respectively, in microcin B17 synthesis (Milne et al., 1999; Zamble et al., 2000).

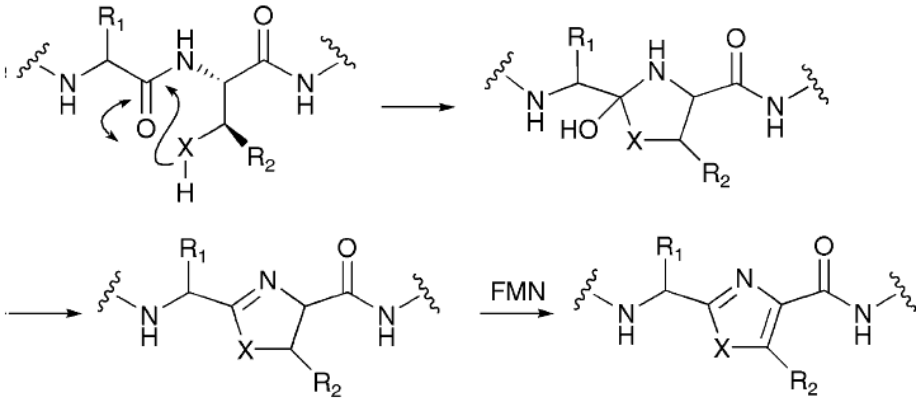

Figure II.15. A general scheme for heterocyclization of Cys or Ser to oxazoline/oxazole or thiazoline/thiazole. X can be either oxygen atom or sulfur atom

Disulfide bonds are also often observed in RPs (Paik et al., 1998; Fontaine and Hols, 2008). In mature RPs, Cys-Cys disulfide bonds have primary function of stabilizing the structure into a rigid active state. Redox activity, however, was not observed for these disulfide bonds. Protein disulfide isomerases (PDI) are often engaged in RP syntheses although RPs rarely have more than two disulfide bonds. Other abnormal structural modifications, such as dehydrated Ser and Thr, lanthionine, prenylation, epimerization,

and macrocyclization are observed in structure of RPs. These, however, will not be discussed here due to their probable absence in methanobactin synthesis.

Nonribosomal peptide (NRP) synthesis is the most common pathway for synthesis of siderophores with peptide backbone structures (Crosa and Walsh, 2002; Schwarzer et al., 2003). Instead of being directly translated from mRNA, these peptides are assembled by a group of enzymes termed nonribosomal peptide synthases (NRPS). These enzymes are organized in modules, which are units for addition of each amino acid to an expanding peptide chain. Each module is made up of domains with different functions, which work together for proper addition of a specific amino acid to peptide chains.

The basic scheme for elongation of peptide chains in NRP synthesis involves adenylation (A) domains, peptidyl carrier protein (PCP) domains, and condensation (C) domains usually arranged in A-PCP-C manner (Mootz et al., 2002; Schwarzer et al., 2003). A-domain confers specificity toward the proper amino acid to be added to the chain by having active site structure specifically fit for accommodation of that specific amino acid, which is then adenylated by enzyme activity (Stachelhaus et al., 1999; Challis et al., 2000). This adenylated amino acid is then transported by PCP domain to the active site for addition to the peptide intermediate, which is mediated by C domain.

NRP syntheses have drawn great attention due to the variability of structural features observed in their products, e.g., epimerization, heterocyclization, macrocyclization, N-methylation, and oxidation, etc (Konz and Marahiel, 1999; Mootz et al., 2002; Schwarzer et al., 2003). This variability is conferred by incorporation of various domains with different functions (Figure II.16) into NRPS modules. An example of NRPS is illustrated in Figure II.17, in which bacitracin A, a decapeptide with relatively

similar size to methanobactin, is synthesized by a three-enzyme-complex with 12 modules (Schwarzer et al., 2003)

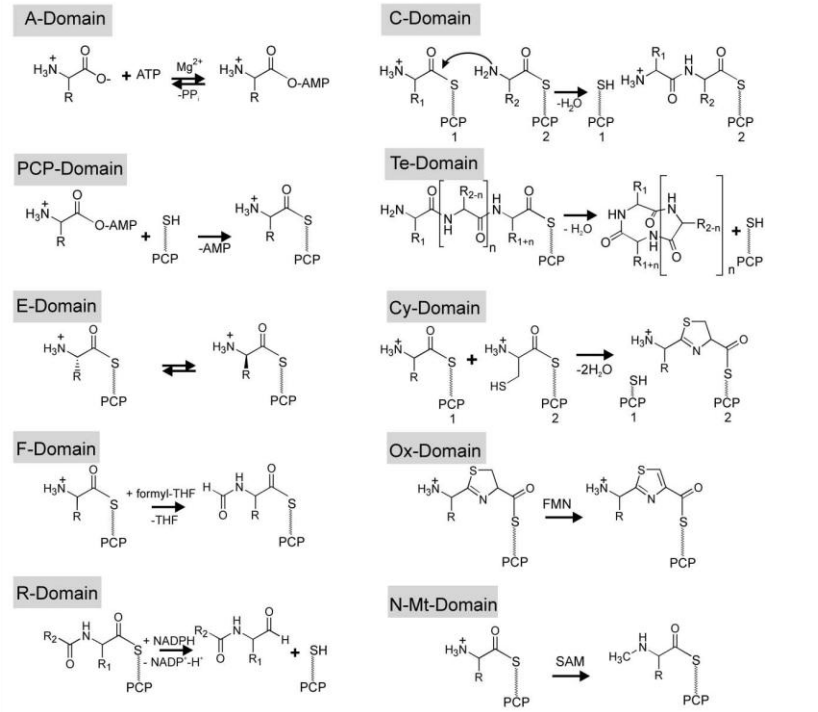

Figure II.16 Domains and their respective function in non-ribosomal peptide synthesis (Schwarzer et al., 2003)

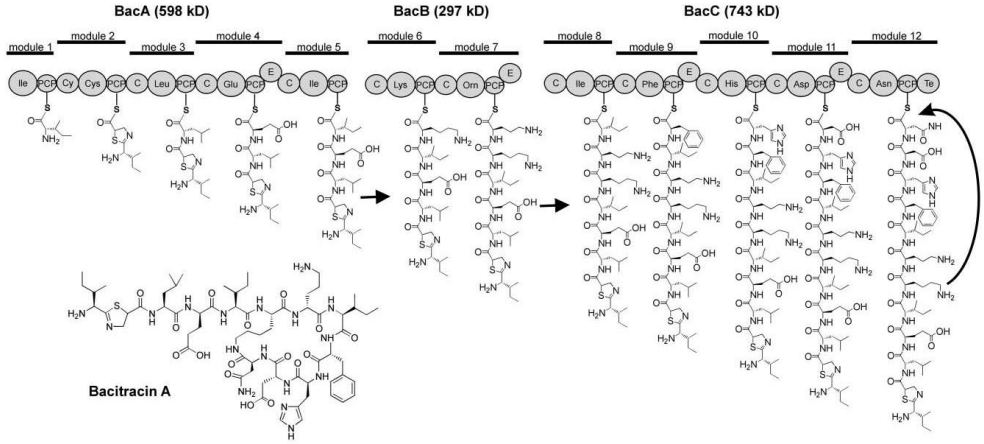

Figure. II.17 A schematic diagram depicting the module arrangement and mechanism of bacitracin A synthesis. Domains labeled with nomenclature for amino acids are adenylation domains specific for the amino acids (Schwarzer et al., 2003)

CHAPTER III

Methods and Materials

III.1 Measurement and modeling of multiple substrate oxidation by methanotrophs at 20˚C

Culture conditions *Methylosinus trichosporium* OB3b was grown at 20˚C in 125 mL of nitrate mineral salt medium (Whittenbury et al., 1970) in 2-L Erlenmeyer flasks shaken at 225 r.p.m. in a methane-to-air ratio of 1:2 at 1 atm of pressure. For pMMO-expressing conditions, 20 μM of copper was added as $CuCl_2$. For sMMO-expressing conditions, no copper was added. To verify which form of the MMO was expressed, the naphthalene assay was performed as described previously (Brusseau et al., 1990).

Chemicals Highest-purity methane (≥99.99%) was obtained from Airgas Company and TCE (≥99.5%) was purchased from Fisher Scientific Company (Fair Lawn, NJ). Trans-dichloroethylene (t-DCE) (≥98%) was purchased from Aldrich (Milwaukee, WI) and vinyl chloride (VC) (≥99.5%) was purchased from Fluka (Ronkonkoma, NY). Distilled deionized water was used (>18MΩ). Before use, all glassware was washed with detergent and then acid washed in 2N HNO_3 for at least 24 h to remove copper and other trace metals. Nitric acid was subsequently removed by rinsing the glassware with distilled deionized water (>18MΩ).

For chlorinated ethenes that are liquid at room temperature, i.e., TCE and *t*-DCE,

saturated stock solutions were prepared by the method developed by Chang and Alvarez-Cohen (1996). Aliquots were taken using Hamilton 1700 series gas-tight syringes (Hamilton, Reno, NV). For methane and VC, which are gaseous at room temperature, aliquots were taken using Precision Lok gas-tight syringes (Precision Sampling Corp., Baton Rouge, LA). Ten percent (v/v) VC was prepared in a 20-mL vial for low VC concentrations. Formate was prepared as 500 mM sodium formate stock solution. The amount of chlorinated solvents to be added was determined by calculation using dimensionless Henry's constants at 20°C. Henry's constants for methane, TCE, *t*-DCE, and VC used in this study were 28.4, 0.291, 0.329, and 0.908, respectively (Perry, 1984; Tse et al., 1992; Gossett, 1987).

Measurement of Michaelis-Menten parameters at 20 °C The whole-cell Michaelis–Menten parameters, V_{max} and K_s, for degradation of TCE, *t*-DCE, VC, and methane by *M. trichosporium* OB3b expressing either pMMO or sMMO were measured using gas chromatography as described earlier (Lontoh et al., 2000). Specifically, *M. trichosporium* OB3b was grown at 20°C as mentioned above to an $OD_{600\ nm}$ of 0.4. Cells were then diluted 1:1 with fresh NMS medium precooled to 20°C. Cells were then grown to an $OD_{600\ nm}$ of ~0.3 to ensure that they were in the exponential phase. The flask was then evacuated and flushed with compressed air at least 10 times to remove methane before 3-mL aliquots were transferred to 20-mL serum vials. After adding 20 mM of sodium formate, the vials were capped with Teflon-coated butyl-rubber stoppers (National Scientific Co., Duluth, GA) and crimp sealed with aluminum caps. The corresponding

protein concentration was determined using the Bio-Rad protein assay kit (Bio-Rad Laboratories, Hercules, CA).

For degradation assays with *M. trichosporium* OB3b expressing sMMO, varying concentration ranges were used for different compounds, specifically 22–220, 8–950, and 18–500 µM for TCE, *t*-DCE, and VC, respectively. Initial samples were taken after the vials were vigorously shaken for 1 min. For TCE and *t*-DCE, 100 mL of headspace was injected into an HP5890 Series II gas chromatograph equipped with a 75 m DB-624 column with 0.53 mm internal diameter (J&W Scientific Co.) using a Precision Lok gas-tight syringe. An electron capture detector (ECD) was used for both TCE and *t*-DCE, with injector, oven, and detector temperatures set to 160, 120, and 250 ℃, respectively. Subsequent injections were made every 2 min for TCE over 14 min and 3 min for *t*-DCE over 16 min. For VC, an HP5890 Series II gas chromatograph was used with a flame ionization detector (FID), with injector, oven, and detector temperatures set to 140, 120 and 250 ℃, respectively. Injections were made every 1.5 min over 6 min. For degradation assays of *M. trichosporium* OB3b expressing pMMO, significantly longer time intervals were used due to the slower degradation rates. Injections were made every 30 min for TCE over 2–3 h, 18 min for *t*-DCE over 72 min, and 5 min for VC over 30 min. The concentration ranges used for pMMO degradation assays were 5–90, 14-300, and 20–510 µM for TCE, *t*-DCE, and VC, respectively.

For methane consumption assays, concentration ranges of 0.5–260 and 8–430 µM were used for *M. trichosporium* OB3b expressing pMMO and sMMO, respectively. Serum vials were shaken at 200 r.p.m. at 20 ℃. For sMMO-expressing cells, samples were taken every 60 min over 8 h. For pMMO expressing cells, samples were taken every

20 min over 80 min for low concentrations (<35 μM), and every 90 min over 6 h for higher concentrations. For methane measurements, an HP6890 gas chromatograph with a flame ionization detector and a GS Molesieve column with 0.53 mm inner diameter and 30 m length was used, with injector, oven, and detector temperatures set to 185, 75, and 250 °C, respectively. The normalized degradation rates were fit to the Michaelis–Menten equation using KALEIDAGRAPH v.4.0 (Synergy Software).

Effect of mixed chlorinated solvents on cell growth at 20 °C The growth rates of *M. trichosporium* OB3b cells in the presence of different concentrations of mixed pollutants were measured using the procedure described previously by Lee et al. (2006). Specifically, *M. trichosporium* OB3b was grown to the mid exponential phase (OD_{600nm} ~ 0.4) and then diluted to an $OD_{600\ nm}$ of ~ 0.04. After the cells were regrown to an $OD_{600\ nm}$ of ~ 0.06 at 20 °C, the headspace was removed by applying a vacuum and replacing with air 10 times. Five milliliters of aliquots were then aseptically transferred into specially constructed serum vials. Sodium formate was added at a concentration of 20 mM and the serum vials were sealed with Teflon-coated butyl-rubber stoppers (National Scientific Co., Duluth, GA). Using a Precision Lok syringe, 5 mL of headspace in the serum vials were replaced with 5 mL of methane to yield an aqueous concentration of 270 μM. VC, *t*-DCE, and TCE were then added to yield initial equimolar concentrations ranging from 10 to 100 μM. The initial and final concentrations of the chlorinated solvents were measured using the procedure developed earlier (Lee et al., 2006). To measure any abiotic loss, the same procedure was repeated with *M. trichosporium* OB3b

cells of the same density inactivated with the addition of 50 µl of 5 N sodium hydroxide as described earlier (Lontoh and Semrau, 1998).

Calculation of the competition parameter, Δ The **Δ** model developed by Lee et al. (2006) was used to evaluate the effect of chlorinated ethenes on the oxidation of methane by methanotrophs. The dimensionless parameter Δ was calculated using the following equation to yield values ranging from 1 (i.e., no chlorinated ethenes present) to negative numbers (i.e., the combined rates of chlorinated ethene turnover are greater than the rate of methane turnover).

$$\Delta = \left(\frac{V_{max}^{G} \times S^{G}}{K_s^{G} + S^{G}} - \sum_{j=1}^{n} \frac{V_{max}^{P_i} \times P_i}{K_s^{P_i} + P_i}\right) \Big/ \frac{V_{max}^{G} \times P_i}{K_s^{G} \times S^{G}}$$

In this equation, S^G and P_i are concentrations of the growth substrate and the *i*th pollutant in the aqueous phases, respectively. V_{max}^{G} and $V_{max}^{P_i}$ are the maximum rates of growth substrate and pollutant transformation, respectively and K_s^G and $K_s^{P_i}$ are the half-saturation constants for the binding of the growth substrate and pollutant, respectively.

III.2 Expression of pMMO by *Methylocystis daltona* SB2 grown on acetate and its implications in degradation of chlorinated ethenes

Culture conditions *Methylocystis daltona* SB2 was grown at 30˚C in 50 ml of nitrate mineral salt medium (Whittenbury et al., 1970) with 10 µM of copper added as $CuCl_2$ in 250-ml Erlenmeyer flasks shaken at 225 r.p.m. For methane-growth conditions, methane was added to the headspace to 1:1 methane-to-air ratio, and for acetate-growth conditions, sodium acetate (≥ 99.5%; Fisher Scientific Company, Pittsburgh, PA) was added to the

final concentration of 1 mM, which was found to be the optimal concentration of acetate for *Methylocystis daltona* SB2 (data not shown).

DNA and RNA extraction *M. daltona* SB2 was initially grown on methane to the mid-exponential phase ($OD_{600\ nm}$ of 0.3 – 0.4). Cell suspensions were then flushed ten times with compressed air by vacuuming and refilling the gas in the headspace and diluted to $OD_{600\ nm} < 0.03$ in 50 ml of fresh media in a 250-ml Erlenmeyer flask. Methane or acetate was then added as described above. These cells were grown to the late-exponential phase and 1.5 ml aliquots collected from each flask. The aliquots were pelleted by centrifugation at 12,000 rpm for 10 min and stored in -80˚C.

Chromosomal DNA was extracted from these pellets by combining protocols used by Han and Semrau (2004) and Dedysh et al. (2005) to maximize extraction efficiency. Cell extraction buffer was prepared with hexadecyltrimethylammonium bromide (CTAB, Sigma, St. Louis, MO) as described by Dedysh et al (1998). One milliliter of cell extraction buffer and 500 g of 0.1 mm diameter zirconia/silica beads (BioSpec products, Bartlesville, OK) were added to the thawed pellets. Zirconia/silica beads were acid washed, rinsed with distilled deionized water, and oven-baked at 240˚C overnight prior to use. The cells were first lysed with bead beating in a Mini-Bead Beater (BioSpec products, Bartlesville, OK) at 4˚C six times for 30 s with 1 min interval in ice to avoid overheating of the samples (Han and Semrau, 2004). To increase the extraction efficiency, the cells then underwent three rapid freeze-and-thaw cycles by alternatively placing the cells in liquid nitrogen and a 65˚C water bath, making sure that the cells were completely frozen or thawed at each step (Dedysh et al., 1998). After the freeze-thaw

cycles, Proteinase K (Sigma, St. Louis, MO) was added to the concentration of 50 µg/ml and the mixture vigorously mixed by vortexing. 100 µl of 20% sodium dodecyl sulfate (Sigma, St. Louis, MO) was then added and mixed by gently inverting the tubes five times (Dedysh et al., 2005). The mixture was then incubated at 65˚C for two hours with gentle inversions every 10 – 15 min. After settling the glass beads, 0.9 ml of the supernatant was carefully transferred to 2-ml Phase Lock Gel tubes (5 PRIME, Gaithersburg, MD) for phenol-chloroform extraction (Dedysh et al,. 2005).

For extraction of total RNA, cell pellets were lysed as described by Han and Semrau (2004). The QIAGEN RNeasy Mini Kit (QIAGEN, Valencia, CA) was used to extract total RNA from the lysates according to kit protocols. The extracted total RNA (30 µl) was treated with 3 µl of RNase-free DNase I (Promega, Madison, WI) at 37˚C for 30 min. The reaction was stopped by adding 3 µl of Stop Solution provided with DNase I and heating the solution at 65˚C for 10 min. PCR reactions were then performed targeting *pmoA* and 16S rRNA genes using A189/mb661 primers (Costello and Lidstrom, 1999) and 27f-1492r primers (Lane, 1991), respectively, on DNase treated total RNA samples to check for any DNA contamination. The reaction mixture for reverse transcription was prepared by adding 1 µl of 3 µg/µl random primers (Invitrogen, Carlsbad, CA) and 2 µl of 2.5 mM dNTP Mix (Invitrogen, Carlsbad, CA) to 9 µl of the RNA solution treated with DNase I. Reverse transcription was then performed using SuperScript II Reverse Transcriptase (Invitrogen, Carlsbad, CA) according to the manufacturer instructions.

The products of DNA and total RNA extractions were checked with PCR and two-step RT-PCR with A189/mb661 primers targeting *pmoA* before proceeding to real-time quantitative PCR and RT-PCR analyses. PCR and RT-PCR amplifications were

performed with 50 µl of mixtures consisting of 5 µl of 10× PCR buffer, 1.5 µl of 50 mM $MgCl_2$, 1 µl of 1 mM dNTP mix, 20 pmoles of each primer, 2.5 units of Taq DNA polymerase (Invitrogen, Carlsbad, CA), and 50 ng of DNA template (Lee et al., 2009). Biometra TPersonal thermal cycler system (Labrepco Inc. Horsham, PA) was used with the following amplification program: denaturation at 94˚C for 3 min; 30 cycles of 94˚C for 30 s, 58˚C for 30 s, and 72˚C for 45 s; and a final extension at 72˚C for 5 min.

Real-time quantitative PCR and RT-PCR assays The primers for amplification of 16S rRNA and *pmoA* genes in the real-time quantitative PCR and RT-PCR analyses were designed *de novo* from the partial 16S rRNA (GU734136) and *pmoA* (GU734137) sequences of *M. daltona* SB2 using Primer3 program (Rozen and Skaletsky, 2000) to limit the amplicon length to less than 150 bp for more accurate quantification (Table III.1). Real-time quantitative PCR assays were performed with RealMasterMix SYBR ROX solution (5 Prime, Gaithersburg, MD) on a Mastercycler ep realplex apparatus (Eppendorf, Hamburg, Germany). PCR master mix was prepared by adding the forward and reverse primers to the final concentration of 0.2 mM in 1X RealMasterMix SYBR ROX solution prepared according to the instruction provided by the manufacturer. One microliter of genomic DNA or cDNA sample was added to 49 µl of PCR master mix pipetted into 96-well PCR plates (Eppendorf, Hamburg, Germany). For analysis of 16S rRNA, the cDNA samples were diluted by 100-fold, as the initial C_t value was out of the range of the standard calibration curve. After all samples were loaded, the 96-well plate was sealed with heat sealing film (Eppendorf, Hamburg, Germany). A three-step cycle with an initial denaturation step was used for assays with both 16S rRNA and *pmoA*

genes: initial denaturation at 94˚C for two minutes and 40 cycles of denaturation (94˚C for 15 s), annealing (58˚C for 20 s), and extension (68˚C for 30 s). All real-time quantitative PCR and RT-PCR analyses were done in triplicates. GraphPad Quickcals Software (GraphPad Software Inc., La Jolla, CA) was used for statistical comparison of the real-time PCR results.

Table III.1 *M. daltona* SB2 primers used in the real-time quantitative PCR and RT-PCR

Gene	Forward primer (5' – 3')	Reverse primer (5' – 3')	Amplicon length (bp)	T_A (˚C)
16S	AGTGGAACTGCGAG TGTAGAGGTG	ACCAGGGTATCTAA TCCTGTTTGCT	131	58
pmoA	GGATCAACCGCTAC GTCAACTTCT	AGCCGAGCGAACCA ACAATC	152	58

To generate a calibration curve relating the threshold cycle (C_t) and the copy number of the target genes, a dilution series of plasmid DNA with known copy number was prepared. 16S rRNA and *pmoA* genes were amplified with their respective primer sets (Table III.1) from the genomic DNA extracted from *M. daltona* SB2. The PCR products were then cloned with TOPO TA Cloning Kit (Invitrogen, Carlsbad, CA) into TOP10 ONESHOT competent cells (Invitrogen, Carlsbad, CA). The plasmids were extracted with QIAGEN Plasmid Mini Kit (QIAGEN, Valencia, CA) and the copy numbers of these plasmids were calculated from nucleic acid concentrations measured with NanoDrop 1000 spectrometer (Thermo Scientific, Wilmington, DE) and the molecular weight of the plasmids provided by the manufacturer. Dilution series ranging from 10^9 to 10^3 copies per microliter were generated by serial dilution.

Growth and degradation of chlorinated solvents The growth of *M. daltona* SB2 and degradation of the mixture of TCE, *t*-DCE, and VC were measured in three different conditions: methane, acetate, and acetate with acetylene (a selective inhibitor of both MMOs; Prior and Dalton, 1985). The method used previously by Lee et al. (2006) was slightly modified for these assays. For all three growth conditions, *M. daltona* SB2 was initially grown on methane to the mid-exponential phase ($OD_{600\ nm}$ of 0.3 – 0.4). This cell suspension was flushed with compressed air as described above to remove residual methane and diluted to $OD_{600\ nm} < 0.03$ in 50 ml of fresh media in 250-ml Erlenmeyer flask. For growth on methane, methane was added to the headspace to an air: methane ratio of 1:1 and the cells were grown back to an $OD_{600\ nm}$ of ~0.06. After the flask was flushed with compressed air as described earlier**,** five millimeter aliquots were transferred to serum vials specially fabricated to measure growth as $OD_{600\ nm}$ over time (Lee, et al., 2006). Teflon-coated butyl-rubber stoppers (National Scientific Co., Duluth, GA) were used to seal the serum vials. After the serum vials were securely sealed, 5 ml of the air in headspace was replaced with 5 ml of methane to ensure supply of sufficient methane for growth. For growth on acetate, 1 mM of sodium acetate (Im et al., unpublished) instead of methane was added to the diluted cell suspension in 250-ml Erlenmeyer flasks. The cells were grown back up to an $OD_{600\ nm}$ of ~ 0.06. After aliquots were transferred as described above, the serum vials were sealed without addition of any additional substrate. After sealed vials were prepared with growth substrates, TCE, *t*-DCE, and VC were injected to the vials to yield an aqueous concentration of 40 µM for each compound. To a subset of serum vials for acetate-grown cells, 0.35 ml of acetylene was injected to the headspace prior to the addition of chlorinated ethenes. To measure any leakage and

abiotic loss from the serum vials, negative controls were prepared with 5 ml of sterile NMS medium. All samples including the negative controls were prepared in duplicates. The growth of *M. daltona* SB2 was monitored until the cell growth was no longer observed. The initial and final concentration of TCE, *t*-DCE, and VC were measured with HP5890 Series II gas chromatograph equipped with a 75 m DB-624 column with 0.53 mm internal diameter (J&W Scientific Co.). 100 µl of headspace from each sample with chlorinated ethenes was manually injected to the gas chromatograph with a Precision Lok gas-tight syringe. TCE and *t*-DCE were detected with an electron capture detector (ECD) with injector, oven, and detector temperatures set to 160, 120, and 250 ˚C. VC was detected with a flame ionization detector (FID) with injector, oven, and detector temperatures set to 140, 120, and 250˚C, respectively.

III.3 Feasibility of atmospheric methane removal using methanotrophic biotrickling filters

The performance of the methane biotrickling filter was modeled using the methodology initially developed by Alonso et al (1997) for biotrickling filtration of volatile organics as shown in Figure III.1. Several assumptions were made in the model development. First, it was assumed that the biofilm develops uniformly around identical spherical packing materials. Second, a two-phase system was assumed with the gas phase in direct contact with the biofilm, or solid phase. A cylindrical reactor was modeled as a one-dimensional system by assuming no concentration gradients in the gas phase in the radial direction. Since growth of the biofilm occurs over much longer time periods than either mass transfer or methane oxidation rates (Alonso et al., 1997), a quasi steady state was assumed in developing the equations characterizing biofilter performance.

Furthermore, diffusion was assumed to be the only means of mass transfer through the biofilm and diffusion in axial direction was assumed to be negligible. Utilization of methane was modeled with Michaelis-Menten kinetics and methane was considered to be the sole growth limiting substrate. Despite its poor solubility in water (Fry et al., 1995) and low half saturation constant (van Bodegom et al., 2001) comparable to those of methane, oxygen was not considered to be a growth limiting factor in our model due to its abundance in the atmospheric air.

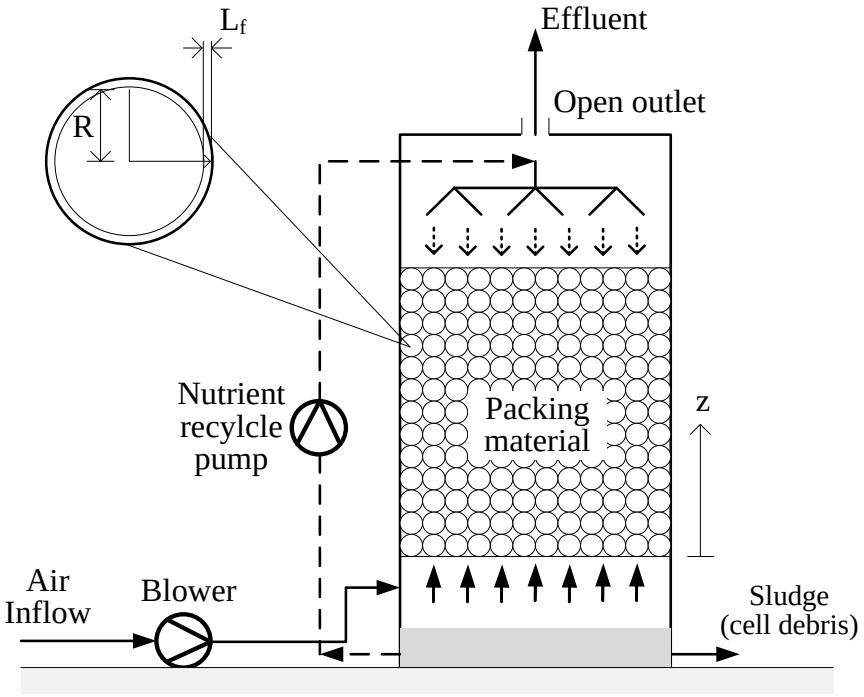

Figure III.1 Schematics of the proposed methane biotrickling filter and the mathematical model

With these assumptions, a differential equation was developed describing mass transfer across the biofilm surrounding a spherical packing material. A spherical coordinate system was used with the point of origin at the center of the sphere. In this

equation, methane diffusion into the biofilm was balanced with methane consumption by bacteria in the biofilm:

$$D_f\left[\frac{d^2C_f}{dr}+\frac{2}{r}\frac{dC_f}{dr}\right]=\frac{X_f V_{\max} C_f}{K_s+C_f} \qquad (1)$$

$$\left.\frac{dC_f}{dr}\right|_{r=R}=0 \qquad (2)$$

$$C_f\Big|_{r=R+L_f}=\frac{C_g}{H} \qquad (3)$$

where D_f is the diffusivity of methane in the biofilm, C_f is the methane concentration in the biofilm, r is the radial distance from the center of a spherical packing material. K_s is the half saturation constant, X_f is the bacterial density in the biofilm, V_{max} is the maximum rate of methane oxidation, R is the radius of the packing material, C_g is the concentration of methane in the gas phase, L_f is the biofilm thickness, and H is the Henry's constant for methane. Boundary conditions were defined from a no-flux condition at the surface of packing material ($r=R$) and concentration at the surface of biofilm equilibrated with methane concentration in gas phase at the respective axial position of the packing material.

The biotrickling filter was assumed to behave as an ideal plug flow reactor. The rate of methane removal from the gas phase is the same as the volumetric transfer into biofilm. Therefore, the mass balance equation in the biofilter can be written as:

$$\frac{dC_g}{dz}=-\frac{Ja_f}{u_0}=-\frac{J_f R_g T a_f}{PM_v u_o} \qquad (4)$$

where z is the distance from the air inlet, J is the flux of methane out of the gas phase, J_f is the flux of methane into the biofilm, a_f is biofilm-gas interfacial surface area per unit

bed volume, u_o is approach velocity of gas, R_g is the universal gas constant, T is temperature, P is system pressure, and M_v is molecular weight of methane.

The biofilm thickness, expressed as L_f in the above equations is not a constant value, since the population of methanotrophic bacteria in the biofilm changes over time upon growth and decay of microorganisms dictated by local methane concentrations. The biofilm thickness can be expressed as:

$$\frac{dL_f}{dt} X_f = \left(D_f \frac{dC_f}{dr}\bigg|_{r=R+L_f} \right) Y - L_f X_f b \qquad (5)$$

where Y is the yield coefficient and b is the specific combined shear/decay coefficient, which is a sum of the specific decay (death) coefficient and the specific shear rate. The specific decay coefficient is a constant property and the specific shear rate is a function of biofilm thickness (Rittman, 1982). The specific combined shear/decay coefficient can be written as:

$$b = b_s^0 \left(\frac{\varepsilon_0}{\varepsilon_f} \right)^2 + b_d \qquad (6)$$

where b_s^0 is the default shear rate coefficient, ε_0 is the clean packed-bed porosity, ε_f is the porosity of the bed with biofilm, and b_d is the specific decay coefficient.

a_f, the biofilm-gas interfacial surface area per unit bed volume can be calculated from geometrical relationships as done by Alonso et al (1997). If it is assumed that the biofilm develops uniformly around packing materials, the volume of the biofilm at the contact points must be excluded from the biofilm-gas interfacial surface area. Then, a_f can be expressed as:

$$a_f = \frac{3(1-\varepsilon_0)}{2R}\left(1+\frac{L_f}{R}\right)((2-n)\frac{L_f}{R}+2) \qquad (7)$$

where n is the number of packing materials in contact with a single packing material. Finally, the bed porosity with biofilm, ε_f, can be calculated in the same way:

$$\varepsilon_f = 1-(1-\varepsilon_0)\left[\left(1+\frac{L_f}{R}\right)^3 - \frac{n}{4}\left(\frac{L_f}{R}\right)^2\left(2\frac{L_f}{R}+3\right)\right] \qquad (8)$$

MATLAB was used to solve these equations to estimate overall methane removal by biofilters under a range of conditions, e.g., temperature, air flow rates, and methane concentration. Using the input parameters shown in Table III.2, methane flux into the biofilm at each incremental depth level was calculated by solving Equation (1) with boundary conditions Equation (2) and (3) with the numerical solver function for boundary value problems in MATLAB. Then, with this flux profile incremental changes in concentration of methane along biofilter depth, $\frac{dC}{dz}$, were calculated. This information is used to acquire the concentration profile along the depth of the biofilter, which in turn, is used in determination of $\frac{dL_f}{dt}$, the incremental change of biofilm depth over time. The model was run until steady-state was established in the system, i.e., there is no more growth or decay in the biofilm. The amount of methane removed in the incremental time at the steady state is calculated by multiplying the difference between inlet and outlet concentration with the air throughput. This steady-state methane removal rate was multiplied to give the total per-month removal rate.

Microbial kinetics parameters of *M. trichosporium* OB3b (NCIMB 11131) expressing pMMO and sMMO (Sipkema et al., 1998) were used as input parameters for

our study. We have also used the mathematical model to evaluate the possibility of using high affinity methanotrophs with parameters obtained by Dunfield et al. (1999). For the diffusivity constant of methane, we used the value reported by Knief et al. (2005). Characteristic parameters for biofilm development were acquired from Alonso et al (1997). Since the optimal temperature for growth and metabolism of *M. trichosporium* OB3b is 30℃ (Lee et al., 2006) and preliminary model results (data not shown) showed that performance increased with temperature, an operating temperature of 30℃ was selected for our analyses. To make cost-benefit analysis more convenient and credible, sizing of our reactor was based on an existing biofiltration system at Grupo Cydsa in Mexico, 3.66 m in diameter and 11.5 m in height (Cox and Deshusses, 2002).

For our cost-benefit analysis, estimates for capital and operating costs from Cox and Deshusses (2002) were used in conjunction with the performance estimates from the modeling results. Since the scale of the reactor in the model was identical to the Grupo Cydsa biofilter, it was assumed that the capital and operating cost of the reactor would be approximately the same as the costs associated with this system. The cost per metric ton of methane removed was then calculated by dividing the annualized total cost by the predicted biofilter performance. This was converted to cost per CO_2 equivalence considering that methane has a global warming potential 23 times that of CO_2.

Table III.2 Microbial and biofilter design parameters used in this study

Symbol	Parameter	Value	Reference
$V_{max\text{-}pMMO}$	Maximum rate of methane oxidation for pMMO-exressing cells (nmol·mg biomass^{-1}·s^{-1})	4.83	(Sipkema et al., 1998)
$K_{s\text{-}pMMO}$	Half-saturation constant of pMMO-expressing cells for methane (µM)	3.0	(Sipkema et al., 1998)
$V_{max\text{-}sMMO}$	Maximum rate of methane oxidation for sMMO-exressing cells (nmol·mg biomass^{-1}·s^{-1})	4.83	(Sipkema et al., 1998)
$K_{s\text{-}sMMO}$	Half-saturation constant of sMMO-expressing cells for methane (µM)	37	(Sipkema et al., 1998)
$V_{max\text{-}LR1}$	Maximum rate of methane oxidation for *Methylocystis* LR1 (nmol·mg biomass^{-1}·s^{-1})	0.125	(Dunfield et al., 1999)
$K_{s\text{-}LR1}$	Half-saturation constant *Methylocystis* LR1 for methane(µM)	0.305	(Dunfield et al., 1999)
b_d	Cell decay rate coefficient (1/d)	0.24	(Arcangeli and Arvin, 1999)
b_s^0	Default shear rate coefficient (1/d)	0.005	(Alonso et al., 1997)
X_f	Film bacterial density (mg/L)	17000	(Alonso et al., 1997)
D_f	CH_4 diffusivity in Biofilm (cm^2/s)	1.55E-05	(Hildebrand, 1969) (Alonso et al., 1997)
$L_{f,0}$	Initial biofilm depth (cm)	0.0042	(Alonso et al., 1997)
H	Henry's constant for methane ((mg/L)/(mg/L))	30	(Hartman, 1998)
ε_0	Empty bed porosity	0.34	(Alonso et al., 1997)
n	Number of spheres in contact with single sphere	10	(Alonso et al., 1997)

III.4 An assay for screening of microbial cultures for chakophore production

Chemicals Chrome azural S (CAS) and hexadecyltrimethylammonium bromide (HDTMA) were purchased from Sigma (St. Louis, MO). PIPES ($\geq$99%) and deferoxamine-B mesylate salt ($\geq$92.5%) derived from *Streptomyces pilosus* were purchased from Sigma (St. Louis, MO). Highest purity methane ($\geq$99.99%) for culturing of methanotrophs was purchased from Airgas Company. Methanobactin was extracted from *Methylosinus trichosporium* OB3b and purified following previously published procedures (Choi et al., 2005). All glassware was acid washed in 5 N HNO_3 overnight to remove adsorbed trace metals including copper and iron. Before use, acid-washed glassware was rinsed with distilled deionized water (>18 MΩ).

Microorganisms Four strains of methanotrophic bacteria were examined: *Methylococcus capsulatus* (Bath) (NCIMB 11132); *Methylosinus trichosporium* OB3B (NCIMB 11131); *Methylocystis parvus* OBBP (NCIMB 11129), and; *Methylomicrobium album* BG8 (NCIMB 11123). *M. capsulatus* Bath was grown at 45°C, while all other strains were incubated at 30°C.

Cu-CAS agar plate assay Nitrate mineral salts (NMS; Whittenbury et al., 1970) agar plates containing either 20 µM or 50 µM Cu^{2+} with CAS and HDTMA were made to examine the growth of methanotrophs and the ability of the chalkophore produced by these methanotrophs to bind copper in the presence of CAS. To ensure complete chelation of Cu^{2+} by CAS, these plates were made with concentrations of CAS and HDTMA slightly higher than copper. For 20 µM Cu-CAS agar plates, 50 ml of 0.42 mM

CAS solution was added to 10 ml of 2 mM $CuCl_2$ solution. This solution was then added to 40 ml of 1.05 mM HDTMA under stirring to give final concentrations of 0.2 mM, 0.21 mM, and 0.42 mM of Cu, CAS, and HDTMA, respectively. For 50 µM Cu-CAS agar plates, the final concentrations of Cu^{2+}, CAS, and HDTMA were 0.5 mM, 0.525 mM, and 1.050 mM, respectively. 450 ml of NMS was prepared separately in a 2-L Erlenmeyer flask. Concentrations of salts were adjusted for 500 ml NMS medium, considering later addition of Cu-CAS solution. The purple-colored Cu-CAS stock solution and NMS agar preparation were then autoclaved separately. After cooling to ~50°C, 50 ml of the purple-colored Cu-CAS solution was carefully pippetted into NMS agar medium. Vitamin (Lidstrom, 1988) and phosphate buffer solutions were then added to the medium as done for NMS agar medium. Interference of phosphate buffer in Cu-CAS NMS agar solution was not observed to be significant and buffering capacity was found to be sufficient to maintain a pH of 6.8. After the agar plates cooled and solidified, methanotrophic strains were inoculated onto these plates and incubated for 16 days.

Modified Cu-CAS Agar Plate Assay A modified version of the Cu-CAS assay for detection of chalkophores was performed as devised by Milagres et al. (1999) for the minimization of HDTMA toxicity. After 50 µM Cu-CAS agar plates were constructed as described above, half of the agar gel was carefully excised with a heat-sterilized razor. The empty space was then filled with sterilized NMS agar medium. Two different copper concentrations were used for the NMS medium, 1 µM or 10 µM as $CuCl_2$, to determine if chalkophore production varied with varying copper concentration. All four strains of methanotrophic cells were streaked onto the NMS half of the hybrid agar plate.

Hybrid CAS plates with iron were also constructed to determine if the tested strains, through the production of methanobactin, could bind iron in the presence of CAS. The procedure was identical to construction of 50 µM Cu-CAS plates as described above with the substitution of 5 mM of $FeCl_3$ prepared in 10 mM HCl for $CuCl_2$. The effect of iron in NMS agar on the ability of the tested strains to sequester iron was tested by omitting Fe-EDTA, a typical component of NMS medium, from a subset of the plates. For Fe-CAS agar, 30 g/L of PIPES was used in place of phosphate buffer, since interference of phosphate buffer in the complexation of Fe by CAS was found to be significant as previously mentioned by Schwyn and Neilands (1987). The pH of the Fe-CAS agar was adjusted to 6.8, the pK_a of PIPES, with 50% w/v NaOH solution before autoclaving.

Addition of purified chalkophores and siderophores onto Cu-CAS and Fe-CAS plates 50 mM solutions of purified methanobactin from *M. trichosporium* OB3b and the siderophore, deferoxamine-B from *Streptomyces pilosus*, were prepared using distilled deionized water. 50 µl of each solution was then spotted onto both 50 µM Cu-CAS and Fe-CAS plates. Color changes were monitored over 12 hours to determine if methanobactin and deferoxamine-B could bind both iron and copper in the presence of CAS.

CHAPTER IV

Measurement and Modeling of Multiple Substrate Oxidation by Methanotrophs at 20˚C

IV.1 Introduction

Previous studies have revealed that both pMMO- and sMMO-expressing methanotrophs can degrade chlorinated hydrocarbons at significant rates (Lontoh and Semrau, 1998; Han et al., 1999; Lee et al., 2006). Although sMMO was generally perceived as a more effective enzyme for degrading chlorinated hydrocarbons due to its broader substrate range (Hanson and Hanson, 1996; van Hylckama Vlieg et al., 1996; Han et al., 1999), competitive inhibition of MMO activity and rapid build-up of intermediates detrimental to whole-cell activity were found to inhibit methanotrophic growth more significantly under sMMO-expressing conditions (Lee et al., 2006). In pMMO expressing cells, this inhibition effect was less profound, likely due mainly to the greater specificity of these cells for methane and slower degradation rates. As a result, pMMO-expressing *M. trichosporium* OB3b cells were found to be more successful at degrading chlorinated hydrocarbon at concentrations higher than 50 μM over prolonged time periods, despite having slower reaction kinetics (Lee et al., 2006).

This previous study revealed a new perspective of methanotrophic degradation of chlorinated ethenes, but it did not consider that growth temperature can and will affect microbial processes and activity. For example, temperature changes are known to

modulate transcription (Gadgil et al., 2005), as well as the activity of expressed enzymes (Morii and Kasama, 2004). The rate of diffusion through the membrane can also be altered because membrane fluidity is known to be affected by temperature (Chu-Ky et al., 2005). Therefore, the results from the previous study may not accurately reflect *in situ* biodegradation by methanotrophs as average groundwater temperatures of contaminated sites in the United States typically range from 13 to 25 ℃ (Wiedemeier et al., 1999).

Because sMMO and pMMO are known to have disparate structures and are differentially transcribed, changes in growth temperature may significantly alter the ability of cells expressing sMMO or pMMO to degrade pollutant(s). Despite its possible significance in pollutant degradation, the effect of temperature on whole-cell kinetics of methanotrophs has not yet been extensively studied, included for the primary substrate, methane. Therefore, we decided to examine mixed pollutant degradation by methanotrophs at 20℃, to better represent *in situ* conditions and to determine what, if any, effect lower growth temperatures had on the ability of methanotrophs to degrade methane and chlorinated solvents. In particular, it was our hypothesis that although lower growth temperature would reduce the growth and activity of both sMMO- and pMMO-expressing cells, pMMO-expressing cells would still be more effective than sMMO-expressing cells at degrading pollutant mixtures.

IV.2 Results

IV.2.1 Kinetics of methane oxidation and chlorinated ethene degradation at 20˚C

For *M. trichosporium* OB3b grown at 20℃ and expressing pMMO, both the V_{max} and V_{max}/K_s values for methane were significantly greater than those for VC, *t*-DCE, and

TCE degradation (Table IV.1). For the same cell expressing sMMO, however, the V_{max} value for methane uptake was considerably smaller than that measured for chlorinated ethenes. Furthermore, for *M. trichosporium* OB3b expressing sMMO, the V_{max}/K_s value for methane uptake was of the same order of magnitude as that measured for VC, *t*-DCE, and TCE degradation. The pseudo-first-order rate constant for methane uptake by *M. trichosporium* OB3b expressing pMMO, however, was one to two orders of magnitude greater than that measured for degradation of the chlorinated ethenes. These results are similar to that found for the same cell grown at 30°C, i.e. both the V_{max} and V_{max}/K_s values of methane oxidation by pMMO-expressing cells were greater than that measured for different chlorinated ethenes, but sMMO-expressing cells degraded chlorinated solvents at rates comparable to that found for methane (Oldenhuis et al., 1991; Lee et al., 2006).

Table IV.1 Michaelis-Menten kinetics of chlorinated ethylene degradation by *Methylosinus trichosporium* OB3b at 20°C expressing either sMMO or pMMO. The numbers in parentheses are SDs of triplicate samples

Expressed MMO	Substrate	V_{max} (nmol·min^{-1}·mg protein^{-1})	K_s (μM)	V_{max} / K_s (ml · min^{-1}·mg protein^{-1})
pMMO	CH_4	149 (5)	9.4 (1.2)	16
	VC	35 (8)	31 (16)	1.1
	t-DCE	22 (0.8)	55 (5)	0.4
	TCE	1.9 (0.4)	65 (24)	0.029
sMMO	CH_4	83 (3)	23 (4)	3.6
	VC	1370 (343)	485 (213)	2.8
	t-DCE	184 (8)	117 (16)	1.6
	TCE	116 (5)	149 (11)	0.78

IV.2.2 The growth of *M. trichosporium* OB3b expressing either sMMO or pMMO at 20˚C in the presence/ absence of chlorinated ethenes

The growth of *M. trichosporium* OB3b expressing either sMMO or pMMO in the presence of varying equimolar concentrations of VC, *t*-DCE, and TCE was examined at 20 ℃ as shown in Table IV.2. The relative growth rate, μ/μ_0, i.e., the ratio of the specific growth rate in the presence of chlorinated ethenes to that in the absence of these cometabolites, was used to determine the effect of these chlorinated ethenes on methanotrophic growth. It is evident from Table IV.2 that an increase in equimolar concentration of the chlorinated ethenes was coupled with a decrease in the relative growth rate of both pMMO- and sMMO-expressing cells. The growth of *M. trichosporium* OB3b expressing sMMO, however, decreased much more significantly in the presence of chlorinated ethenes than the same cell expressing pMMO. Notably, there was no growth observed for sMMO-expressing cells when the equimolar concentrations of chlorinated ethenes were greater than 50 µM, whereas the relative growth rate of pMMO-expressing cells was relatively high (≥ 0.25) at concentrations higher than 50 µM.

Table IV.2 Growth of *M. trichosporium* OB3b at 20℃ expressing either sMMO or pMMO in the presence of varying concentrations of mixture of TCE, *t*-DCE, and VC

Enzyme	Substrate (s)	μ (h^{-1})	μ/μ_0	Max OD_{600nm}
pMMO	CH_4	0.024 (0.0004)	1.0	0.77
	CH_4+10 µM VC, *t*-DCE and TCE	0.017 (0.0004)	0.71	0.53
	CH_4+30 µM VC, *t*-DCE and TCE	0.014 (0.0003)	0.58	0.45
	CH_4+50 µM VC, *t*-DCE and TCE	0.010 (0.0002)	0.42	0.31
	CH_4+100 µM VC, *t*-DCE and TCE	0.006 (0.0002)	0.25	0.21
sMMO	CH_4	0.027 (0.0005)	1.0	0.64
	CH_4+10 µM VC, *t*-DCE and TCE	0.016 (0.0008)	0.59	0.58
	CH_4+30 µM VC, *t*-DCE and TCE	0.0084 (0.0003)	0.31	0.32
	CH_4+50 µM VC, *t*-DCE and TCE	0	0	0.08
	CH_4+100 µM VC, *t*-DCE and TCE	0	0	0.08

Along with the growth experiments, the total amounts of VC, *t*-DCE, and TCE degraded during growth were measured as shown in Table IV.3. For *M. trichosporium* expressing sMMO, equimolar mixtures of 10 and 30 µM TCE, t-DCE, and VC were completely degraded. However, at equimolar concentrations of 50 µM and greater, little degradation of *t*-DCE and TCE was observed and only ~ 20% of initial amount of VC was removed. An abiotic loss of 4–5% was measured for all chlorinated ethenes in negative controls, (data not shown), indicating the losses of *t*-DCE and TCE at high initial concentrations were not due to microbial activity. It is likely that the observed loss of VC was due to the initial activity of the inoculum used to seed these experiments as such loss was not observed for negative control samples. The inhibition of pollutant degradation was more severe at 20℃ than at 30℃, as some growth and chlorinated ethene degradation was observed at higher concentrations of chlorinated ethenes at 30℃ (Lee et al., 2006).

Table IV.3 Extent of mixed chlorinated ethene degradation by *Methylosinus trichosporium* OB3b grown at 20℃ expressing either sMMO or pMMO

Enzyme	Substrate (s)	% Pollutant degraded (range)			Time (h)
		VC	*t*-DCE	TCE	
pMMO	CH_4				
	CH_4+10 µM VC, *t*-DCE and TCE	94 (1)	91 (1)	48 (13)	160
	CH_4+30 µM VC, *t*-DCE and TCE	94 (3)	95 (1)	52 (0)	175
	CH_4+50 µM VC, *t*-DCE and TCE	69 (0)	84 (1)	45 (2)	145
	CH_4+100 µM VC, *t*-DCE and TCE	45 (0)	42 (7)	29 (7)	185
sMMO	CH_4				
	CH_4+10 µM VC, *t*-DCE and TCE	100 (0)	100 (0)	100 (0)	150
	CH_4+30 µM VC, *t*-DCE and TCE	100 (0)	100 (0)	98 (3)	230
	CH_4+50 µM VC, *t*-DCE and TCE	19 (2)	5 (2)	8 (4)	115
	CH_4+100 µM VC, *t*-DCE and TCE	20 (4)	2 (4)	3 (5)	115

M. trichosporium OB3b expressing pMMO was not as effective as sMMO-expressing cells degrading chlorinated ethenes at equimolar concentrations lower than 30 µM, especially for TCE. However, at higher equimolar concentrations, *M. trichosporium* OB3b expressing pMMO continued to grow and thus, degrade the chlorinated ethenes to a greater extent than the same cell expressing sMMO (Table IV.3). Thus, bioremediation of sites that are highly contaminated with chlorinated ethenes might not be feasible by stimulating methane-oxidizing bacteria expressing sMMO. In many sites contaminated with chlorinated ethenes, these pollutants are found at concentrations exceeding 50 µM (Wiedemeier et al., 1999). Therefore a new approach inducing pMMO expression should be considered for methanotrophic bioremediation of such sites.

IV.2.3 Calculation of Δ and validation of the Δ model

A model was developed earlier to quantify the effect of competing pollutants to turnover of the growth substrate (Lee et al., 2006). In this model, kinetic parameters for turnover of growth substrate and competing substrate were used to calculate a dimensionless number Δ. Using the kinetic parameters measured at 20°C (Table IV.1), Δ values were calculated to determine if this model qualitatively described the effect of mixed chlorinated solvents on growth and biodegradation capacity of *M. trichosporium* OB3b when grown at 20°C. In calculating Δ values, the maximum rate of methane degradation was assumed. As can be seen in Figure IV.1, the Δ values for *M. trichosporium* OB3b expressing sMMO decreased much more rapidly with increasing pollutant concentration than for pMMO-expressing cells. Even in the presence of relatively high concentrations (≥100 µM) of chlorinated ethenes, a relatively high

positive Δ value was predicted for *M. trichosporium* OB3b expressing pMMO. For sMMO-expressing cells, however, negative Δ values were predicted at a relatively low concentrations (~20 μM), indicating that the rate of chlorinated ethane degradation was faster than the methane oxidation.

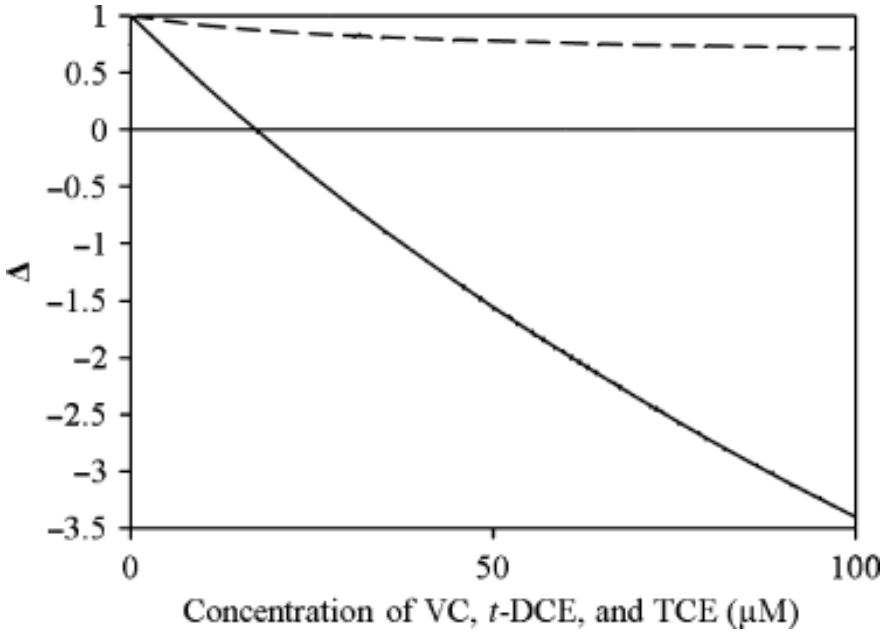

Figure IV.1 The specificity of *M. trichosporium* OB3b expressing either pMMO (dashed line) or sMMO (solid line) for methane when the cells are grown at 20℃ and in presence of TCE, *t*-DCE, and VC as estimated using the Δ model

A semi-quantitative relationship was observed between the Δ values and the relative growth rates of *M. trichosporium* OB3b expressing either pMMO or sMMO (Figure IV.1 and Table IV.3). Specifically, the Δ value appears to be a good indicator in estimating the severity of growth inhibition by the presence of chlorinated ethenes, as conditions with Δ values below -1.5 resulted in no growth at 20℃ as was also observed at 30℃ (Lee et al., 2006). The more pronounced negative impact of the chlorinated

ethenes at 20℃ can also be explained with this model, as Δ reached -1.5 at 100 μM at 30℃. As such Δ model may be applied for *in situ* bioremediation efforts to estimate the effectiveness of methanotrophic biodegradation of various pollutants.

IV.3 Discussion

The findings here extend the conclusions of earlier work (Lee et al., 2006) that methanotrophs expressing pMMO have a distinct advantage over those cells expressing sMMO in mixed waste systems and may be more numerous, particularly at elevated concentrations of cometabolites. Again, the 'tortoise', or pMMO-expressing cell, by selectively binding its growth substrate, methane, is ultimately able to degrade cometabolites to a greater extent than the 'hare', or sMMO-expressing cell, that exhausts itself from its rapid, yet counter-productive oxidation of cometabolites.

The data collected here raise an interesting question that is still unresolved – under what conditions do sMMO expressing cells have a selective advantage over pMMO expressing cells, particularly in pristine environments? It is well known that copper strongly regulates sMMO/pMMO expression by those cells that can express both forms (Stanley et al., 1983), and copper positively affects the activity of pMMO-expressing cells (Lontoh and Semrau, 1998). From the data collected here when juxtaposed with earlier work (Oldenhuis et al., 1991; Lee et al., 2006) it appears sMMO expressing cells have a selective growth advantage at elevated temperatures (i.e., at 30℃) as maximal methane uptake rates are greater than for pMMO-expressing cells, but the inverse appears to be true at 20℃. Future work should examine in more detail how temperature affects MMO expression, particularly by mixed methanotrophic cultures.

Such information may provide insights as to why some, but not all, methanotrophs can express sMMO, as well as help provide strategies to control the composition and activity of mixed methanotrophic cultures.

CHAPTER V

Expression of pMMO by *Methylocystis daltona* SB2 Grown on Acetate and Its Implications in Degradation of Chlorinated Ethenes

V.1 Introduction

Until recently, methanotrophs were considered to be obligately methanotrophic or methylotrophic, i.e., incapable of growth on multi-carbon substrates. The discovery of the first facultatively methanotrophic bacteria, *Methylocella silvestris* BL2, suggested that there might be more diverse groups of methane-oxidizing bacteria capable of growth on multi-carbon substrates (Dedysh et al., 2005). As a result of continuous effort to isolate and identify such microorganisms, the Dunfield research group and our research group have succeeded in identifying two more facultatively methanotrophic strains that are under different phylogenetic groups and have divergent characteristics (Dunfield et al., 2010; Im et al., submitted). These findings suggested that the facultative methanotrophs may be more widely distributed in the environment than previously thought. Therefore we made a hypothesis that if these cells are, indeed, present in diverse environment and are able to express and utilize either form of MMO, it might be possible to improve aerobic bioremediation procedures involving methanotrophs.

Unfortunately, the first facultatively methanotrophic strain ever to be discovered and analyzed, *M. silvestris* BL2, lacked the ability to constitutively express sMMO when acetate was present in the medium (Theisen et al., 2005). RT-PCR of *pmoA* with genomic DNA of *M. daltona* SB2, however, found constitutive expression in the presence of

actetate without methane (Im et al., unpublished). As the ability of pMMO-expressing methanotrophs to degrade chlorinated ethenes has been verified in the previous studies in our lab, we hypothesized that *M. daltona* SB2 may be able to degrade these priority pollutants in complete absence of methane. In an effort to verify this hypothesis, we have used real-time quantitative RT-PCR technique to first verify the expression of pMMO upon growth on acetate and quantify the expression of pMMO in acetate-growth conditions as compared to the methane-growth conditions. To verify the presence and the activity of pMMO, we also examined the long-term degradation of mixture of TCE, *trans*-DCE, and VC under acetate-growth conditions. After initial confirmation of degradation activity, a selective inhibitor of pMMO, acetylene, was used to verify that pMMO was responsible for the observed degradation.

V.2 Result

V.2.1 Real-time quantitative RT-PCR Analyses

The two-step RT-PCR of *M. daltona* SB2 grown on acetate revealed the presence of *pmoA* mRNA in the extracted RNA (Figure V.1). Real-time quantitative RT-PCR was performed to confirm the expression of pMMO in *M. daltona* SB2 grown on acetate and quantify the level of pMMO expression for cells grown with acetate as compared to cells grown with methane. Absolute quantification relying solely on the copy numbers of *pmoA* transcripts is subject to a broad margin of error that might originate from sample preparation. Also, absolute quantification was deemed inappropriate for the purpose of this experiment since *M. daltona* SB2 exhibits different growth patterns in methane- and acetate-growth conditions and thus, is expected to have varied activities under these

different conditions. Therefore, the copy numbers of *pmoA* and 16S rRNA transcripts were first normalized with the copy numbers of the respective genes in the genomic DNA. The ratio of 16S rRNA transcripts to 16S rRNA gene copy number was used as a surrogate for the overall transcription activity for normalizing *pmoA* expression under different conditions and growth stages.

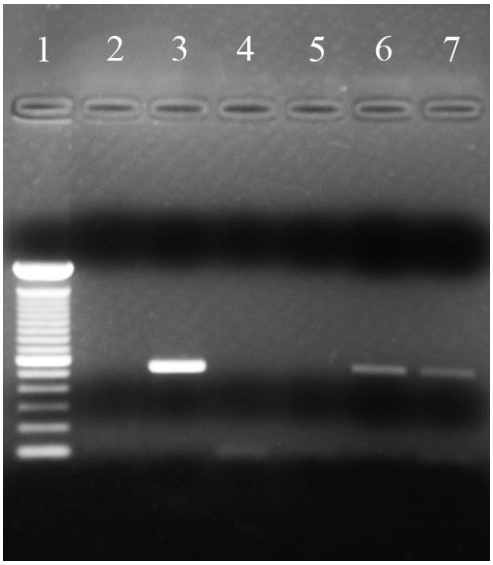

Figure V.1 PCR amplification of cDNA prepared from duplicate samples of *M. daltona* SB2 grown with 1 mM acetate as the sole substrate. 50 ng of each DNA sample was amplified with A189/mb661 primers (Costello and Lidstrom, 1999). *Shewanella oneidensis* MR-1 DNA was used as the negative control (Lane 2) and the genomic DNA of *M. daltona* SB2 was used as the positive control (Lane 3). Lane 4 and 5 are PCR amplification of mRNA samples treated with DNaseI before reverse transcription. Lane 6 and 7 are RT-PCR amplification of the cDNA samples from reverse transcription. Lane 1: 100 bp DNA ladder (Invitrogen, Carlsbad, CA)

16S rRNA expression levels were quantified first. The copy numbers of 16s rRNA in genomic DNA and transcripts of *M. daltona* SB2 grown on methane and acetate were calculated from the measured C_t values using a calibration curve generated for 16S rRNA using five plasmid preparations with known copy numbers ranging from 10^4 to 10^8

per microliter. The ratios of the copy number of 16S rRNA transcripts to the copy number of 16S rRNA in genomic DNA remained relatively constant regardless of either stage of growth or the growth substrate, save for a two-fold decrease in the sample collected at late-exponential phase in acetate-growth conditions as compared to the sample collected at mid-exponential phase in acetate-growth condition (significantly different at 97% confidence interval, Table V.1). This result indicated that cell activity is reduced as *M. daltona* SB2 approaches the stationary phase when grown on acetate while the same trend does not happen when grown on methane. In general, however, the small magnitudes of differences in transcription activity were somewhat unexpected, as in the absence of chlorinated ethenes, the specific growth rate on acetate was approximately one tenth of the specific growth rate on methane (Table V.2).

Table V.1 Expression level of *pmoA* and 16S rRNA genes as measured by the real-time quantitative RT-PCR and normalized by gene copy numbers. The numbers in parenthesis are the standard errors calculated using propagation of error

Substrate	Phase	$OD_{600\ nm}$	$\frac{pmoA\ transcript}{pmoA\ gene}$	$\frac{16S\ transcript}{16S\ gene}$	$\frac{pmoA}{16S}$
CH_4	Early-exp	0.15	4.09 (0.30)	1940 (435)	2.11×10^{-3} (4.96×10^{-4})
	Mid-exp	0.30	2.88 (0.28)	1410 (405)	2.06×10^{-3} (6.23×10^{-4})
	Late-exp	0.43	2.84 (0.64)	1680 (311)	1.69×10^{-3} (4.89×10^{-4})
CH_3COOH	Mid-exp	0.11	1.84×10^{-1} (2.78×10^{-2})	1270 (322)	1.45×10^{-4} (4.28×10^{-5})
	Late-exp	0.15	2.71×10^{-2} (5.43×10^{-3})	606 (129)	4.48×10^{-5} (1.31×10^{-5})

The copy numbers of *pmoA* in genomic DNA and transcripts of *M. daltona* SB2 grown on methane and acetate were calculated from the measured C_t values using a

calibration curve generated for *pmoA* using six plasmid preparations with known copy numbers ranging from 10^3 to 10^8 per microliter. At three different stages of growth for cells grown on methane [early-exponential phase ($OD_{600\ nm}$ = 0.15), mid-exponential phase ($OD_{600\ nm}$ = 0.30) and late-exponential phase ($OD_{600\ nm}$ = 0.45)], the quantities of *pmoA* transcripts normalized with the copy number of *pmoA* in chromosomal DNA were fairly constant, and statistically similar (Table V.1). The same trend was maintained after these values were normalized with the respective quantities of 16S rRNA. This result indicated that the transcription of *pmoA* gene remained unchanged regardless of the stage of growth when *M. daltona* SB2 were grown on methane. Expression of *pmoA* was detected in acetate-grown *M. daltona* SB2 at both mid-exponential phase ($OD_{600\ nm}$ = 0.11) and late-exponential phase ($OD_{600\ nm}$ = 0.15) but the quantity of expression was not constant for the samples extracted at different phases, i.e., the quantity of *pmoA* transcript was eight-fold lower in the late-exponential phase than the mid-exponential phase (significantly different at at 99% confidence interval). Normalization with the overall transcription activity, i.e., the quantity of 16S rRNA transcript, reduced this difference to a three-fold difference but still, the change was statistically different (significantly different at 99% confidence interval).

pmoA expression levels of *M. daltona* SB2 grown on methane and the same cells grown on acetate were then compared for the samples taken at the mid-exponential phase. The copy number of *pmoA* transcripts in the cells grown on acetate, as normalized by the copy number of *pmoA* genes in the chromosomal DNA, was reduced by ~15-fold with respect to the cells grown on methane (Table V.1). The significant decrease in *pmoA* expression (significantly different at 99% confidence interval) was not a result of general

decrease in overall cell activity since normalization with 16S rRNA expression did not reduce this gap.

V.2.2 Growth and chlorinated ethene degradation

When grown on methane, growth of *M. daltona* SB2 was inhibited in the presence of the equimolar mixture of TCE, *t*-DCE, and VC (Figure V.2A). The specific growth rate was 6.0×10^{-2} h^{-1} in the absence of chlorinated ethenes, and decreased to 3.0×10^{-2} h^{-1} in the presence of 40 μM each of TCE, *t*-DCE, and VC (Table V.2). The maximum cell concentration, however, was unaffected by the addition TCE, *t*-DCE, and VC. After 97.5 h of growth on methane at 30˚C, *M. daltona* SB2 completely degraded *t*-DCE and VC and removed ~40% of TCE (Table V.3). This result was comparable to the previous results obtained with another type II methanotroph, *M. trichosporium* OB3b expressing pMMO, i.e., in the presence of 20 μM of copper (Lee et al., 2006). When *M. daltona* SB2 was grown on acetate with 10 μM copper, no inhibition of growth was observed during the initial phase of growth (0 – 3 days). Later, however, cell growth halted in the presence of chlorinated ethenes at an $OD_{600\ nm}$ of ~0.08 (Figure V.2B). Although the cells did not grow to high concentrations in the presence of the chlorinated ethenes, significant removal of chlorinated ethenes, especially *t*-DCE and VC, was observed. As can be seen in Table V.3, ~30% of *t*-DCE and VC was removed during the nine days of incubation. Removal of TCE was not significantly distinguishable from abiotic loss (Table V.3).

Table V.2 Growth of *M. daltona* SB2 under growth on methane and acetate either in presence or absence of acetylene. The numbers in parentheses are standard errors of duplicate samples

Substrate (s)	μ (h^{-1})	μ / μ_0	Max OD_{600}
CH_4	0.057 (0.002)	1.0	0.71 (0.01)
CH_4 + TCE, *t*-DCE, and VC	0.030 (0.0005)	0.52	0.70 (0.01)
CH_3COOH	0.0055 (0.0004)	1.0	0.13 (0.007)
CH_3COOH + TCE, *t*-DCE, and VC	0.0056 (0.0008)	1.02	0.084 (0.001)
CH_3COOH + C_2H_2	0.0055 (0.0005)	1.0	0.114 (0.002)
CH_3COOH + C_2H_2 + TCE, *t*-DCE, and VC	0.0057 (0.0004)	1.04	0.121 (0.001)

Acetylene, an effective inhibitor of pMMO, was added to *M. daltona* SB2 cells grown on acetate in the absence and presence of chlorinated ethenes to confirm that the degradation was due to the presence of active pMMO. As can be seen in Figure V.2B, when acetylene was added to the headspace of the serum vials, the maximum growth of *M. daltona* SB2, as well as the initial specific growth rate, was unaffected by the presence of the chlorinated ethenes. No degradation of chlorinated ethenes was observed for these samples (Table V.3), indicating that the degradation of *t*-DCE and VC was catalyzed by pMMO in *M. daltona* SB2.

Table V.3 Degradation of *M. daltona* SB2 under growth on methane and acetate in the presence and absence of acetylene. The numbers in parentheses are the range of duplicate samples

	% Chlorinated ethene degraded (range)		
Substrates (s)	TCE	*t*-DCE	VC
CH_4 + TCE, *t*-DCE, and VC	41 (11)	100 (0)	100 (0)
CH_3COO^- + TCE, *t*-DCE, and VC	6.5 (1)	30 (3)	30 (5)
CH_3COO^- + C_2H_2 + TCE, *t*-DCE, and VC	3.3 (0)	0 (0)	0 (0)
Abiotic loss	5.2 (1)	0 (0)	1.8 (1)

A.

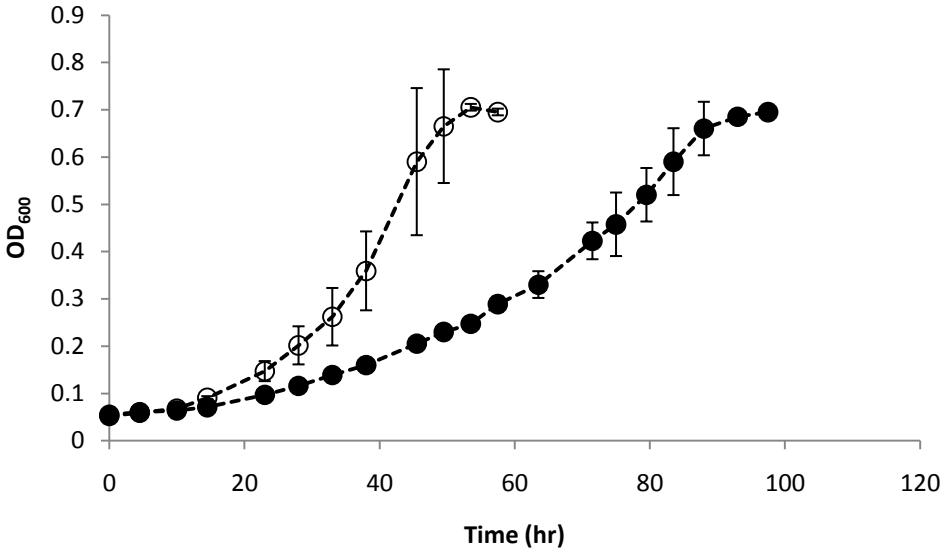

B.

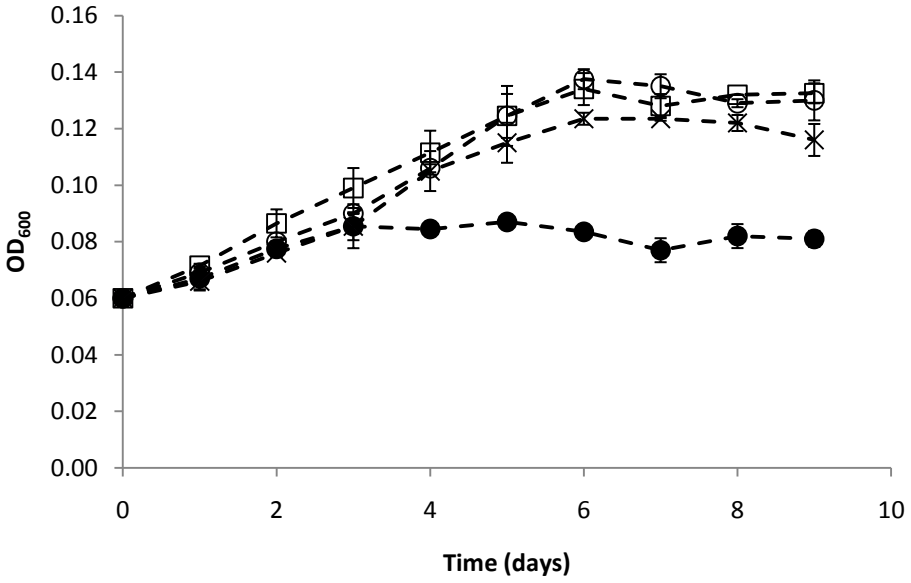

Figure V.2 Growth of *M. daltona* SB2 solely on either (A) methane (14.9% v/v in the headspace) or (B) acetate (1 mM) in the presence/absence of equimolar concentration (40 µM) of trichloroethylene (TCE), *trans*-dichloroethylene (*t*-DCE), and vinyl chloride (VC) and/or acetylene (1% v/v in the headspace). Symbols in (A): ○ – methane only (positive control), ● – methane and 40 µM each of TCE, *t*-DCE, and VC. Symbols in (B): ○ – acetate only (positive control), ● – acetate and 40 µM each of TCE, *t*-DCE, and VC, □ – acetate, and acetylene, × – acetate, acetylene, and 40 µM each of TCE, *t*-DCE, and VC

V.3 Discussion

Methanotrophs can effectively degrade chlorinated ethenes including TCE, *t*-DCE, and VC through the action of both forms of MMO. The rates of these reactions are, in fact, greater than most known microbial reactions (Van Hylckama Vlieg et al., 2001). Since it was initially believed that methanotrophs are obligately methanotrophic, a continuous supply of methane was deemed to be necessary to stimulate biodegradation mediated by MMOs. This can act as a significant drawback given the poor solubility of methane in aqueous solutions and slow mass-transfer rates. The recent discovery of facultative methanotrophs (Dedysh et al., 2005; Dunfield et al., 2010; Im et al., unpublished), however, indicates that methanotrophic degradation of chlorinated ethenes without methane might be possible, provided that either form of methane monooxygenase is constitutively expressed and remains active in the presence of the alternative growth substrate, e.g., acetate. Chlorinated ethene degradation utilizing these facultative methanotrophs in the absence of methane, if possible, may be advantageous in bioremediation given the greater solubility of the alternative growth substrates (acetate and ethanol). It is well-known that chlorinated ethenes compete with methane for binding to both forms of MMO. When grown on secondary substrates, facultative methanotrophs, however, do not rely on either MMO for growth (Im et al., submitted; Dunfield et al., 2010; Dedysh et al., 2005). Therefore, it was expected that the presence of chlorinated ethenes would not affect the growth of *M. daltona* SB2 on acetate.

The experimental results from RT-PCR indicated that pMMO is constitutively expressed in *M. daltona* SB2 in the absence of methane, when its alternate substrate, acetate, was present. This was, in fact, the first time that expression of either methane

monooxygenase was observed for facultative methanotrophs grown on multi-carbon substrates, as sMMO expression in *M. silvestris* BL2 was found to be repressed in the presence of acetate (Theisen et al., 2005) and *M. aurea* KYG has yet been examined for pMMO expression under acetate-growth conditions. The real-time quantitative RT-PCR results presented in this study confirmed that pMMO was, indeed, constitutively expressed regardless of the presence or absence of methane. Under growth on methane, the level of *pmoA* expression normalized by quantity of 16S rRNA transcripts was relatively constant at all examined growth stages with reasonable range of variability. This result agreed with the previous study on the change in *pmoA* expression at different stages of growth (Han and Semrau, 2004). Their competitive RT-PCR analysis differed from this study in that *M. trichosporium* OB3b was examined and the rate of CH_4 uptake was used to normalize the quantity of *pmoA* expression to the cell activities. The quantity of *pmoA* mRNA, however, had a linear relationship with the cell activity regardless of the examined growth stages, i.e., exponential growth phase, stationary phase, and death phase, consistent with the results from this study.

pmoA expression decreased significantly when grown on acetate as compared to growth on methane, although such expression was measurable. The level of *pmoA* expression in *M. daltona* SB2 grown on acetate was approximately 10- to 15-fold lower than in the same cells grown on methane. Another three-fold decrease in *pmoA* transcription amid an overall decrease in transcription activity for cells grown on acetate was observed as these cells approached the stationary phase. Carryover of *pmoA* mRNA is very unlikely due to the long incubation time in absence of methane. The copper-to-biomass ratio is known to regulate *pmoA* expression (Murrell et al., 2000b), and it is

possible, from the results presented here, that positive regulation by methane may be another mechanism regulating the expression of pMMO in *M. daltona* SB2. Such substrate stimulation of transcription has been observed for the expression of hydroxylamine oxidoreductase (HAO) genes in *Methylococcus capsulatus* Bath (Poret-Peterson et al., 2008). The magnitude of shift in *pmoA* expression level presented here was also comparable to the magnitude of change in gene expression of *pmoA* when the copper concentration was varied from 1 μM to 59 μM (Choi et al., 2003). This might be an indication that the copper regulation and the hypothesized substrate regulation might involve a common mechanism downstream of initial signal reception.

The chlorinated ethene degradation experiments presented here provided evidence that not only were *pmo* genes transcribed, but that pMMO was active in *M. daltona* SB2 grown on acetate. Such cells were able to remove a significant portion of the added chlorinated ethenes. The complete loss of such degradation upon addition of acetylene, a selective inhibitor of pMMO, further indicates that the degradation activity was mediated by pMMO in these cells. Growth on acetate was much slower than growth on methane regardless of the addition of the chlorinated ethenes, indicating lower overall cellular activity in acetate-grown cells. The chlorinated ethenes themselves had little effect on *M. daltona* SB2, as the growth rate of *M. daltona* SB2 with added acetylene was not hampered by the presence of the chlorinated ethenes. However, the growth of these cells was reduced in the presence of chlorinated solvents but absence of acetylene. Since the acetate-utilizing catabolic and anabolic pathways are independent of the pathway of methane metabolism, these results provide evidence of the importance of intermediate/product toxicity in affecting overall degradation rates.

This study has revealed the expression and activity of pMMO in a facultative methanotroph grown on acetate in the absence of methane. This information will be critical in developing more effective and efficient *in situ* biodegradation strategy with methanotrophic bacteria. Knowing that at least some subgroups of methanotrophs can grow and express active MMOs in absence of methane, more sophisticated bioremediation strategies such as periodic addition of methane along with continuous addition of acetate might prove promising. More research is needed, however, to apply these facultative methantotrophs to actual remediation practices. For example, developing the means to assess the abundance of these cells *in situ*, and finding ways to selectively stimulate growth of these cells and maintain high level of pMMO expression are among the issues that need to be examined.

CHAPTER VI

Feasibility of Atmospheric Methane Removal Using Methanotrophic Biotrickling Filters

VI.1 Introduction

Methane is a potent greenhouse gas that counts for ~15% of total contribution to greenhouse effect, despite of its low concentration in atmosphere (Rodhe, 1990). In both natural and anthropogenic environments, methanotrophs have played a major role in mitigating emission of methane to atmosphere (King, 1992). Along with the study on natural attenuation of methane in the environment, studies on engineered systems that provide favorable environment for methanotrophic activity have been carried out by several research groups (Gebert et al., 2003; Melse and Van der Werf, 2005; Nikiema et al., 2005; Gebert and Gröngröft, 2006). Considering the characterisitics of methane and methanotrophs, biofiltration was thought to be the most appropriate engineering methodology in enhanced removal of methane.

Biofiltration is an engineered biological treatment process that utilizes the metabolic activity of microorganisms attached onto a variety of packing materials to treat a wide range of organic and inorganic contaminants (Cohen, 2001; Cox and Deshusses, 2002). In a biofilter, contaminants in the gas phase diffuse into biofilms, a thin layer of microbial consortium on the packing material, to be consumed by microorganisms therein. Biofilters are filled with a variety of packing materials to provide the surface area for establishment of biofilms. Appropriate packing materials have sufficient porosity and a

high moisture holding capacity to allow for the establishment of biofilms (Nikiema et al., 2005). Inert materials such as a variety of plastics (e.g., propylene and polyurethane) and silicates, e.g., celite and perlite (Kennes et al., 1996; Alonso et al., 1997; Cox et al., 1997; Cox and Deshusses, 1999; Okkerse et al., 1999; Song and Kinney, 2001; Iranpour et al., 2005) have been used for this purpose. These materials are known to be cost effective in long-term biofiltration due to their durability, which allows for lower operating cost in general (Kennes and Veiga, 2002). Typical sizes of commercial biotrickling filters range from ca. 1.5 to 4.0 m in diameter and 9 to 12 m in height (Cox and Deshusses, 2002; Gabriel and Deshusses, 2003).

Studies to remove methane via biofiltration typically have not considered removal of low concentrations of methane (< 7000 ppmv), nor have they considered that methanotrophic activity is strongly dependent on environmental conditions, most notably the availability of copper (Hanson and Hanson, 1996; Lontoh and Semrau, 1998). The key, rate-limiting step in biotic methane removal is the transformation of methane to methanol by the methane monooxygenase, or MMO (Dalton, 1991). pMMO-expressing cells are known to exhibit significantly higher affinities to methane than sMMO-expressing cells, as well as have higher reaction rates at lower methane concentrations, as implied by its lower half saturation constant (K_s) and higher pseudo-first order-rate constant values ($\frac{V_{\max}}{K_s}$) (Sipkema et al., 1998). As the overall activity of sMMO-expressing cells in low methane environments will be restricted, it is likely to be advantageous to have pMMO-expressing conditions present in either natural or engineered systems to optimize atmospheric methane oxidation by methanotrophs.

Here, we propose a design for the removal of methane using biotrickling filtration. This design is based on existing biotrickling filtration systems used for the removal of gaseous organic and sulfuric compounds (Aizpuru et al., 2003; Iranpour et al., 2005). A general mathematical model to estimate methane removal under both sMMO- and pMMO-expressing conditions is presented, as well as a cost – benefit analysis to determine the economic feasibility of using such a system to reduce global emissions of methane.

VI.2 Results

VI.2.1. Biofilter design and modeling

With the mathematical model using MATLAB, methane removal was estimated under a wide range of conditions, including different methane concentrations, pMMO- vs sMMO-expressing cells, and temperature. First, however, different inlet air velocities were tested with a fixed methane concentration, 1,000 ppmv, for both sMMO- and pMMO-expressing cells to determine the most appropriate inlet air velocity to be used in further analysis. As can be seen in Figure VI.1, the methane removal rate for pMMO-expressing cells was constant above an inlet air velocity of ~0.3 m/s, while sMMO-expressing cells failed to reach steady state under any assumed inlet velocities at this concentration of methane. An inlet velocity of 0.5 m/s (equal to a flow rate of 5.26 m^3/s) was thus used in further analyses.

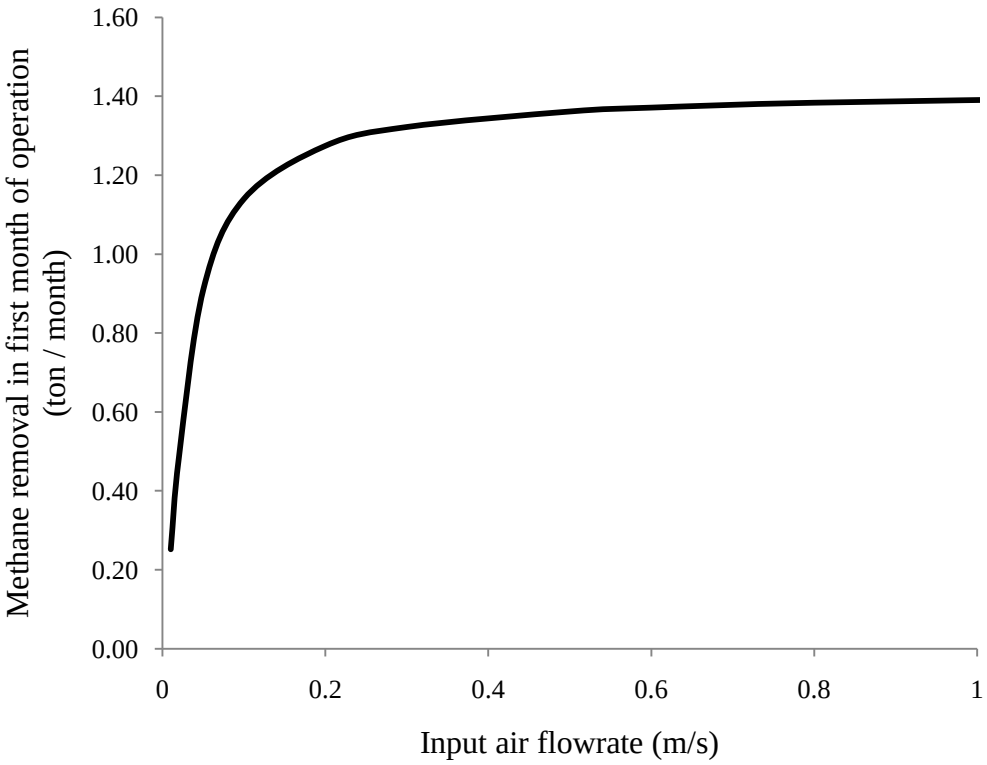

Figure VI.1 Optimization of input air flowrate for removal of atmospheric methane using methanotrophic biofilters composed of *M. trichosporium* OB3b expressing pMMO

As mentioned above, input methane concentration was varied from average atmospheric concentration, 1.7 ppmv, to 6,000 ppmv to evaluate the feasibility of methane biofiltration for cells expressing either sMMO or pMMO in locations with varying methane concentrations. The highest concentration, 6,000 ppmv, was based on the highest atmospheric methane concentrations measured in the vicinity of landfills by Carman and Vincent (1998). It was found that methane removal using biotrickling filtration is not feasible if the global average atmospheric methane concentration, 1.7 ppmv, is assumed. This concentration is too low to support cell growth for either sMMO- or pMMO-expressing cells such that complete washout (i.e., death) of the biofilm occurs in less than a month (data not shown). As shown in Figure VI.2, however, above 500

ppmv both biofilm thickness and methane removal by pMMO-expressing cells achieved steady state within the first two months of operation, while sMMO-expressing cells achieved steady state at methane concentrations above 3,000 ppmv. Furthermore, as seen in Figure VI.2, sMMO-expressing biofilters consumed less methane than pMMO-expressing cells over the entire concentration range tested. Given these findings, only pMMO-expressing cells will be discussed in detail further.

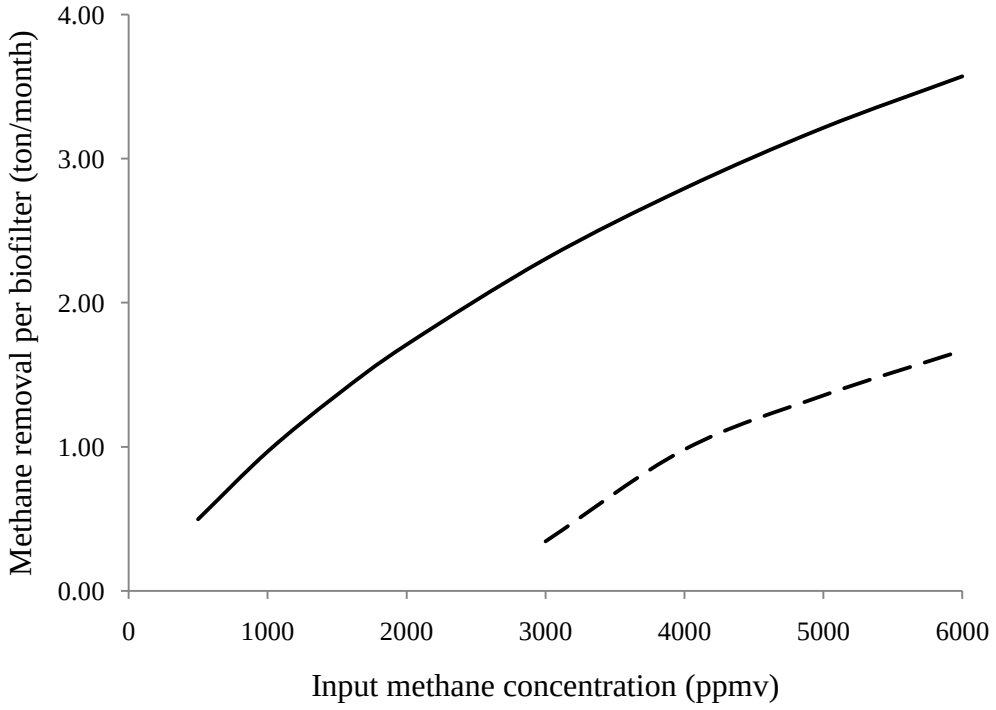

Figure VI.2 Steady state methane removal rate for *M. trichosporium* OB3b as a function of input methane concentration in methanotrophic biofilters (—: pMMO-expressing cells, - - -: sMMO-expressing cells)

From numerical simulations, if a methanotrophic biofilter expressing pMMO is placed in an environment with a local methane concentration of 500 ppmv, 498 kg of methane is removed per month after steady state is reached. The methane degradation rate increased to 3.57 tons of methane per month when the local atmospheric

concentration of methane was raised to 6,000 ppmv (Figure VI.2). If pMMO-expressing biofilters are operated for 10 months of year with two months downtime for maintenance, we estimate that up to 35.7 tons of methane per year can be removed at 6,000 ppmv methane. For the entire concentration range tested, the steady-state biofilm depth did not exceed 1.4×10^{-2} cm at the inlet end, where the cells exhibit the fastest growth (Figure VI.3).

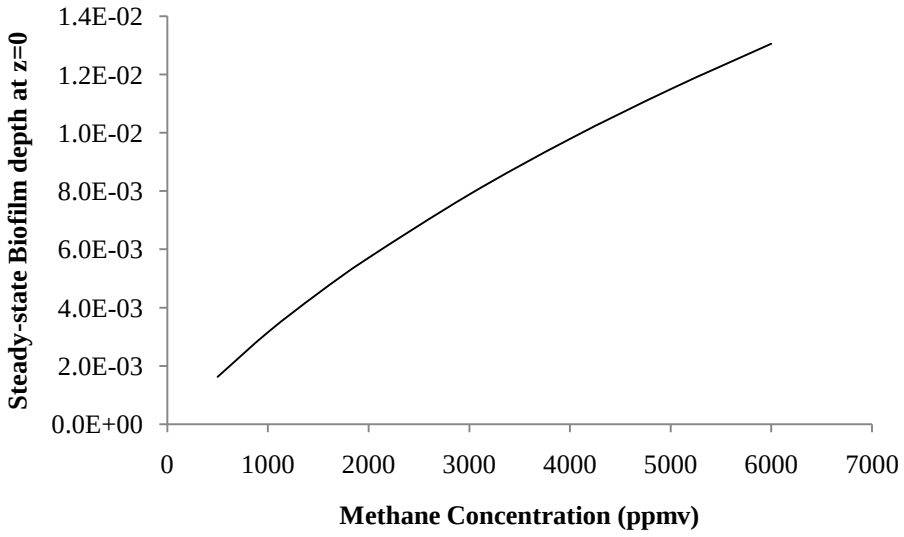

Figure VI.3 Biofilm depth at the inlet end (z=0) after steady-state is established.

VI.2.2 Economic analysis

These estimates of biotrickling filter performance were then used to determine the unit cost of methane removal. As the methanotrophic biotrickling filter proposed here has the same dimensions and composition and will be operated under similar conditions as a well-characterized biofilter at the Grupo Cydsa facility (Cox and Deshusses, 2002), we based our cost estimates on the financial data provided in the literature for this system.

The costs were adjusted for inflation by using the cumulative inflation rate between 2002 and 2008 of 19%. Collectively, the capital cost of our proposed biofilter would be approximately $595,000.

The proposed biofiltration system requires electricity for three purposes: (1) to operate blowers, (2) to recycle nutrient medium, and (3) to maintain optimal temperature in the reactor. The electrical demand for blower operation is estimated to be 216 MWh per year based on the data presented by Gabriel and Deshusses (2003). The air inflow rate in our biotrickling filter is 10% larger but it was reported that blowers with capacity ranging from 17,000 to 68,000 m^3/h do not have more than 10% variation in their electrical demand (Gabriel et al., 2004). Reported electricity requirements for nutrient recycling in specific biofilters are 0.64 MWh per year for a flow rate of 1 m^3/h (Gabriel and Deshusses, 2003). Thus, it is estimated that electrical demand for nutrient recycling will be 11 MWh per year for our proposed system. Finally, in some situations, both the influent air and nutrient medium may require heating to provide the optimal conditions of methanotrophic growth. If it is assumed that heating from 20℃ to 30℃ is required and that the heat capacities of water and air are 4.18 and 1.003 kJ/kg/K, respectively, it is estimated that an additional 485 MWh per year is required per biofilter for heating. Collectively, it is estimated that total energy requirements vary from 227 to 712 MWh per year, dependent on heating requirements. Using an average cost of electricity of 6.16 ¢/kWh for industrial use (EIA, 2007), total electricity costs due to heating will range from $14,000 to $44,000 per year per biofilter.

Assuming that our biofilter has a lifetime of 20 years, and the discount factor is 3% (the average inflation rate for the past 5 years), the annualized capital cost of a

methanotrophic biofilter is calculated to be ~ $40,000 per biofilter per year, with the total annualized cost varying between $74,000 and $104,000 per biofilter per year, depending on heating costs. When compared to the amount of methane removed as a function of influent methane concentration, the costs vary from $2,070 to $20,900 per ton of methane removed or $75 to $860 per equivalent ton of CO_2 (Figure VI.3), depending on the methane concentration and if heating is required.

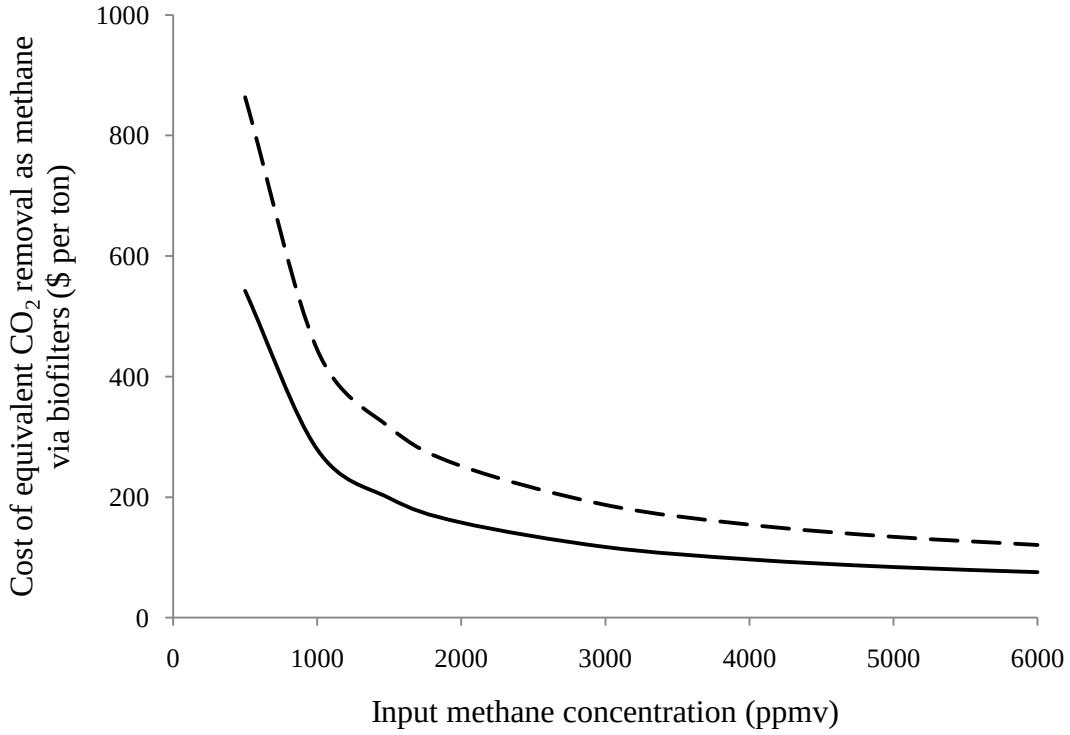

Figure VI.4 Cost of equivalent CO_2 removal as methane using methanotrophic biofilters composed of *M. trichosporium* OB3b expressing pMMO when heating is either unnecessary (—) or necessary (- - -)

As of Mar 3, 2010, 1 ton of CO_2 for year 2014 was traded at ~ €14 or $22 (www.Co2prices.eu). Our estimated costs of removal of an equivalent amount of CO_2 as methane are approximately 3.4- to 39-fold higher. CO_2 market, however, have been unstable and there is possibility that the CO_2 price might rise again. At some point in the

future, the price of CO_2 may exceed the cost of methane removal using the biofiltration systems described here, but it is unknown when this might occur.

VI.3 Discussion

From the model analysis, removal of methane at a significant rate is feasible by pMMO-expressing biofilters at concentrations greater than 500 ppmv and that these systems significantly outperform sMMO-expressing systems. Methane removal with this biotrickling filtration, however, is not economically feasible at current stage as the estimated cost of removal exceeds the current market price of CO_2 emissions in the European carbon market. The price of CO_2 emission, however, is subject to change as the carbon trading market is growing, and it may be possible to reduce the cost of building and operating these biotrickling filters if they are mass-produced.

Another issue that will determine success of greenhouse gas removal with these trickling biofilters is the carbon footprint associated with electricity generation. Carbon dioxide emitted during generation of the power required for operating the biofilter must be considered in conjunction with methane removal rates and costs when considering the feasibility of these biofilters for removal of greenhouse gases from the atmosphere. Carbon footprints of electricity generation range from 5 to 1,000 g/kWh depending on the methods of generation (Parliamentary Office of Science and Technology, 2006). Therefore, the carbon footprint of electricity used in removal of methane by our proposed biofilters will be 3.56–712 tons of CO_2 per year if heating is necessary and 1.13–227 tons of CO_2 per year if it is not. Considering that the expected removal rate is 4.98–35.7 tons of methane per year per biofilter, equivalent to 115–821 tons of CO_2 per year (assuming

influent methane concentrations ranging from 500 to 6,000 ppmv), it will be difficult to have net carbon removal if electricity is supplied by conventional fossil fuel power plants (>500 g CO_2 emitted/kWh). If energy can be supplied from a low carbon energy source, e.g., wind power (<10 g CO_2 emitted/kWh), however, net removal of carbon using these biofilters will be feasible by a wide margin regardless of the electricity requirement for heating.

Biofilters and synthetic packing materials, in general, are known to have very long lifetimes of at least 10 years (van Groenestijn and Kraakman, 2005). However, clogging due to uncontrolled accumulation of biomass is a recurring problem in the operation of biofiltration that deteriorates biofilter function over time (Alonso et al., 1997; Cox and Deshusses, 2002). For the removal of methane, however, clogging is not a significant issue due to the low concentrations of the growth substrate, methane, even at the elevated concentrations assumed here. In our modeling studies, even at the highest atmospheric methane concentrations used in the study, e.g., 6,000 ppmv, steady-state biofilm thickness did not exceed 1.3×10^{-2} cm. Therefore, it is expected that the use of biofilters for atmospheric methane removal will require less maintenance due to clogging.

The major difficulty in removal of atmospheric methane, as mentioned earlier, is the extremely low atmospheric concentration of methane. This restricts use of these biofilters, even those expressing pMMO to local "hot spots" of methane such as that found above landfills and in concentrated animal feeding operations (factory farms). This is due to the relatively low affinity for methane assumed here as compared to the global average atmospheric concentration. Here, the K_s value by the type strain *M.*

trichosporium OB3b expressing pMMO used was 3 μM, equivalent to an atmospheric concentration of 2,170 ppmv.

It should be noted that much of the work on methanotrophs has focused on bacteria isolated from high-methane environments, including *M. trichosporium* OB3b, and as such, it is not surprising that these cells have relatively low affinities for methane. More recently, high-affinity methanotrophs with very low half-saturation constants (40.5 to 134.5 ppmv) have been found to exist in some environments, e.g., organic agricultural soils, with such cells able to consume methane at concentrations as low as 1.7 ppmv (Dunfield et al., 1999; Bull et al., 2000; Dunfield and Conrad, 2000; Knief et al., 2005). Their maximum capacity to degrade methane, however, was found to be very limited (Dunfield and Conrad, 2000). Using the average V_{max} and K_s values (0.125 nmol mg biomass^{-1} s^{-1} and 0.305 μM, respectively) obtained by Dunfield and Conrad (2000) for *Methylocystis* strain LR1, less than 6 kg per month was estimated to be removed under optimal conditions (i.e., an influent methane concentration of 6,000 ppmv, negligible cell death rates and an initial biofilm thickness of 42 μm). It should be noted that even under these conditions, the system failed to achieve steady state, i.e., the biofilm was continuously degraded as cell loss through shearing was greater than cell growth. Therefore, their direct application in engineering practices for removal of atmospheric methane seems infeasible at this time, although their existence suggests the possibility of engineering other methanotrophic strains to have higher affinities toward methane while maintaining high turnover rates, i.e., reduce K_s while maintaining a high V_{max} value. If the pMMO of a strain such as *M. trichosporium* OB3b could be modified to reduce the half-saturation constant to 100 nM (equivalent to 70 ppmv in air assuming equilibrium)

and V_{max} is assumed to remain at 4.83 nmol mg biomass^{-1} s^{-1}, our model predicts that it is possible remove 0.385 ton of methane per month per biofilter at a methane concentration of 100 ppmv without the cells being washed out (as was the case with *M. trichosporium* OB3b expressing pMMO at the same methane concentration). Such a scenario, although potentially feasible, would require more extensive consideration on whole-cell metabolic fluxes of carbon and energy to ensure that relatively simple modifications of the pMMO would be stably maintained.

In summary, the use of pMMO-expressing methanotrophic biotrickling filters for controlling methane emissions is technically feasible and an attractive option for control of methane emission, provided that a low-carbon energy source is used for power supply. The costs associated with such removal must be reduced, however, to enhance the economic attractiveness of this solution. It is possible that these systems may become economically attractive in the near future with improved biofilter designs coupled with cost reduction via mass production and increased value of future CO_2 credits.

CHAPTER VII

An Assay for Screening of Microbial Cultures for Chakophore Production

VII.1 Introduction

Methanobactin has been known to have important roles of mediating the interactions between methanotrophs and copper in that its was found to be deeply involved in copper uptake from the environment and regulation of expression and activity of pMMO and sMMO (Phelps et al., 1992; Fitch et al., 1993; Morton et al., 2000a, b; Knapp et al., 2007). Therefore, understanding the genetics of methanotrophs and the use of molecular markers, e.g., DNA probes, primer sets, targeting methanobactin synthase genes will significantly enhance the knowledge on expression of MMOs in context of microbial ecology of methanotrophs. Also, potential applications of methanobactin in the industry, e.g., for reduction of Au(III) to gold nanoparticles, will require larger amounts of methanobactin, which can only be acquired by heterologous expression of the methanobactin synthases in a less fastidious host such as *E. coli*. To design such a process, the genetic information on methanobactin is indispensable. Use of high-throughput experiments to detect the targeted genes, e.g., transposon mutagenesis, however, has been impeded by the lack of simple and efficient screening methods. Thus, investigations have been limited to single-gene mutations. As for the single mutations targeted on putative NRPS genes (Murrell, Personal communications) the defects in methanobactin production have been difficult to screen, due to insufficient knowledge on

properties and functions of methanobactin in various methanotrophic bacterial strains. The lack of a screening methodology has limited further investigation for genes involved in methanobactin synthesis.

To resolve this problem and facilitate the investigation of methanobactin, we have devised a novel method to qualitatively screen for production of chalkaphores through a simple plate assay. This assay was developed by adopting the chromo azural S (CAS) for siderophore production (Schwyn and Neilands, 1987), to instead screen cultures for chalkophore production by substituting copper for iron. In the original assay, a blue complex is formed between iron and CAS in the presence of a detergent, hexadecyltrimethylammonium bromide (HDTMA). The removal of iron by a competing ligand, e.g., a siderophore, results in a color change, typically from blue to orange. Here copper was substituted for iron, as CAS also has a high affinity for copper (log K = 13.2) (Cha and Abruna, 2002) with a blue complex also being observed, with a similar color change observed in the presence of chalkophores expressed by methanotrophs.

The primary utility of this newly developed method, we expect, will be screening putative mutants of methanobactin synthesis. However, this assay can be also used to screen other cells for production of chalkophores to determine how wide-spread the expression of such compounds may be.

VII.2 Results

VII.2.1 Growth of methanotrophs on Cu-CAS agar plates

To screen for siderophore production (Schwyn and Neilands, 1987), methanotrophs were initially cultured directly on Cu-CAS plates. As can be seen in

Figure VII.1A and C, on 50 µM Cu-CAS plates, only *M. trichosporium* OB3b grew to any extent, with a concomitant color change in the Cu-CAS agar visible from blue to yellow. Growth of the other tested methanotrophs, *M. capsulatus* Bath, *M. album* BG8, and *M. parvus* OBBP was severely limited, possibly due to the toxicity of HDTMA used to solubilize the metal-CAS complex, and no substantial colorimetric changes in the Cu-CAS agar were observed for these strains.

To overcome the inhibition of growth, 20 µM Cu-CAS plates were examined to determine if lower concentrations of Cu-CAS could be used to provide a strong initial coloration, as well as to determine if a lower corresponding concentration of HDTMA would facilitate methanotrophic growth. As can be seen in Figure VII.1B and D, three of the four tested strains grew after 16 days, the exception being *M. parvus* OBBP. The low initial concentration of Cu-CAS did not give a strong blue coloration, however, making it difficult to use these conditions for screening of chalkophore production. Given these results suggesting that HDTMA is toxic to these Gram-negative cells, the plate method suggested by Milagres, et al (1999) to mitigate the toxicity of HDTMA to Gram-positive cells was next examined.

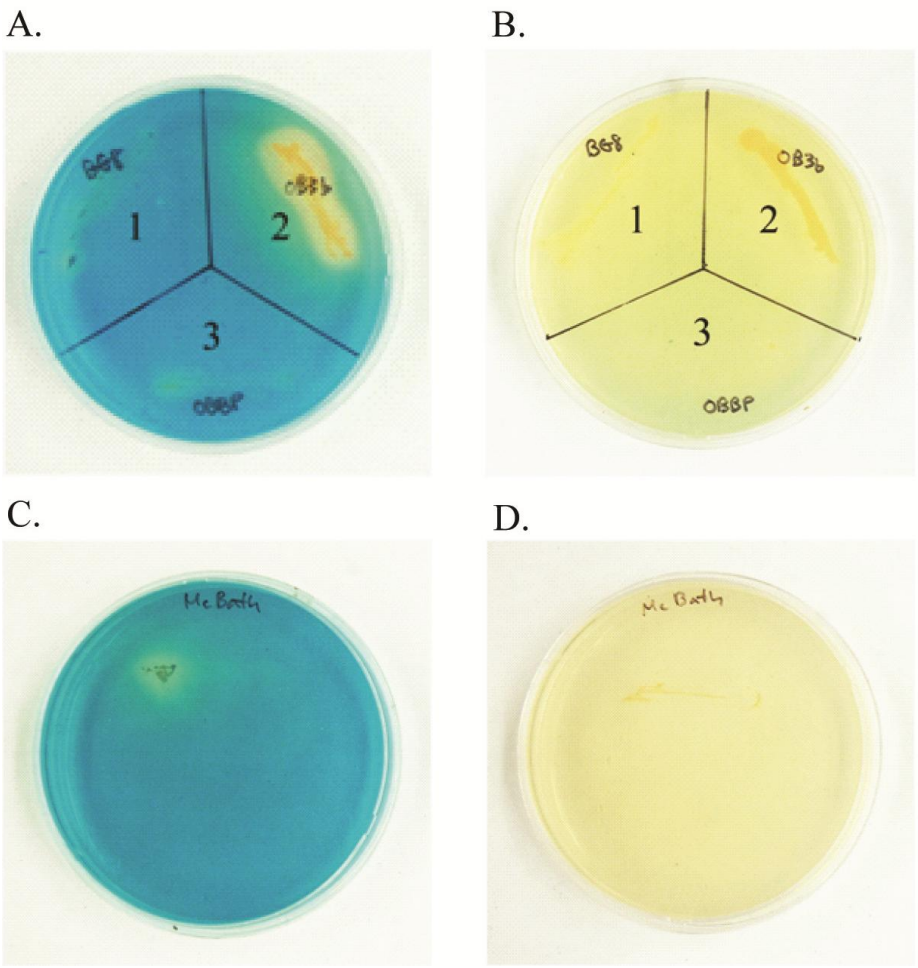

Figure VII.1 (A) Growth of *M. album* BG8 (1), *M. trichosporium* OB3b (2) and *M. parvus* OBBP (3) directly on 50 μM Cu-CAS agar. (B) Growth of *M. album* BG8 (1), *M. trichosporium* OB3b (2), and *M. parvus* OBBP (3) directly on 20 μM Cu-CAS agar. (C) Growth of *M. capsulatus* Bath directly on 50 μM Cu-CAS agar. (D). Growth of *M. capsulatus* Bath directly on 20 μM Cu-CAS agar.

VII.2.2 Screening of Chalkophore Production on Split NMS/Cu-CAS Plates

As can be seen in Figure VII.2 and Figure VII.3, by streaking methanotrophs onto NMS agar with 1 μM copper immediately adjacent to 50 μM Cu-CAS agar, growth is readily observable for all tested methanotrophs. Two strains, *M. trichosporium* OB3b and *M. album* BG8, showed significant change in the coloration of the Cu-CAS agar within 15 days (from blue to yellow), while plates incubated with *M. capsulatus* Bath

showed a similar color change within 6 days, and such a color shift increased over more of the Cu-CAS plate over time, indicating that more copper was removed from the Cu-CAS complex over time by these cells. *M. parvus* OBBP, however, did not show significant color shift, although after 21 days, the Cu-CAS agar blue color changed slightly to green. These assays were repeated with the NMS agar containing 10 μM copper, and the results were identical to when the copper concentration was 1 μM (Figure VII.4 and VII.5), indicating that the assay is insensitive to the amount of copper in NMS agar.

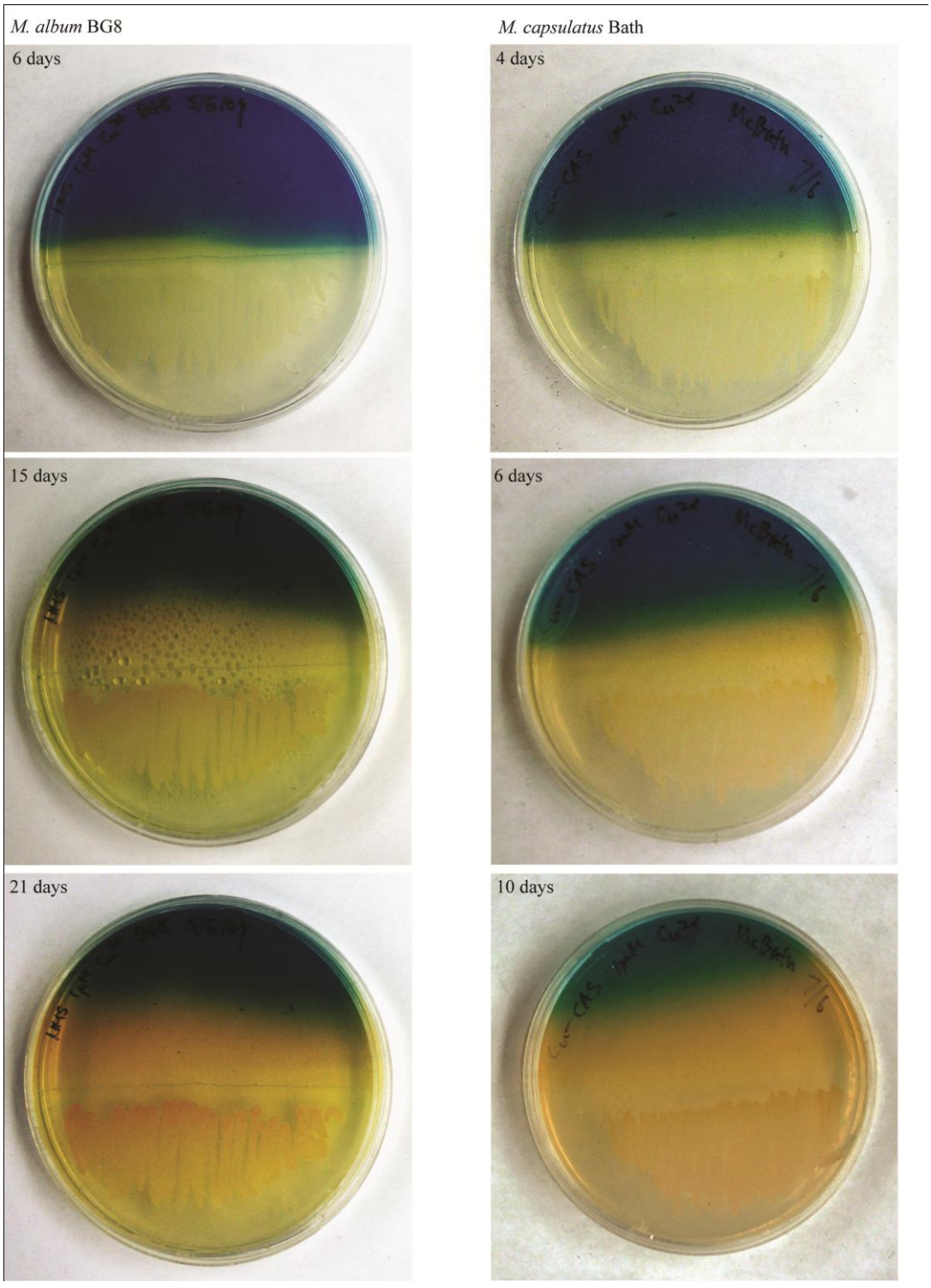

Figure VII.2 Modified split NMS/Cu-CAS plates for detection of chalkophore production over time by type I methanotrophs: left - *M. album* BG8; right - *M. capsulatus* Bath. NMS media was supplemented with 1 μM copper as $CuCl_2$

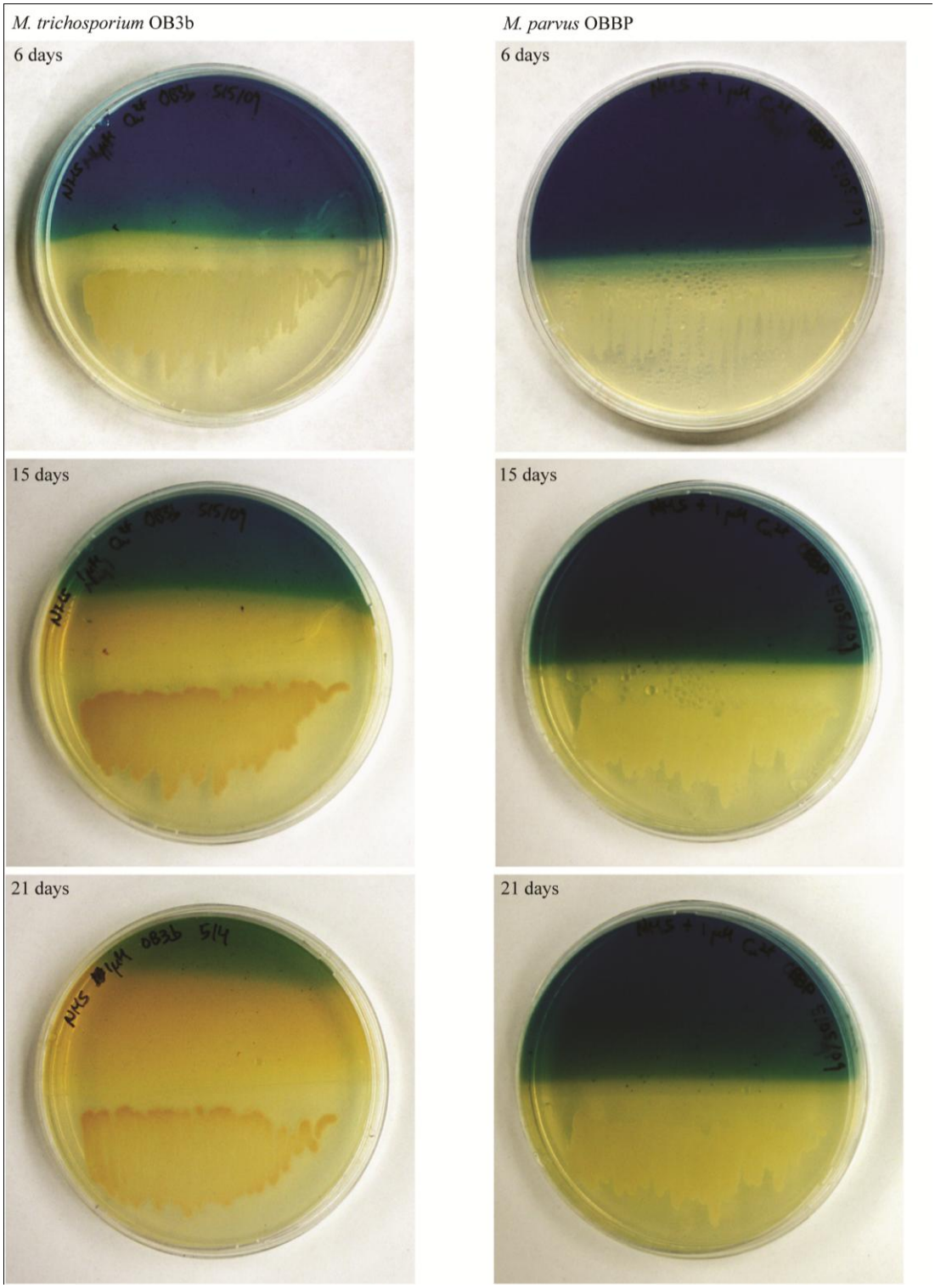

Figure VII.3 Modified split NMS/Cu-CAS plates for detection of chalkophore production over time by type II methanotrophs: left - *M. trichosporium* OB3b; right - *M. parvus* OBBP. NMS media was supplemented with 1 μM copper as $CuCl_2$

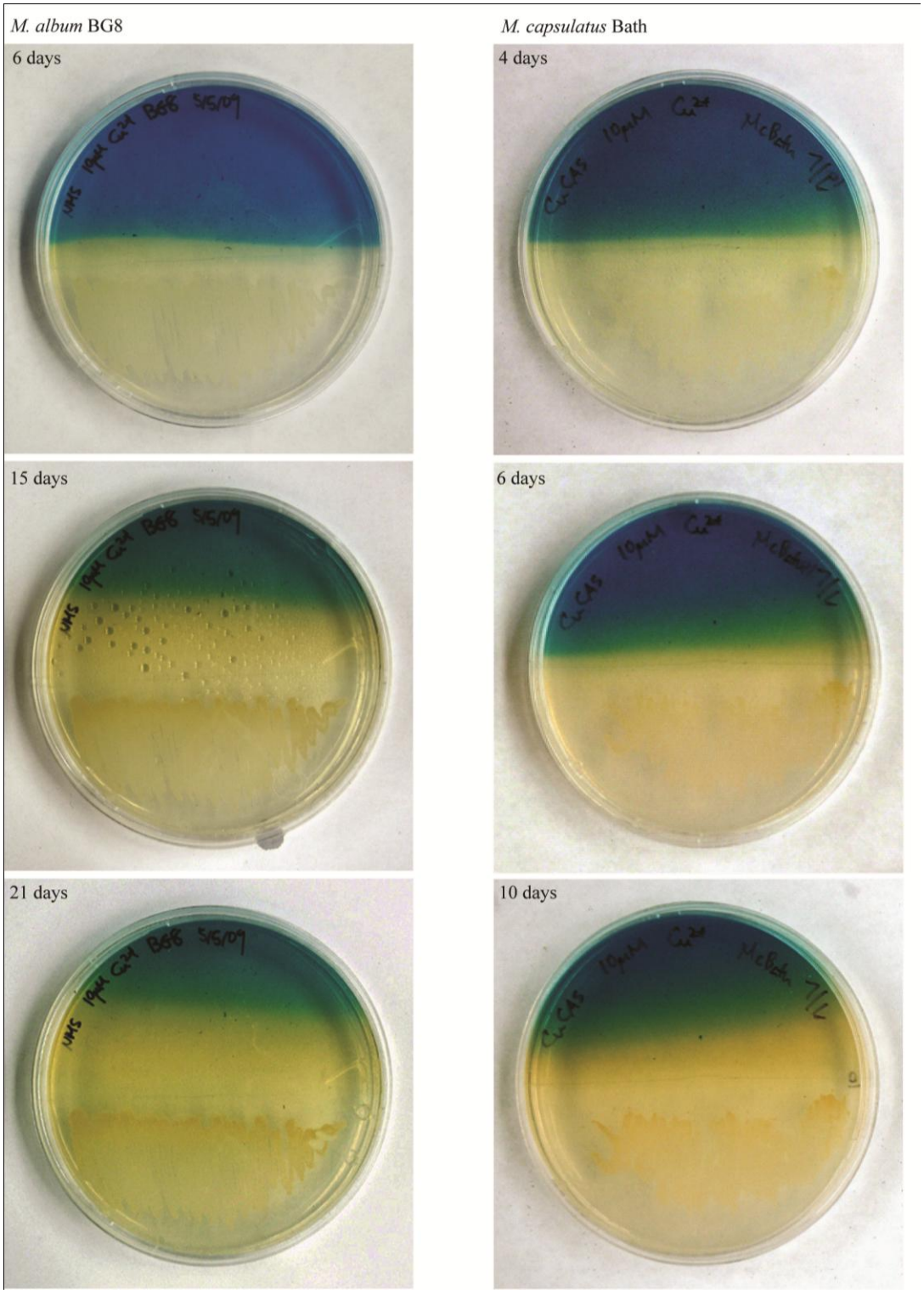

Figure VII.4 Modified split NMS/Cu-CAS plates for detection of chalkophore production over time by type I methanotrophs: left - *M. album* BG8; right - *M. capsulatus* Bath. NMS media was supplemented with 10 μM copper as $CuCl_2$

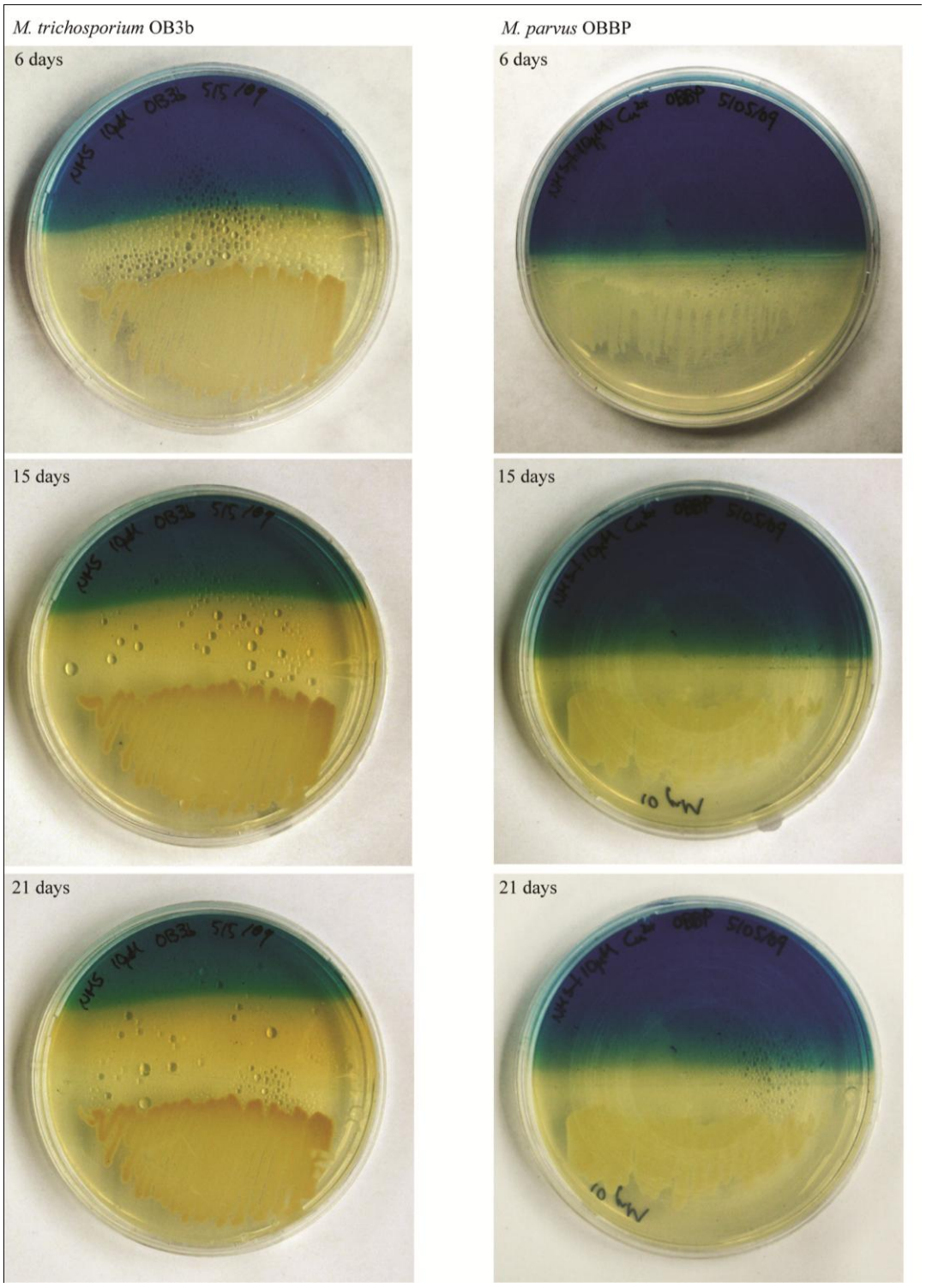

Figure VII.5 Modified split NMS/Cu-CAS plates for detection of chalkophore production over time by type II methanotrophs: left - *M. trichosporium* OB3b; right - *M. parvus* OBBP. NMS media was supplemented with 10 μM copper as $CuCl_2$

VII.2.3 Production of siderophores by methanotrophs

To determine if the color change of Cu-CAS plates was due to non-specific metal binding by compounds other than chalkophores, e.g., siderophores, split plates were prepared with NMS with 10 μM copper and Fe-CAS agars. As can be seen in Figure VII.6 and Figure VII.7, a slight color change of the Fe-CAS agar was observed at the periphery of the Fe-CAS and NMS agar for plates streaked with *M. album* BG8 and *M. trichosporium* OB3b, but no color change is apparent for plates streaked with *M. capsulatus* Bath and *M. parvus* OBBP. In these plates, iron was added as Fe-EDTA to the NMS agar as this is a standard component of NMS medium. To determine if the availability of iron in the NMS medium prevented uptake of iron from the Fe-CAS agar, these assays were repeated with Fe-EDTA omitted from the NMS agar. As can be seen in Figure VII.8 and Figure VII.9, for *M. trichosporium* OB3b and *M. album* BG8, a more substantial color change was observed in the Fe-CAS agar, and the zone of the color change increased in size over time. *M. capsulatus* Bath and *M. parvus* OBBP, however, again showed little color change after 10 and 21 days, respectively. Collectively, these results suggest that *M. trichosporium* OB3b and *M. album* BG8 produced siderophores, particularly when grown under iron limitation on NMS agar. Alternatively, methanobactin from these methanotrophs may have bound iron and have been responsible for the observed color changes.

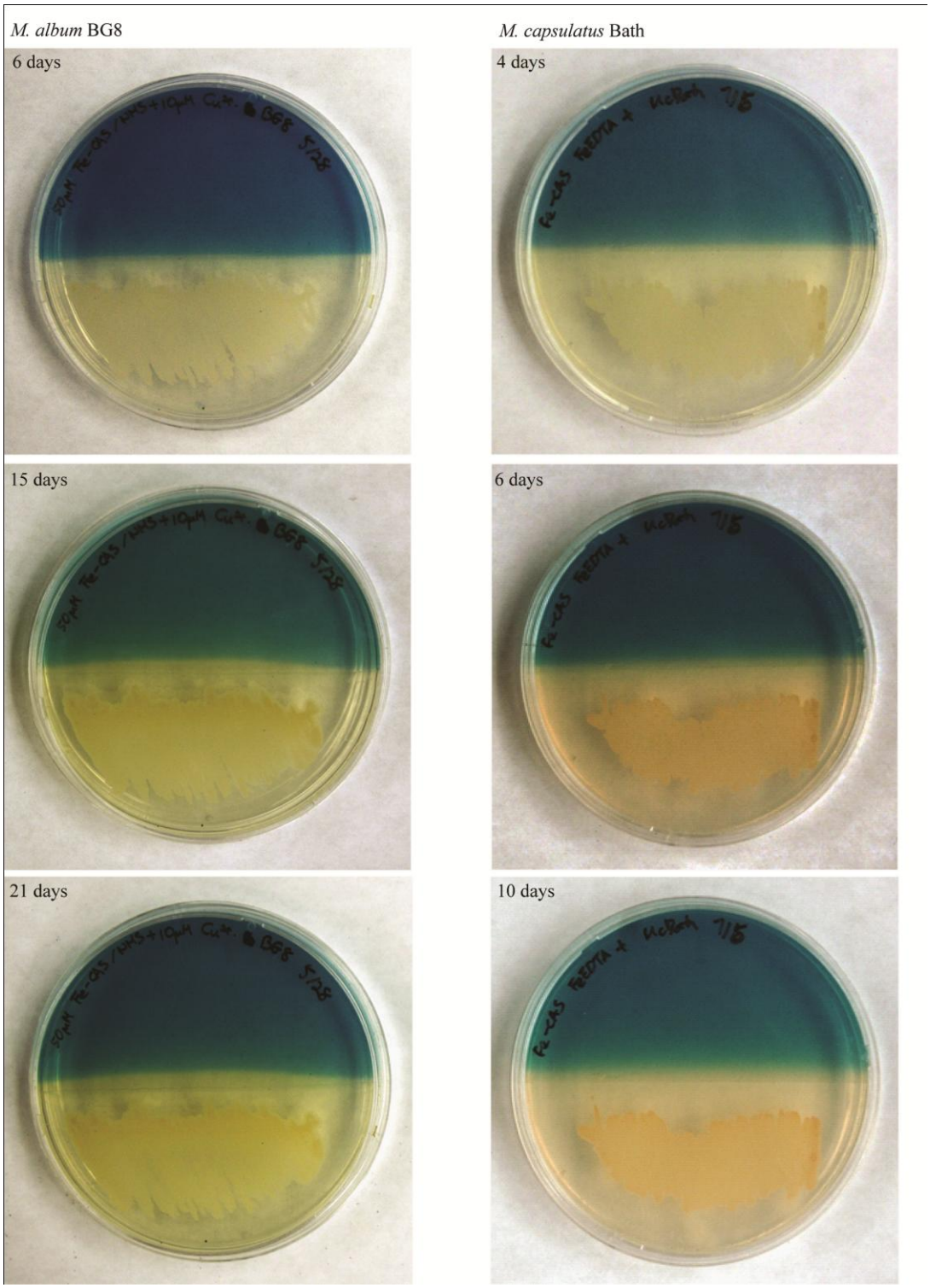

Figure VII.6 Modified split NMS/Fe-CAS plates for detection of siderophore production over time by type I methanotrophs: left - *M. album* BG8; right - *M. capsulatus* Bath. NMS agar was supplemented with 0.1% w/v Fe-EDTA

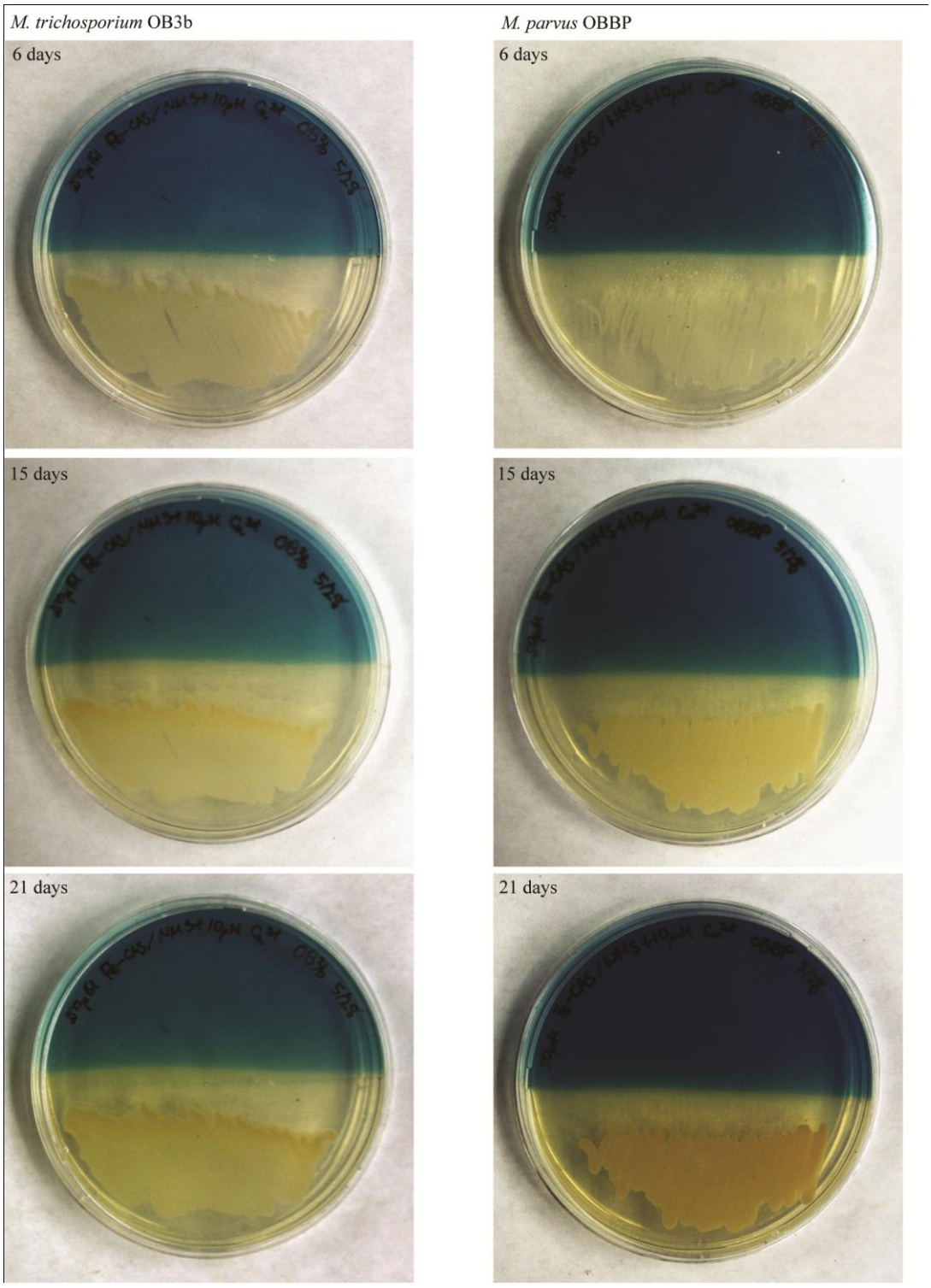

Figure VII.7 Modified split NMS/Fe-CAS plates for detection of siderophore production over time by type II methanotrophs: left - *M. trichosporium* OB3b; right - *M. parvus* OBBP. NMS agar was supplemented with 0.1% w/v Fe-EDTA

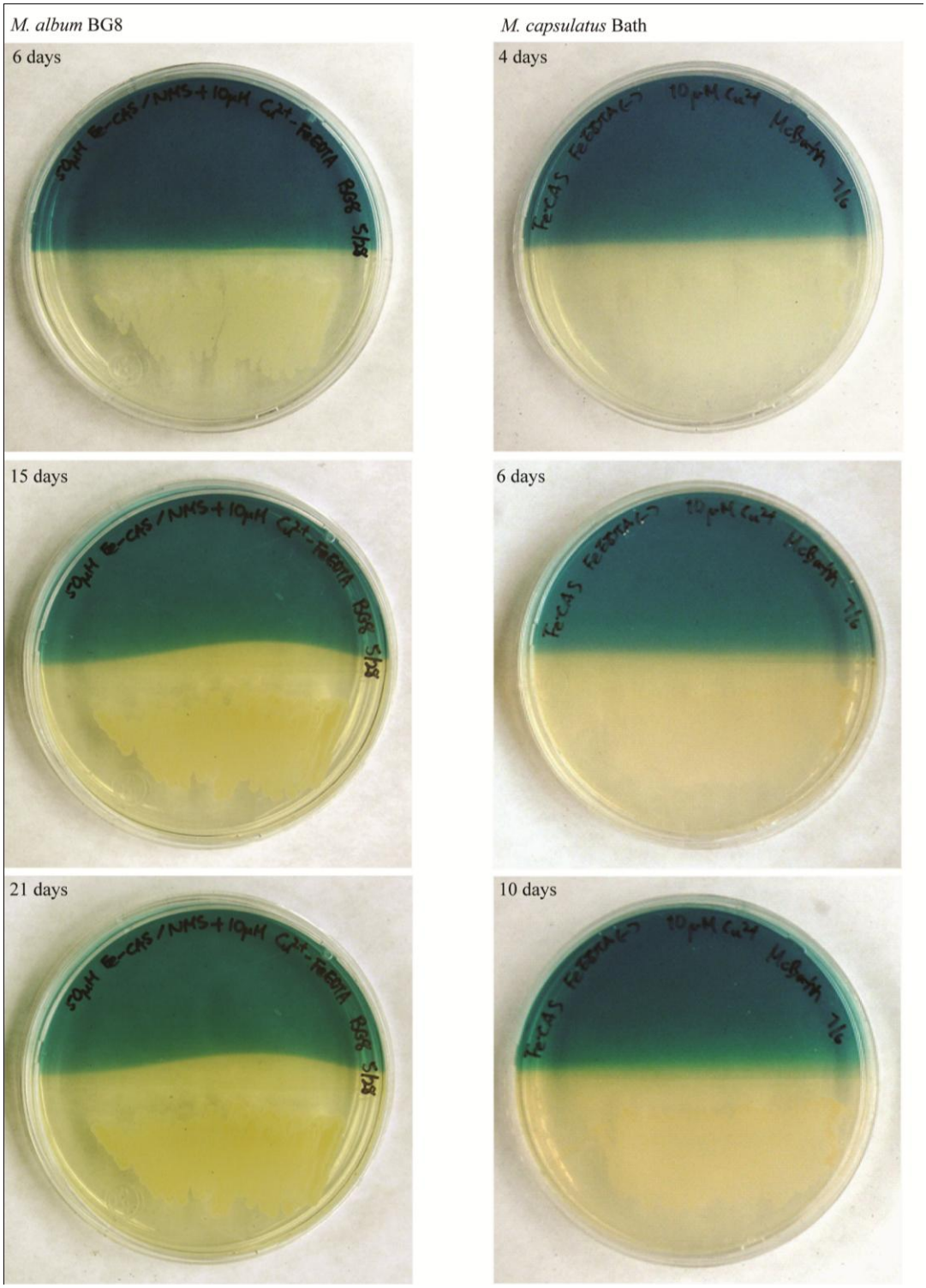

Figure VII.8 Modified split NMS/Fe-CAS plates for detection of siderophore production over time by type I methanotrophs: left - *M. album* BG8 ; right - *M. capsulatus* Bath. Fe-EDTA was omitted from NMS agar

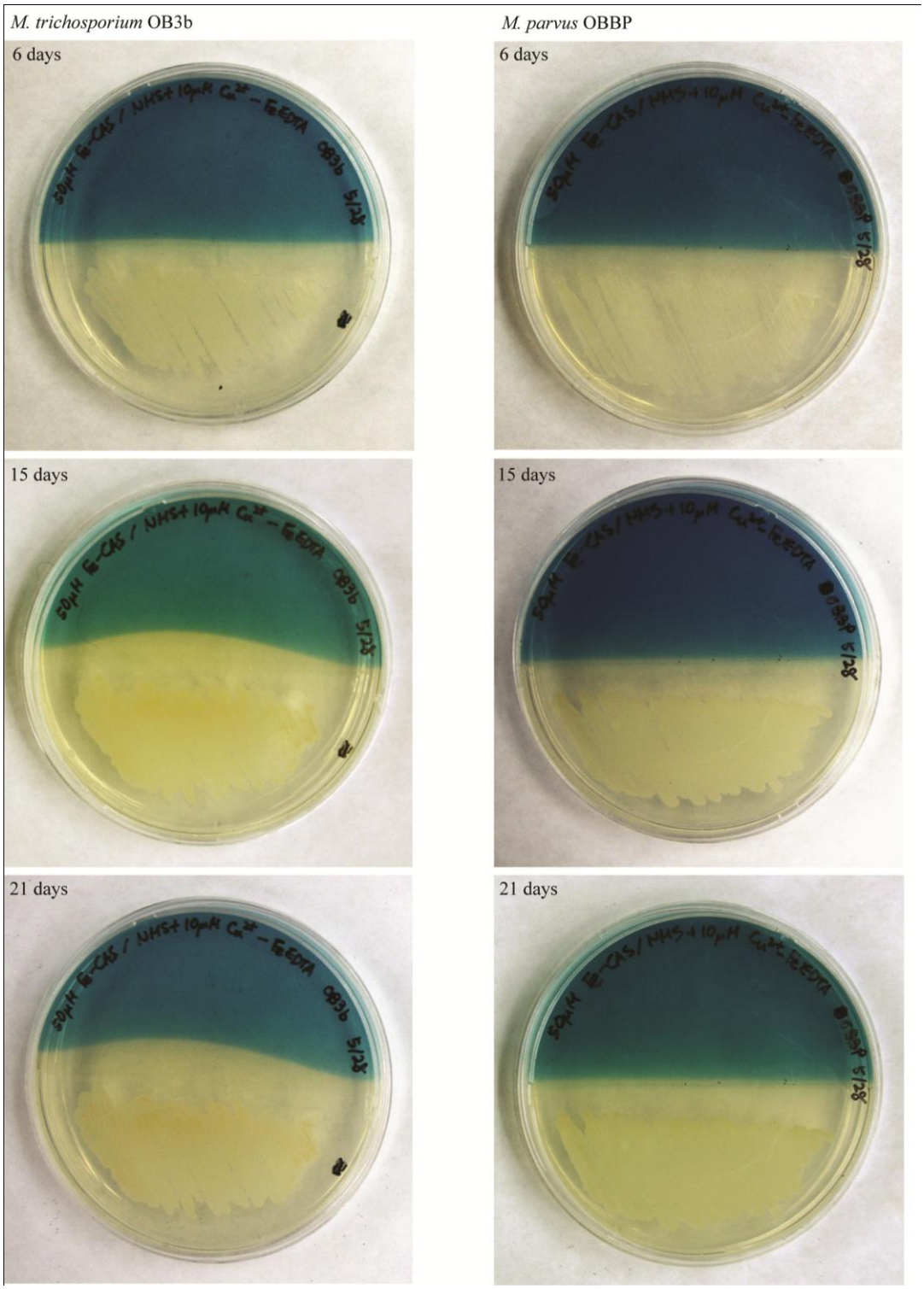

Figure VII.9 Modified split NMS/Cu-CAS plates for detection of siderophore production over time by type II methanotrophs: left - *M. trichosporium* OB3b; right - *M. parvus* OBBP. Fe-EDTA was omitted from NMS agar

VII.2.4 Examination of metal binding by purified methanobactin and deferoxamine-B

To determine if iron binding in the presence of CAS was due to either a siderophore or a chalkophore expressed by *M. trichosporium* OB3b or *M. album* BG8, purified methanobactin from *M. trichosporium* OB3b and deferoxamine-B (purchased from Sigma Aldrich) were spotted onto both 50 µM Cu-CAS and Fe-CAS agar plates. 50 mM of methanobactin did cause a color change within 1 hour when spotted onto Cu-CAS agar, but not on Fe-CAS agar after 12 hours (Figure VII.10). Deferoxamine-B caused a color change on Cu-CAS within 1 hour and Fe-CAS agar within 12 hours. The green coloration observed when methanobactin from *M. trichosporium* OB3b was spotted onto Fe-CAS agar is not due to iron binding by methanobactin, but is due to the yellow color of the methanobactin solution.

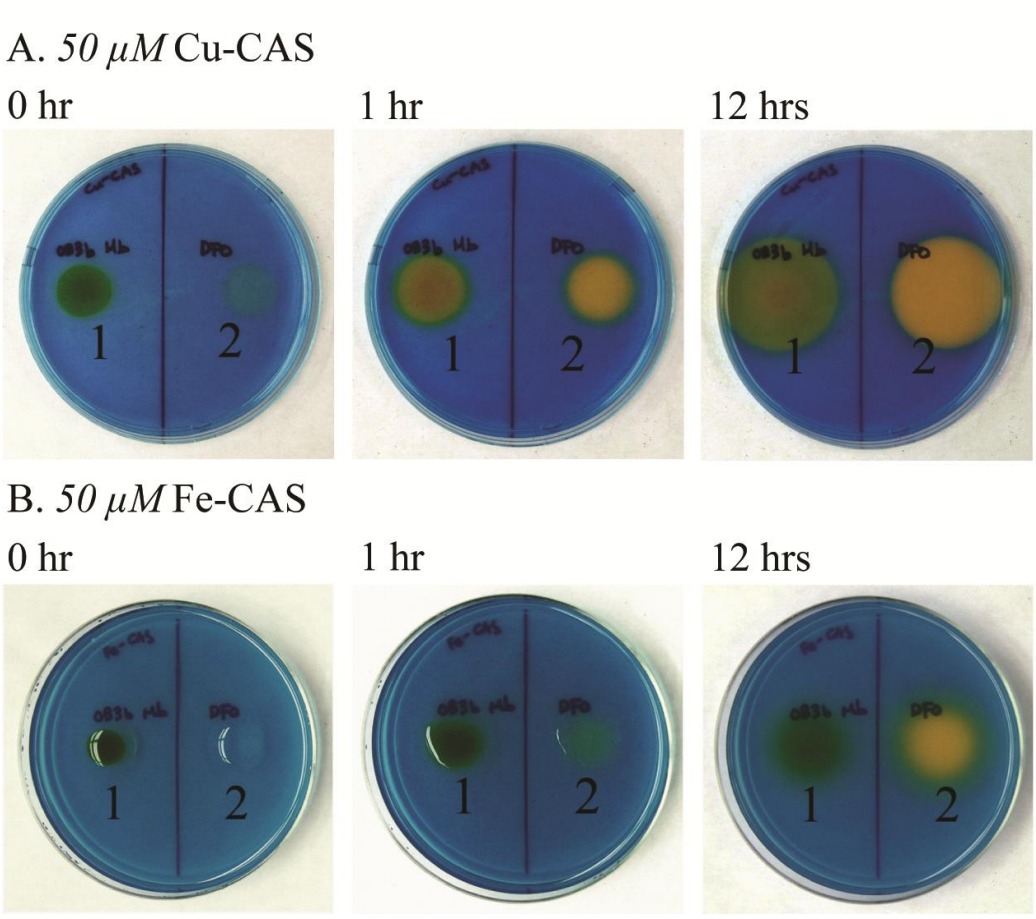

Figure VII.10 (A) Binding of copper in the presence of CAS by either: (1) 50 µl of 50 mM copper-free methanobactin from *M. trichosporiu*m OB3b, or; (2) 50 µl of 50 mM deferoxamine-B from *Streptomyces pilosus*. (B) Binding of iron in the presence of CAS by either (1) 50 µl of 50 mM copper-free methanobactin from *M. trichosporiu*m OB3b, or; (2) 50 µl of 50 mM deferoxamine-B from *Streptomyces pilosus*.

VII.3 Discussion

Here we described the development of a simple assay for screening of chalkophore production by different organisms. The assay was developed using NMS agar and methanotrophs as a model system as at least one of these cells, *M. trichosporium* OB3b, is known to express a high-affinity copper uptake system, although the assay can

be modified to screen other cells for chalkophore production by substituting the appropriate growth medium for NMS agar.

From the data presented here, it is clear that simple plate assays can detect the expression of chalkophores in methanotrophs, and that in the case of best characterized chalkophore, methanobactin from *M. trichosporium* OB3b, it does not bind iron in the presence of CAS to a sufficient extent to cause a color change from blue to yellow. These results are consistent with the known properties of methanobactin from *M. trichosporium* OB3b, where the apparent stability constant of this compound for copper is $3.3\times10^{34} \pm 3.0\times10^{11}$ M^{-1}, while the affinity for iron is many orders of magnitude lower, $9.7 \times 10^{5} \pm 6 \times 10^{4}$ M^{-1} (Choi et al., 2006b). Although siderophores have very high affinities for iron, many also have relatively high affinities for copper. For example, the 1:1 log formation constants for copper and iron complexes of deferoxamine-B are 14.12 and 30.6 respectively (at 20 ℃ and an ionic strength of 0.1 M (Martell et al., 2001). Given that siderophores can also bind copper in the presence of CAS (Shenker et al., 1995), it is important that when screening novel isolates for chalkophore production, cells should be streaked on both Cu-CAS and Fe-CAS plates under nominally iron-sufficient conditions and on Fe-CAS plates under iron-limiting conditions. A chalkophore should only react with Cu-CAS unless it has an unusually high affinity for iron, while siderophore production should be more apparent under iron-limiting conditions.

Here the use of Cu-CAS/NMS agar plates revealed that several, but not all methanotrophs have high affinity copper uptake systems. It is possible that the competition between methanotrophs for copper, and the varying affinities of methanobactin produced by different methanotrophs regulates overall methanotrophic

community composition, size, and activity, and that the relative (in)ability to sequester copper thereby has an important effect on methane cycling in the environment. Specifically, it can be expected as conditions become more reducing, copper speciation will change from potentially readily available Cu (II) complexes to less available Cu (I) sulfides. As such, one could predict that in low redox environments, methanotrophs with high affinity copper uptake systems would predominate, while in high redox environments, cells with lower affinity systems would become competitive. It is interesting to note that conflicting data have been reported as to the distribution of methanotrophs in different redox conditions. Early work found that type II strains tended to dominate in areas with low O_2 and high CH_4 concentrations while type I methanotrophs were preferentially found in inverse conditions (Amaral and Knowles, 1995). Other studies, however, have found that type II methanotrophs can be enriched under both high CH_4: low O_2 and low CH_4 : high O_2 ratios (Auman et al., 2000) and that both type I and II methanotrophs are found in landfill cover soils were the CH_4: O_2 ratio is typically quite high (Bodrossy et al., 2003; Stralis-Pavese et al., 2004). In the methanotrophic strains examined here, two type I strains (*M. album* BG8 and *M. capsulatus* Bath) and one type II strain (*M. trichosporium* OB3b) were found to have relatively high affinity copper uptake systems, while another type II strain (*M. parvus* OBBP) did not. As the presence of high-affinity copper uptake systems is irrelevant to the phylogenetic relationship among the methanotrophic bacteria, it can be suggested that the yet unidentified methanobactin synthase genes may have been transferred via horizontal gene transfer. It is possible that the methanotrophic distribution along redox gradients may be more a function of a cell's ability to sequester copper rather than its

phylogeny. Further work should be done to verify the affinity of methanobactin from the strains other than those screened here, as well as to determine if different forms of methanobactin are found in methanotrophic cultures cultivated under a variety of conditions that influence copper bioavailability.

While high affinity copper uptake systems have been discovered only recently in methanotrophic bacteria, high affinity iron uptake systems are known to be widespread among aerobic bacteria (Wandersman and Delepelaire, 2004). The biochemical importance of iron stems from the ubiquitous nature of iron bearing metalloenzymes including sMMO and possibly pMMO. Iron homeostasis can be severely challenged by the presence of iron-oxides, -hydroxides and –oxohydroxides that limit the solubility and dissolution rates of iron under aerobic conditions in the circumneutral pH-range (Kraemer, 2004). The precipitation of iron along a redox gradient can therefore pose a problem to oxygen dependent methanotrophic bacteria. In this study, the use of Fe-CAS/NMS agar plates revealed that some of the methanotrophs responded to low iron conditions by the exudation of a siderophore that was suppressed under iron sufficient conditions. This siderophore appears to be distinct from the chalkophore that is also exuded. To the best of the authors' knowledge, this is the first evidence of an organism that uses two distinct high affinity metal uptake systems for two different metal nutrients. The use of two high affinity metal uptake systems as well as the fact that not all methanotrophs possess each system may also have important ecological implications.

At this time, it is still unclear how methanobactin, or any other putative chalkophore is synthesized. It is possible that such compounds are produced via non-ribosomal polypeptide synthases (NRPS), as are many siderophores (Challis and

Naismith, 2004). NRPS genes have been found in the one published methanotrophic genome of *M. capsulatus* Bath (Ward et al., 2004), but to date no data have been published showing that such genes are involved in methanobactin production. The simple plate assay presented here will allow putative chalkophore-minus mutants to be more easily screened, thus enabling more rapid progress in determining the genetics and biochemistry of chalkophore production, similar to the use of the Fe-CAS assay for screening of siderophore-defective mutants (Schwyn and Neilands, 1987; Carreró et al., 2002).

Chapter VIII

Conclusions and Future Works

VIII.1 Conclusions

The general objective of this study was to enhance the physiological knowledge on methanotrophs for improved applications. First, a laboratory strain of type II methanotroph, *Methylosinus trichosporium* OB3b, was examined for the effectiveness of sMMO and pMMO in degradation of chlorinated ethenes at 20˚C. This temperature was specifically chosen as it is significantly lower than the optimal growth temperature of *M. trichosporium* OB3b (30˚C) and at the same time, close to the average *in situ* ground water temperature. Congruent with the previous result obtained from the experiments at 30˚C (Lee et al., 2006), sMMO had much faster initial degradation kinetics towards TCE, *trans*-DCE, and VC than pMMO. In long-term batch degradation experiments with growth in consideration, however, pMMO-expressing cells were better in degrading the chlorinated ethenes at high concentrations. As suggested by the Δ dimensionless numbers calculated from the whole-cell kinetics measured at 20˚C, the competitive binding of the chlorinated ethenes, especially VC, to sMMO is likely to have had great negative impact on the uptake of methane by *M. trichosporium* OB3b expressing sMMO. The degree of inhibition was observed to be more severe at 20˚C, congruent with the estimation from the Δ model. Although it has yet been tested, the V_{max} values of the whole-cell kinetics data suggested that the transcription of sMMO might be negatively

affected at the average *in situ* groundwater temperature. As the catabolic and anabolic systems downstream of MMOs are currently known to be the same regardless of the presence of copper, the larger magnitude of decrease in maximum degradation rates in *M. trichosporium* OB3b observed only at sMMO expression condition strongly suggests that sMMO expression may be repressed to some degree at suboptimal temperature conditions, while pMMO expression is not.

Second, the recently isolated facultative methanotroph, *Methylocystis daltona* SB2 was examined for the expression of pMMO and degradation of chlorinated ethene compounds under growth on acetate in absence of methane. The real–time quantitative RT–PCR analyses confirmed the constitutive expression of pMMO in *M. daltona* SB2 cells grown in acetate at two different stages of growth, mid-exponential growth phase and late-exponential (or the beginning of the stationary phase), although the quantity of expression was not constant at the two different time points. That is, a significant drop in pMMO expression was observed as *M. daltona* SB2 approached the stationary phase. The same trend of decrease in pMMO expression was not observed for the same cells grown on methane. In the subsequent long-term degradation experiment, significant degradation of *t*-DCE and VC was observed from the mixture of chlorinated ethenes added to the batch cultures of *M. daltona* SB2. The degradation activity was not observed at all when acetylene, the effective inhibitor of MMOs, was added prior to the degradation experiment, strongly supporting that the active pMMO was actually present and responsible for degradation of the chlorinated ethenes. The total amount degraded, however, was much lower than when the same cells were grown on methane. We contemplated that two reasons may have contributed to the lower degree of degradation

at acetate-growth condition: the low overall housekeeping activity of the cells leading to increased vulnerability to the toxicity of the intermediates/products and/or the decrease of pMMO expression over time. This study was significant in that it was the first time degradation of the chlorinated ethenes by a facultative methanotroph was evidenced in absence of methane. As diverse population of facultative methanotrophs are being discovered and thus expected to exist in soils of varying environmental conditions, this may lead to development of more sophisticated strategies for utilization of methanotrophic community in the soil for bioremediation of the sites contaminated with chlorinated ethenes.

Third, a thorough assessment was made of the feasibility of employing biotrickling filters loaded with methanotrophic community for removal of methane from the atmosphere. A design of such a biofilter was developed from the existing biofiltration systems used for removal of organic/inorganic pollutants and our current knowledge on methanotrophs. MATLAB was used to calculate the removal efficiency of the reactors through mathematical modeling and with the data on the estimated rate of removal, economic feasibility was analyzed. The model result indicated that such biofiltration systems were able to remove methane from the atmosphere, provided that they are located in local "hotspots" of methane (> 500 ppmv) in vicinity of major anthropogenic sources and that pMMO expression condition is induced. The consistent supply of copper, therefore, is thought to be essential in operating these hypotical biotrickling filters. Another important consideration was the carbon footprint associated with the electricity. As electricity requirement is not negligible in operating these biotrickling filters, overall removal of carbon dioxide equivalence was found to be obtainable only when renewable

resources are used for power generation. Considering the estimated costs associated with this biofiltration system, removal of the greenhouse gas using methanotrophic biofiltration is not profitable with current technology. It is possible, however, that these systems may become economically attractive in the near future with improved biofilter designs based on enhanced knowledge on methanotrophic community coupled with cost reduction via mass production and increased value of future CO_2 credits.

Fourth, for better understanding of methane oxidation in both isolated cultures and *in situ*, better knowledge on methanobactin is important as it appears to play a key role in regulating expression and activity of methane monooxygenase. As a primer for studies on the genetics of methanobactin, we have developed a method for screening methanotrophs or any other cells for production of chalkophores (biological copper chelators) by modifying a widely known experimental procedure, CAS assay, used in identification of siderophore expression. The modified CAS assay with agar split into halves of NMS agar and blue-colored Cu-CAS agar was successful in identifying exusion of methanobactin from the methanotrophs grown on the NMS agar with no inhibition from the toxicity of CAS or HDTMA. Contradicting previous hypotheses, not every known methanotroph produced chalkophores that have high enough affinity to abstract copper from CAS. The two type I methanotrophs tested, *Methylomicrobium album* BG8 and *Methylococcus capsulatus* Bath, were confirmed of methanobactin production despite of their relatively far phylogenetic distance. More intriguingly, however, the two type II strains from the *Methylocysceae* family, *M. trichosporium* OB3b and *Methylocystis parvus* OBBP differed in their ability to abstract copper. Only *M. trichosporium* OB3b was able to abstract copper from Cu-CAS complex, while *M. parvus*

OBBP lacked the ability. Thus, we concluded that the tendency of producing chalkophores had little, if any, correlation with phylogeny, suggesting that the ability to express methanobactin may be horizontally transferred. Based on these results, it was hypothesized that the differing ability of the cells to abstract copper from environment might be critically related to the distribution of methanotrophs in environments with varying redox conditions. Another interesting finding in this study was that *M. album* BG8 and *M. trichosporium* OB3b were found to express siderophores. The abundance of putative NRPS genes in the draft genome of *M. trichosporium* OB3b suggests the existence of multiple siderophore synthases in the methanotroph.

VIII.2 Future work

As presented in this study, methanotrophs are intriguing groups of microorganisms with a huge potential in environmental industry. Their physiology, genetics, and genomics are, however, not very well understood even after 100 years of vigorous research. Although the pieces of knowledge gained about the methanotrophs from this study has contributed to knowing a little more about these bacteria, there still remains a lot to be unveiled. Therefore, I would like to propose a few research topics that can be studied extending the studies performed here.

In this study, it was found that the temperature change had differential effects on the activity of *M. trichosporium* OB3b expressing pMMO and the sMMO. The growth rates of these cells, however, were not significantly different at given concentration of methane regardless of the temperature (20˚C or 30˚C), indicating that methane uptake might not be the rate-limiting step when methane concentration is much greater than the

half saturation constants (K_s) of methane uptake by *M. trichosporium* OB3b expressing sMMO and pMMO, which is not usually observed in natural systems. Therefore, it may be interesting to see how growth of pMMO- and sMMO- expressing methanotrophs are impacted by temperature if the methane concentration is significantly lower. The expression levels of pMMO and sMMO under different temperature conditions can be measured using real-time quantitative RT-PCR techniques developed in this study or competitive RT-PCR developed earlier (Han and Semrau, 2004) and correlated to the cell growth to examine how differential expression of these enzymes affect the growth of methanotrophs. It would also be interesting to see whether temperatures lower than 20˚C, e.g., 4˚C, differentially affect survivability and growth of the pMMO-expressing and sMMO-expressing methanotrophs and/or the expressions of pMMO and/or sMMO. These may be able to provide the rationale for difficulty in detection of sMMO transcripts in mRNA extracted from environmental samples (Lee et al., 2009). If consistent trends are observed from *in vitro* experiments with isolated cells, this study can be extended to the study of methanotrophic community *in situ*, e.g., the microbial community in landfill cover soil.

The expression of methane monooxygenase in facultative strains of methanotrophs in the absence of methane deserves a closer observation. In this study, we have observed that *M. daltona* SB2 was able to constitutively express pMMO in absence of methane. The quantity of expression, however, was found to decrease after prolonged period of absence of methane. It might be interesting to observe the change in expression of *pmo* genes upon periodical addition of methane along with the change in cell physiology associated with the shift in availability of methane. An unpublished set of

results in our laboratory indicated that addition of methane to *M. daltona* SB2 grown on acetate induces these cells to regain the higher growth rate observed in abundance of methane. If these cells are actually able to maintain relatively high levels of pMMO expression with occasional occurance of inducible methane concentration, such finding will provide significant enhancement in understanding and application of methanotrophs. Such cells may be the reason why overall methane reduction from atmosphere has been observed in habitats of methanotrophs where methane concentrations experience periodic fluctuations. Also, as mentioned above, community of facultative methanotroph might prove useful at developing more advanced bioremediation schemes *in situ*. As methanotrophs from diverse groups are discovered to be facultative, it is expected that there are facultative methanotrophs with broader physiological diversity. Among them might be cells that lack the regulation mechanism for downregulation of pMMO or sMMO expression in absence of methane. These cells may be involved with the enigmatic methanotrophy of atmospheric methane, as the growth and methane oxidation can be uncoupled in such cases as observed with the acetate and chlorinated ethenes in *M. daltona* SB2.

After more information is available about the facultative methanotrophs from laboratory experiments with isolated strains, provided that our hypotheses on the physiology of these cells prove to be true, the next step will be to extend our *in vitro* experiments to experiments *in situ*. To do so, probes or primers that can specifically target different facultative methanotrophs needs to be designed, as molecular analysis of total soil DNA and mRNA samples should be performed in parallel with the *in situ* measurement of methane and/or chlorinated ethene uptake rates. As methanotrophs in

these soils comprise at best a minority population, it might be essential to adopt state-of-art molecular technologies, e.g., DNA- or RNA- standard isotope probing (SIP) and/or metagenomic/metatranscriptomic analyses that enable the detection of difficult-to-culture subpopulations. Interactions of these bacteria with other groups of microorganisms can also be explored by analyzing metagenome and metatranscriptiome of these soil samples. If successful, this research topic will be able to address one of the most sought after question in the study of methanotrophs.

In this study the use of applying biotrickling filtration systems for removal of methane was considered. The model, however, has to be verified and refined with experimental data, as the feasibility and economical assessment was based solely on simplified mathematical models and data from pre-existing biofiltration systems designed for removal of other gaseous pollutants. A small-scale biofilter system should be constructed to acquire the experimental data. Based on the experimental results, the mathematical models will incorporate more subtleties such as the effect of a thin liquid layer between air and biofilm. With the refined model, more precise estimates of the cost and practical feasibility will be attainable. Molecular analysis of the microbial population in the biofilter will provide important pieces of information as well. The difference in the composition of microbial community analysis at different axial positions in the pilot-scale biofilter will be very useful information in improving the design, e.g., flow velocity, of the biofilter. The change in the composition over time will be critical information in long-term performance of methane biofilter. We can also observe the change in methanotrophic community structure as methane input concentration is varied and find

important information on methanotrophic population related with high-affinity methane oxidation.

With the methodology to screen for methanobactin synthesis in isolates of methanotrophs and more available genome sequences (or draft genome sequences) of methanotrophs, it may be finally possible to identify the genes involved with synthesis of methanobactin. There has been only one available genome sequence of methanotroph, i.e., *Methylococcus capsulatus* Bath. Recently, however, at least four more genome sequences of methanotrophic strains are either completed or nearly completed. The genome sequences of two strains representative of model mesophilic neutrophilic obligate methanotrophs, *Methylomicrobium album* BG8 and *Methylosinus trichosporium* OB3b, will be especially helpful in identifying methanobactin synthases. As mentioned above, methanobactin synthesis is likely to be involved in ribosomal or non-ribosomal peptide synthesis. There are signature genes in either pathway. The genes involved in NRPS are especially well conserved across different secondary metabolites and this enables relatively easy detection of such genes in genome sequences. In fact, from preliminary investigation of the draft genome of *M. trichosporium* OB3b (acquired by personal communication), unusually large number of putative NRPS genes were found, which was not observed in the genome of *M. capsulatus* Bath. As it is highly likely that expression of methanobactin synthesis is, to some degree, regulated by copper concentration, it might be possible to apply the real-time quantitative PCR developed in this study to find which, if any, NRPS genes are overexpressed in the presence of copper. Negative mutants of these suspect genes can then be screened for methanobactin production with the Cu-CAS plate assay. If none of the NRPS genes are found to be

relevant to the copper uptake and the gene cluster for ribosomal peptide synthesis is not identified, transposon mutagenesis can be employed for detection of a unique peptide-building mechanism *de novo*. The possibility of these genes being encoded from plasmids cannot be ruled out if the study on the chromosomal DNA does not provide any positive results.

REFERENCES

Aizpuru, A., Khammar, N., Malhautier, L., and Fanlo, J.L. (2003) Biofiltration for the treatment of complex mixtures of VOC - influence of the packing material. *Acta Biotechnol* 23: 211-226.

Alonso, C., Suidan, M.T., Sorial, G.A., Smith, F.L., Biswas, P., Smith, P.J., and Brenner, R.C. (1997) Gas treatment in trickle-bed biofilters: biomass, how much is enough? *Biotechnol Bioeng* 54: 583-594.

Alvarez-Cohen, L., and McCarty, P.L. (1991) Product toxicity and cometabolic competitive inhibition modeling of chloroform and trichloroethylene transformation by methanotrophic resting cells. *Appl Environ Microbiol* 57: 1031-1037.

Amaral, J.A., and Knowles, R. (1995) Growth of methanotrophs in methane and oxygen counter gradients. *FEMS Microbiol Lett* 126: 215-220.

Arcangeli, J.P., and Arvin, E. (1999) Modelling the growth of a methanotrophic biofilm: estimation of parameters and variability. *Biodegradation* 10: 177-191.

Auman, A.J., Stolyar, S., Costello, A.M., and Lidstrom, M.E. (2000) Molecular characterization of methanotrophic isolates from freshwater lake sediment. *Appl Environ Microbiol* 66: 5259-5266.

Bakke, B., Stewart, P.A., and Waters, M.A. (2007) Uses of and exposure to trichloroethylene in US industry: a systematic literature review. *J Occup Environ Hyg* 4: 375-390.

Balasubramanian, R., and Rosenzweig, A.C. (2008) Copper methanobactin: a molecule whose time has come. *Curr Opin Chem Biol* 12: 245-249.

Bambini, S., and Rappuoli, R. (2009) The use of genomics in microbial vaccine development. *Drug Discov Today* 14: 252-260.

Behling, L.A., Hartsel, S.C., Lewis, D.E., DiSpirito, A.A., Choi, D.W., Masterson, L.R. et al. (2008) NMR, mass spectrometry and chemical evidence reveal a different chemical structure for methanobactin that contains oxazolone rings. *J Am Chem Soc* 130: 12604-12605.

Blaha, D., Bartlett, K., Czepiel, P., Harriss, R., and Crill, P. (1999) Natural and anthropogenic methane sources in New England. *Atmos Environ* 33: 243-255.

Blazyk, J.L. and Lippard, S.J. (2002) Expression and characterization of ferredoxin and flavin adenine dinucleotide binding domains of the reductase component of soluble methane monooxygenase from *Methylococcus capsulatus* (Bath). *Biochemistry* 41: 15780-15794.

Blazyk, J.L. and Lippard, S.J. (2004) Domain engineering of the reductase component of soluble methane monooxygenase from *Methylococcus capsulatus* (Bath). *J Biol Chem* 279: 5630-5640.

Bodrossy, L., Holmes, E.M., Holmes, A.J., Kovacs, K.L., and Murrell, J.C. (1997) Analysis of 16S rRNA and methane monooxygenase gene sequences reveals a novel group of thermotolerant and thermophilic methanotrophs, *Methylocaldum* gen. nov. *Arch Microbiol* 168: 493-503.

Bodrossy, L., Kovács, K.L., McDonald, I.R., and Murrell, J.C. (1999) A novel thermophilic methane-oxidising *γ-Proteobacterium*. *FEMS Microbiol Lett* 170: 335-341.

Bodrossy, L., Stralis-Pavese, N., Murrell, J.C., Radajewski, S., Weilharter, A., and Sessitsch, A. (2003) Development and validation of a diagnostic microbial microarray for methanotrophs. *Environ Microbiol* 5: 566-582.

Bolt, H.M. (2005) Vinyl chloride - a classical industrial toxicant of new interest. *Crit Rev Toxicol* 35: 307-323.

Börjesson, G., Sundh, I., Tunlid, A., and Svensson, B.H. (1998) Methane oxidation in landfill cover soils, as revealed by potential oxidation measurements and phospholipid fatty acid analyses. *Soil Biol Biochem* 30: 1423-1433.

Bousquet, P., Ciais, P., Miller, J.B., Dlugokencky, E.J., Hauglustaine, D.A., Prigent, C., et al. (2006) Contribution of anthropogenic and natural sources to atmospheric methane variability. *Nature* 443: 439-443.

Bowman, J.P., McCammon, S.A., and Skerrat, J.H. (1997) *Methylosphaera hansonii* gen. nov., sp. nov., a psychrophilic, group I methanotroph from Antarctic marine-salinity, meromictic lakes. *Microbiology* 143: 1451-1459.

Brazeau, B.J., and Lipscomb, J.D. (1999) Effect of temperature on the methane monooxygenase compound Q formation and decay processes. *J Inorg Biochem* 74: 81-81.

Brazeau, B.J., and Lipscomb, J.D. (2000) Kinetics and activation thermodynamics of methane monooxygenase compound Q formation and reaction with substrates. *Biochemistry* 39: 13503-13515.

Brusseau, G.A., Tsien, H.C., Hanson, R.S., and Wackett, L.P. (1990) Optimization of trichloroethylene oxidation by methanotrophs and the use of a colorimetric assay to detect soluble methane monooxygenase activity. *Biodegradation* 1: 19-29.

Bull, I.D., Parekh, N.R., Hall, G.H., Ineson, P., and Evershed, R.P. (2000) Detection and classification of atmospheric methane oxidizing bacteria in soil. *Nature* 405: 175-178.

Cardy, D.L.N., Laidler, V., Salmond, G.P.C., and Murrell, J.C. (1991) Molecular analysis of the methane monooxygenase (MMO) gene cluster of *Methylosinus trichosporium* OB3b. *Mol Microbiol* 5: 335-342.

Carman, R.E., and Vincent, R.K. (1998) Measurements of soil gas and atmospheric methane content on one active and two inactive landfills in Wood County, Ohio. *Environ Eng Geosci* **4**: 317-329.

Carreró, M.I.G., Sangari, F.J., Agüero, J., and Lobo, J.M.G. (2002) *Brucella abortus* strain 2308 produces brucebactin, a highly efficient catecholic siderophore. *Microbiology* 148: 353-360.

Cha, S.K., and Abruna, H.D. (2002) Determination of copper at electrodes modified with ligands of varying coordination strength: a preamble to speciation studies. *Anal Chem* 62: 274-278.

Challis, G.L. (2005) A widely distributed bacterial pathway for siderophore biosynthesis independent of nonribosomal peptide synthetases. *ChemBioChem* 6: 601-611.

Challis, G.L., and Naismith, J.H. (2004) Structural aspects of non-ribosomal peptide biosynthesis. *Curr Opin Struct Biol* 14: 748-756.

Challis, G.L., Ravel, J., and Townsend, C.A. (2000) Predictive, structure-based model of amino acid recognition by nonribosomal peptide synthetase adenylation domains. *Chem Biol* 7: 211-224.

Chan, S.I., Chen, K.H.C., Yu, S.S.F., Chen, C.-L., and Kuo, S.S.J. (2004) Toward delineating the structure and function of the particulate methane monooxygenase from methanotrophic bacteria. *Biochemistry* 43: 4421-4430.

Chang, H.L., and Alvarez-Cohen, L. (1996) Biodegradation of individual and multiple chlorinated aliphatic hydrocarbons by methane-oxidizing cultures. *Appl Environ Microbiol* 62: 3371-3377.

Chatwood, L.L., Müller, J., Gross, J.D., Wagner, G., and Lippard, S.J. (2004) NMR structure of the flavin domain from soluble methane monooxygenase reductase from *Methylococcus capsulatus* (Bath). *Biochemistry* 43: 11983-11991.

Cheng, W.H. and Kung, H.H. (1994) Methanol Production and Use: Marcel Dekker, Inc., New York.

Choi, D.W., Antholine, W.E., Do, Y.S., Semrau, J.D., Kisting, C.J., Kunz, R.C., et al. (2005) Effect of methanobactin on the activity and electron paramagnetic resonance spectra of the membrane-associated methane monooxygenase in *Methylococcus capsulatus* Bath. *Microbiology* 151: 3417-3426.

Choi, D.W., Kunz, R.C., Boyd, E.S., Semrau, J.D., Antholine, W.E., Han, J.I., et al. (2003) The membrane-associated methane monooxygenase (pMMO) and pMMO-NADH:quinone oxidoreductase complex from *Methylococcus capsulatus* Bath. *J Bacteriol* 185: 5755-5764.

Choi, D.W., Semrau, J.D., Antholine, W.E., Hartsel, S.C., Anderson, R.C., Carey, J.N., et al. (2008) Oxidase, superoxide dismutase, and hydrogen peroxide reductase activities of methanobactin from types I and II methanotrophs. *J Inorg Biochem* 102: 1571-1580.

Choi, D.W., Zea, C.J., Do, Y.S., Semrau, J.D., Antholine, W.E., Hargrove, M.S., et al. (2006a) Spectral, kinetic, and thermodynamic properties of Cu(I) and Cu(II) binding by methanobactin from *Methylosinus trichosporium* OB3b. *Biochemistry* 45: 1442-1453.

Choi, D.W., Do, Y.S., Zea, C.J., McEllistrem, M.T., Lee, S.W., Semrau, J.D., et al. (2006b) Spectral and thermodynamic properties of Ag(I), Au(III), Cd(II), Co(II), Fe(III), Hg(II), Mn(II), Ni(II), Pb(II), U(IV), and Zn(II) binding by methanobactin from *Methylosinus trichosporium* OB3b. *J Inorg Biochem* 100: 2150-2161.

Chu-Ky, S., Tourdot-Marechal, R., Marechal, P.A., and Guzzo, J. (2005) Combined cold, acid, ethanol shocks in *Oenococcus oeni*: Effects on membrane fluidity and cell viability. *Biochim Biophys Acta (BBA) - Biomembranes* 1717: 118-124.

Cohen, Y. (2001) Biofiltration - the treatment of fluids by microorganisms immobilized into the filter bedding material: a review. *Bioresour Technol* 77: 257-274.

Colby, J., and Dalton, H. (1978) Resolution of the methane mono-oxygenase of *Methylococcus capsulatus* (Bath) into three components. Purification and properties of component C, a flavoprotein. *Biochem J* 171: 461-468.

Colby, J., Stirling, D.I., and Dalton, H. (1977) The soluble methane mono-oxygenase of *Methylococcus capsulatus* (Bath) - its ability to oxygenate *n*-alkanes, *n*-alkenes, ethers, and alicyclic aromatic and heterocyclic compounds. *Biochem J* 165: 395-402.

Coleman, N.V., Mattes, T.E., Gossett, J.M., and Spain, J.C. (2002) Phylogenetic and kinetic diversity of aerobic vinyl chloride-assimilating bacteria from contaminated sites. *Appl Environ Microbiol* 68: 6162-6171.

Costello, A.M., and Lidstrom, M.E. (1999) Molecular characterization of functional and phylogenetic genes from natural populations of methanotrophs in lake sediments. *Appl Environ Microbiol* 65: 5066-5074.

Cox, H.H.J., and Deshusses, M.A. (1999) Chemical removal of biomass from waste air biotrickling filters: screening of chemicals of potential interest. *Water Res* 33: 2383-2391.

Cox, H.H.J., and Deshusses, M.A. (2002) Biotrickling filters for air pollution control. In The encyclopedia of environmental microbiology. Bitton, G. (ed). New York, NY, USA: John Wiley & Sons, pp. 782-795.

Cox, H.H.J., Moerman, R.E., van Baalen, S., van Heiningen, W.N.M., Doddema, H.J., and Harder, W. (1997) Performance of a styrene-degrading biofilter containing the yeast *Exophiala jeanselmei*. *Biotechnol Bioeng* 53: 259-266.

Crosa, J.H., and Walsh, C.T. (2002) Genetics and assembly line enzymology of siderophore biosynthesis in bacteria. *Microbiol Mol Biol Rev* 66: 223-249.

Csáki, R., Bodrossy, L., Klem, J., Murrell, J.C., and Kovács, K.L. (2003) Genes involved in the copper-dependent regulation of soluble methane monooxygenase of *Methylococcus capsulatus* (Bath): cloning, sequencing and mutational analysis. *Microbiology* 149: 1785-1795.

Dalton, H. (1991) Structure and mechanism of action of the enzyme(s) involved in methane oxidation. In Applications of Enzyme Biotechnology. Kelly, J.W., Baldwin, T.O. (eds). New York, NY, USA: Plenum, pp. 55-68.

Dedysh, S.N., Liesack, W., Khmelenina, V.N., Suzina, N.E., Trotsenko, Y.A., Semrau, J.D., et al. (2000) *Methylocella palustris* gen. nov., sp. nov., a new methane-oxidizing acidophilic bacterium from peat bogs, representing a novel subtype of serine-pathway methanotrophs. *Int J Syst Evol Microbiol* 50: 955-969.

Dedysh, S.N., Knief, C., and Dunfield, P.F. (2005) *Methylocella* species are facultatively methanotrophic. *J Bacteriol* 187: 4665-4670.

Dedysh, S.N., Khmelenina, V.N., Suzina, N., Trotsenko, Y.A., Semrau, J.D., Liesack, W., and Tiedje, J.M. (2002) *Methylocapsa acidiphila* gen. nov., sp. nov., a novel methane-oxidizing and dinitrogen-fixing acidophilic bacterium from Sphagnum bog. *Int J Syst Evol Microbiol* 52: 251-261.

Dedysh, S.N., Panikov, N.S., and Tiedje, J.M. (1998) Acidophilic methanotrophic communities from sphagnum peat bogs. *Appl Environ Microbiol 64*: 922-929.

Demain, A.L., and Sanchez, S. (2009) Microbial drug discovery: 80 years of progress. *J Antibiot* 62: 5-16.

DiSpirito, A.A., Zahn, J.A., Graham, D.W., Kim, H.J., Larive, C.K., Derrick, T.S., et al. (1998) Copper-binding compounds from *Methylosinus trichosporium* OB3b. *J Bacteriol* 180: 3606-3613.

Dunfield, P.F., Belova, S.E., Vorob'ev, A.V., Cornish, S.L., and Dedysh, S.N. (2010) *Methylocapsa aurea* sp. nov., a facultatively methanotrophic bacterium possessing a particulate methane monooxygenase. *Int J Syst Evol Microbiol*, DOI: doi:ijs.0.020149-0

Dunfield, P.F. and Conrad, R. (2000) Starvation alters the apparent half-saturation constant for methane in the type II methanotroph *Methylocystis* strain LR1. *Appl Environ Microbiol* 66: 4136-4138.

Dunfield, P.F., Khmelenina, V.N., Suzina, N.E., Trotsenko, Y.A., and Dedysh, S.N. (2003) *Methylocella silvestris* sp. nov., a novel methanotroph isolated from an acidic forest cambisol. *Int J Syst Evol Microbiol* 53: 1231-1239.

Dunfield, P.F., Liesack, W., Henckel, T., Knowles, R., and Conrad, R. (1999) High-affinity methane oxidation by a soil enrichment culture containing a type II methanotroph. *Appl Environ Microbiol* 65: 1009-1014.

Dunfield, P.F., Yuryev, A., Senin, P., Smirnova, A.V., Stott, M.B., Hou, S., et al. (2007) Methane oxidation by an extremely acidophilic bacterium of the phylum *Verrucomicrobia*. *Nature* 450: 879-882.

EIA (2007). Average retail price of electricity to ultimate customers by end-use sector. URL http://www.eia.doe.gov/cneaf/electricity/epa/epat7p4

Elango, N.A., Radhakrishnan, R., Froland, W.A., Wallar, B.J., Earhart, C.A., Lipscomb, J.D., and Ohlendorf, D.H. (1997) Crystal structure of the hydroxylase component of

methane monooxygenase from *Methylosinus trichosporium* OB3b. *Protein Sci* 6: 556-568.

Etheridge, D.M., Steele, L.P., Francey, R.J., and Langenfelds, R.L. (1998) Atmospheric methane between 1000 A.D. and present: evidence of anthropogenic emissions and climatic variability. *J Geophys Res* 103: 15979-15993.

Fitch, M.W., Graham, D.W., Arnold, R.G., Agarwal, S.K., Phelps, P., Speitel, G.E., Jr, and Georgiou, G. (1993) Phenotypic characterization of copper-resistant mutants of *Methylosinus trichosporium* OB3b. *Appl Environ Microbiol* 59: 2771-2776.

Fogel, M.M., Taddeo, A.R., and Fogel, S. (1986) Biodegradation of chlorinated ethenes by a methane-utilizing mixed culture. *Appl Environ Microbiol* 51: 720-724.

Fontaine, L., and Hols, P. (2008) The inhibitory spectrum of thermophilin 9 from *Streptococcus thermophilus* LMD-9 depends on the production of multiple peptides and the activity of BlpGSt, a thiol-disulfide oxidase. *Appl Environ Microbiol* 74: 1102-1110.

Foster, J.W., and Davis, R.H. (1966) A methane-dependent coccus, with notes on classification and nomenclature of obligate, methane-utilizing bacteria. *J Bacteriol* 91: 1924-1931.

Fox, B.G., Froland, W.A., Dege, J.E., and Lipscomb, J.D. (1989) Methane monooxygenase from *Methylosinus trichosporium* OB3b. Purification and properties of a three-component system with high specific activity from a type II methanotroph. *J Biol Chem* 264: 10023-10033.

Fox, B.G., Borneman, J.G., Wackett, L.P., and Lipscomb, J.D.(1990) Haloalkene oxidation by the soluble methane monooxygenase from *Methylosinus trichosporium* OB3b: mechanistic and environmental implications. *Biochemistry* 29: 6419-6427.

Freedman, D.L. and Gossett, J.M. (1989) Biological reductive dechlorination of tetrachloroethylene and trichloroethylene to ethylene under methanogenic conditions. *Appl Environ Microbiol* 55: 2144-2151.

Fry, V.A., Istok, J.D., Semprini, L., O'Reilly, K.T., and Buscheck, T.E. (1995) Retardation of dissolved oxygen due to a trapped gas phase in porous media. *Ground Water* 33: 391-398.

Fung, I., John, J., Lerner, J., Matthews, E., Prather, M., Steele, L.P., and Fraser, P.J. (1991) Three-dimensional model synthesis of the global methane cycle. *J Geophys Res* 96: 13033-13065.

Futamata, H., Harayama, S., and Watanabe, K. (2001) Diversity in kinetics of trichloroethylene-degrading activities exhibited by phenol-degrading bacteria. *Appl Microbiol Biotechnol* 55: 248-253.

Gabriel, D. and Deshusses, M.A. (2003) Retrofitting existing chemical scrubbers to biotrickling filters for H_2S emission control. *Proc Nat Acad Sci USA* 100: 6308-6312.

Gabriel, D., Cox, H.H.J., and Deshusses, M.A. (2004) Conversion of full-scale wet scrubbers to biotrickling filters for H_2S control at publicly owned treatment works. *J Environ Eng* 130: 1110-1117.

Gadgil, M., Kapur, V., and Hu, W.S. (2005) Transcriptional response of *Escherichia coli* to temperature shift. *Biotechnol Prog* 21: 689-699.

Gebert, J. and Gröngröft, A. (2006) Performance of a passively vented field-scale biofilter for the microbial oxidation of landfill methane. *Waste Manag* 26: 399-407.

Gebert, J., Groengroeft, A., and Miehlich, G. (2003) Kinetics of microbial landfill methane oxidation in biofilters. *Waste Manag* 23: 609-619.

Gilbert, B., McDonald, I.R., Finch, R., Stafford, G.P., Nielsen, A.K., and Murrell, J.C. (2000) Molecular analysis of the pmo (particulate methane monooxygenase) operons from two type II methanotrophs. *Appl Environ Microbiol* 66: 966-975.

Gossett, J.M. (1987) Measurement of Henry's law constants for C1 and C2 chlorinated hydrocarbons. *Environ Sci Technol* 21: 202-208.

Green, J., and Dalton, H. (1986) Steady-state kinetic analysis of soluble methane mono-oxygenase from *Methylococcus capsulatus* (Bath). *Biochem J* 236: 155-162.

Haas, H. (2003) Molecular genetics of fungal siderophore biosynthesis and uptake: the role of siderophores in iron uptake and storage. *Appl Microbiol Biotechnol* 62: 316-330.

Hakemian, A.S., Kondapalli, K.C., Telser, J., Hoffman, B.M., Stemmler, T.L., and Rosenzweig, A.C. (2008) The metal centers of particulate methane monooxygenase from *Methylosinus trichosporium* OB3b. *Biochemistry* 47: 6793-6801.

Han, J.I., Lontoh, S., and Semrau, J.D. (1999) Degradation of chlorinated and brominated hydrocarbons by *Methylomicrobium album* BG8. *Arch Microbiol* 172: 393-400.

Han, J.I., and Semrau, J.D. (2004) Quantification of gene expression in methanotrophs by competitive reverse transcription-polymerase chain reaction. *Environ Microbiol* 6: 388-399.

Hanson, R.S., and Hanson, T.S. (1996) Methanotrophic bacteria. *Microbiol Rev* 60: 439-471.

Hartman, B. (1998) Investigation and remediation: oh Henry! (a constant). *LUSTLine Bull* 29: 17-18.

Hildebrand, J.H. (1969) Relative diffusivities of methane in water and carbon tetrachloride. *Proc Nat Acad Sci USA* 64: 1329-1330.

Holmes, A.J., Costello, A.M., Lidstrom, M.E., and Murrell, J.C. (1995) Evidence that participate methane monooxygenase and ammonia monooxygenase may be evolutionarily related. *FEMS Microbiol Lett* 132: 203-208.

Hou, S., Makarova, K., Saw, J., Senin, P., Ly, B., Zhou, Z. et al. (2008) Complete genome sequence of the extremely acidophilic methanotroph isolate V4, *Methylacidiphilum infernorum*, a representative of the bacterial phylum *Verrucomicrobia*. *Biol Direct* 3: 26-50.

IPCC (2007). Climate change 2007: the physical science basis: contribution of working group I to the fourth assessment report of the intergovernmental panel on climate change; technical summary. URL http://www.ipcc.ch/pdf/assessment-report/ar4/wg1/ar4-wg1-ts.pdf

Iranpour, R., Coxa, H.H.J., Deshusses, M.A., and Schroeder, E.D. (2005) Literature review of air pollution control biofilters and biotrickling filters for odor and volatile organic compound removal. *Environ Prog* 24: 254-267.

Islam, T., Jensen, S., Reigstad, L.J., Larsen, Ø ., and Birkeland, N.-K. (2008) Methane oxidation at 55°C and pH 2 by a thermoacidophilic bacterium belonging to the *Verrucomicrobia* phylum. *Proc Nat Acad Sci USA* 105: 300-304.

Kennes, C., and Veiga, M.C. (2002) Inert filter media for the biofiltration of waste gases: characteristics and biomass control. *Rev Environ Sci Biotechnol* 1: 201-214.

Kennes, C., Cox, H.H.J., Doddema, H.J., and Harder, W. (1996) Design and performance of biofilters for the removal of alkylbenzene vapors. *J Chem Technol Biotechnol* 66: 300-304.

Khmelenina, V.N., Kalyuzhnaya, M.G., Starostina, N.G., Suzina, N.E., and Trotsenko, Y.A. (1997) Isolation and characterization of halotolerant alkaliphilic methanotrophic bacteria from Tuva soda lakes. *Curr Microbiol* 35: 257-261.

Kim, H.J., Galeva, N., Larive, C.K., Alterman, M., and Graham, D.W. (2005) Purification and physical-chemical properties of methanobactin: a chalkophore from *Methylosinus trichosporium* OB3b. *Biochemistry* 44: 5140-5148.

Kim, H.J., Graham, D.W., DiSpirito, A.A., Alterman, M.A., Galeva, N., Larive, C.K. et al. (2004) Methanobactin, a copper-acquisition compound from methane-oxidizing bacteria. *Science* 305: 1612-1615.

King, G.M. (1992) Ecological aspects of methane oxidation, a key determinant of global methane dynamics. *Adv Microb Ecol* 12: 431-468.

Knapp, C.W., Fowle, D.A., Kulczycki, E., Roberts, J.A., and Graham, D.W. (2007) Methane monooxygenase gene expression mediated by methanobactin in the presence of mineral copper sources. *Proc Nat Acad Sci USA* 104: 12040-12045.

Knief, C., Vanitchung, S., Harvey, N.W., Conrad, R., Dunfield, P.F., and Chidthaisong, A. (2005) Diversity of methanotrophic bacteria in tropical upland soils under different land uses. *Appl Environ Microbiol* 71: 3826-3831.

Konz, D., and Marahiel, M.A. (1999) How do peptide synthetases generate structural diversity? *Chem Biol* 6: R39-R48.

Kraemer, S.M. (2004) Iron oxide dissolution and solubility in the presence of siderophores. *Aquat Sci - Res Across Bound* 66: 3-18.

Krylov, O.V. (1993) Catalytic reactions of partial methane oxidation. *Catal Today* 18: 209-302.

Lane, D.J. (1991) 16S/23S rRNA sequencing. In Nucleic Acid Techniques in Bacterial Systematics. Stackebrant, E., Goodfellow, M. (eds). New York, NY, USA: John Wiley & Sons, pp 115-175.

Le Mer, J., and Roger, P. (2001) Production, oxidation, emission and consumption of methane by soils: a review. *Eur J Soil Biol* 37: 25-50.

Le Texier, H., Solomon, S., and Garcia, R.R. (1988) The role of molecular hydrogen and methane oxidation in the water vapour budget of the stratosphere. *Q J R Meteorol Soc* 114: 281-295.

Leahy, J.G., Batchelor, P.J., and Morcomb, S.M. (2003) Evolution of the soluble diiron monooxygenases. *FEMS Microbiol Rev* 27: 449-479.

Lee, S.K., and Lipscomb, J.D. (1999) Oxygen activation catalyzed by methane monooxygenase hydroxylase component: proton delivery during the O-O bond cleavage steps. *Biochemistry* 38: 4423-4432.

Lee, S.K., Nesheim, J.C., and Lipscomb, J.D. (1993) Transient intermediates of the methane monooxygenase catalytic cycle. *J Biol Chem* 268: 21569-21577.

Lee, S.W., Keeney, D.R., Lim, D.H., Dispirito, A.A., and Semrau, J.D. (2006) Mixed pollutant degradation by *Methylosinus trichosporium* OB3b expressing either soluble or particulate methane monooxygenase: can the tortoise beat the hare? *Appl Environ Microbiol* 72: 7503-7509.

Lee, S.W., Im, J., DiSpirito, A.A., Bodrossy, L., Barcelona, M., and Semrau, J.D. (2009) Effect of nutrient and selective inhibitor amendments on methane oxidation, nitrous oxide production, and key gene presence and expression in landfill cover soils: characterization of the role of methanotrophs, nitrifiers, and denitrifiers. *Appl Microbiol Biotechnol* 85: 389-403.

Lemos, S.S., Collins, M.L.P., Eaton, S.S., Eaton, G.R., and Antholine, W.E. (2000) Comparison of EPR-visible Cu^{2+} sites in pMMO from *Methylococcus capsulatus* (Bath) and *Methylomicrobium album* BG8. *Biophys J* 79: 1085-1094.

Lidstrom, M.E. (1988) Isolation and characterization of marine methanotrophs. *Antonie van Leeuwenhoek* 54: 189-199.

Lieberman, R.L., and Rosenzweig, A.C. (2004) Biological methane oxidation: regulation, biochemistry, and active site structure of particulate methane monooxygenase. *Crit Rev Biochem Mol Biol* 39: 147-164.

Lieberman, R.L., and Rosenzweig, A.C. (2005) Crystal structure of a membrane-bound metalloenzyme that catalyses the biological oxidation of methane. *Nature* 434: 177-182.

Lieberman, R.L., Shrestha, D.B., Doan, P.E., Hoffman, B.M., Stemmler, T.L., and Rosenzweig, A.C. (2003) Purified particulate methane monooxygenase from *Methylococcus capsulatus* (Bath) is a dimer with both mononuclear copper and a copper-containing cluster. *Proc Nat Acad Sci USA* 100: 3820-3825.

Lieberman, R.L., Kondapalli, K.C., Shrestha, D.B., Hakemian, A.S., Smith, S.M., Telser, J. et al. (2006) Characterization of the particulate methane monooxygenase metal centers in multiple redox states by X-ray absorption spectroscopy. *Inorg Chem* 45: 8372-8381.

Lipscomb, J.D. (1994) Biochemistry of the soluble methane monooxygenase. *Ann Rev Microbiol* 48: 371-399.

Liu, K.E., Wang, D., Huynh, B.H., Edmondson, D.E., Salifoglou, A., and Lippard, S.J. (1994) Spectroscopic detection of intermediates in the reaction of dioxygen with the reduced methane monooxygenase/hydroxylase from *Methylococcus capsulatus* (Bath). *J Am Chem Soc* 116: 7465-7466.

Liu, Y., Nesheim, J.C., Lee, S.-K., and Lipscomb, J.D. (1995) Gating effects of component B on oxygen activation by the methane monooxygenase hydroxylase component. *J Biol Chem* 270: 24662-24665.

Lontoh, S., and Semrau, J.D. (1998) Methane and trichloroethylene degradation by *Methylosinus trichosporium* OB3b expressing particulate methane monooxygenase. *Appl Environ Microbiol* 64: 1106-1114.

Lontoh, S., Zahn, J.A., DiSpirito, A.A., and Semrau, J.D. (2000) Identification of intermediates of in vivo trichloroethylene oxidation by the membrane-associated methane monooxygenase. *FEMS Microbiol Lett* 186: 109-113.

Malashenko, I.R., Romanovskaia, V.A., Bogachenko, V.N., and Shved, A.D. (1975) Thermophilic and thermotolerant bacteria that assimilate methane. *Mikrobiologiia* 44: 855-862.

Martell, A.E., Smith, R.M., and Motekaitis, R.J. (2001) NIST critically selected stability constants of metal complexes. NIST standard reference database 46, Version 6.0, NIST Gaithersburg, MD.

Martinho, M., Choi, D.W., DiSpirito, A.A., Antholine, W.E., Semrau, J.D., and Munck, E. (2007) Mossbauer studies of the membrane-associated methane monooxygenase from *Methylococcus capsulatus* Bath: evidence for a diiron center. *J Am Chem Soc* 129: 15783-15785.

Maymo-Gatell, X., Anguish, T., and Zinder, S.H. (1999) Reductive dechlorination of chlorinated ethenes and 1,2-dichloroethane by "*Dehalococcoides ethenogenes*" 195. *Appl Environ Microbiol* 65: 3108-3113.

McCue, T., Hoxworth, S., and Randall, A.A. (2002) Degradation of halogenated aliphatic compounds utilizing sequential anaerobic/aerobic treatments. *Water Sci Technol*: 47:79-84.

McDonald, I.R., Miguez, C.B., Rogge, G., Bourque, D., Wendlandt, K.D., Groleau, D., and Murrell, J.C. (2006) Diversity of soluble methane monooxygenase-containing methanotrophs isolated from polluted environments. *FEMS Microbiol Lett* 255: 225-232.

McIntosh, J.A., Donia, M.S., and Schmidt, E.W. (2009) Ribosomal peptide natural products: bridging the ribosomal and nonribosomal worlds. *Nat Prod Rep* 26: 537-559.

Melse, R.W., and Van der Werf, A.W. (2005) Biofiltration for mitigation of methane emission from animal husbandry. *Environ Sci Technol* 39: 5460-5468.

Merkx, M., and Lippard, S.J. (2002) Why OrfY? Characterization of mmoD, a long overlooked component of the soluble methane monooxygenase from *Methylococcus capsulatus* (Bath). *J Biol Chem* 277: 5858-5865.

Milagres, A.M.F., Machuca, A., and Napoleão, D. (1999) Detection of siderophore production from several fungi and bacteria by a modification of chrome azurol S (CAS) agar plate assay. *J Microbiol Methods* 37: 1-6.

Milne, J.C., Roy, R.S., Eliot, A.C., Kelleher, N.L., Wokhlu, A., Nickels, B., and Walsh, C.T. (1999) Cofactor requirements and reconstitution of microcin B17 synthetase: a multienzyme complex that catalyzes the formation of oxazoles and thiazoles in the antibiotic microcin B17 *Biochemistry* 38: 4768-4781.

Miyaji, A., Kamachi, T., and Okura, I. (2002) Improvement of the purification method for retaining the activity of the particulate methane monooxygenase from *Methylosinus trichosporium* OB3b. *Biotechnol Lett* 24: 1883-1887.

Mootz, H.D., Schwarzer, D., and Marahiel, M.A. (2002) Ways of assembling complex natural products on modular nonribosomal peptide synthetases. *ChemBioChem* 3: 490-504.

Morel, F.M. and Hering, J.G. (1991) Principles and Application of Aquatic Chemistry. New York, NY, USA: John Wiley & Sons.

Morii, H., and Kasama, K. (2004) Activity of two histidine decarboxylases from *Photobacterium phosphoreum* at different temperatures, pHs, and NaCl concentrations. *J Food Prot* 67: 1736-1742.

Morton, J.D., Hayes, K.F., and Semrau, J.D. (2000a) Bioavailability of chelated and soil-adsorbed copper to *Methylosinus trichosporium* OB3b. *Environ Sci Technol* 34: 4917-4922.

Morton, J.D., Hayes, K.F., and Semrau, J.D. (2000b) Effect of copper speciation on whole-cell soluble methane monooxygenase activity in *Methylosinus trichosporium* OB3b. *Appl Environ Microbiol* 66: 1730-1733.

Müller, J., Lugovskoy, A.A., Wagner, G., and Lippard, S.J. (2002) NMR structure of the [2Fe-2S] ferredoxin domain from soluble methane monooxygenase reductase and interaction with its hydroxylase. *Biochemistry* 41: 42-51.

Murrell, J.C., Gilbert, B., and McDonald, I.R. (2000a) Molecular biology and regulation of methane monooxygenase. *Arch Microbiol* 173: 325-332.

Murrell, J.C., McDonald, I.R., and Gilbert, B. (2000b) Regulation of expression of methane monooxygenases by copper ions. *Trends Microbiol* 8: 221-225.

Nguyen, H.H.T., Elliott, S.J., Yip, J.H.K., and Chan, S.I. (1998) The particulate methane monooxygenase from *Methylococcus capsulatus* (Bath) Is a novel copper-containing three-subunit enzyme. Isolation and characterization. *J Biol Chem* 273: 7957-7966.

Nguyen, H.H.T., Shiemke, A.K., Jacobs, S.J., Hales, B.J., Lidstrom, M.E., and Chan, S.I. (1994) The nature of the copper ions in the membranes containing the particulate methane monooxygenase from *Methylococcus capsulatus* (Bath). *J Biol Chem* 269: 14995-15005.

Nielsen, A.K., Gerdes, K., and Murrell, J.C. (1997) Copper-dependent reciprocal transcriptional regulation of methane monooxygenase genes in *Methylococcus capsulatus* and *Methylosinus trichosporium*. *Mol Microbiol* 25: 399-409.

Nielsen, A.K., Gerdes, K., Degn, H., and Murrell, J.C. (1996) Regulation of bacterial methane oxidation: transcription of the soluble methane mono-oxygenase operon of *Methylococcus capsulatus* (Bath) is repressed by copper ions. *Microbiology* 142: 1289-1296.

Nikiema, J., Bibeau, L., Lavoie, J., Brzezinski, R., Vigneux, J., and Heitz, M. (2005) Biofiltration of methane: an experimental study. *Chem Eng J* 113: 111-117.

Okkerse, W.J.H., Ottengraf, S.P.P., Diks, R.M.M., Osinga-Kuipers, B., and Jacobs, P. (1999) Long term performance of biotrickling filters removing a mixture of volatile organic compounds from an artificial waste gas: dichloromethane and methylmethacrylate. *Bioprocess Eng* 20: 49-57.

Oldenhuis, R., Vink, R.L., Janssen, D.B., and Witholt, B. (1989) Degradation of chlorinated aliphatic hydrocarbons by *Methylosinus trichosporium* OB3b expressing soluble methane monooxygenase. *Appl Environ Microbiol* 55: 2819-2826.

Oldenhuis, R., Oedzes, J.Y., van der Waarde, J.J., and Janssen, D.B. (1991) Kinetics of chlorinated hydrocarbon degradation by *Methylosinus trichosporium* OB3b and toxicity of trichloroethylene. *Appl Environ Microbiol* 57: 7-14.

Olivieri, N.F., and Brittenham, G.M. (1997) Iron-chelating therapy and the treatment of thalassemia. *Blood* 89: 739-761.

Omelchenko, M.V., Vasilyeva, L.V., and Zavarzin, G.A. (1993) Psychrophilic methanotroph from tundra soil. *Curr Microbiol* 27: 255-259.

Paik, S.H., Chakicherla, A., and Hansen, J.N. (1998) Identification and characterization of the structural and transporter genes for, and the chemical and biological properties of, sublancin 168, a novel lantibiotic produced by *Bacillus subtilis* 168. *J Biol Chem* 273: 23134-23142.

Parliamentary Office of Science and Technology, U.K. (2006) Carbon footprint of electricity generation. POST Rep. 66.

Perry, J.H. (1984) *Chemical Engineers' Handbook*: McGraw-Hill Book Co., New York.

Pfeifer, B.A., Wang, C.C.C., Walsh, C.T., and Khosla, C. (2003) Biosynthesis of yersiniabactin, a complex polyketide-nonribosomal peptide, using *Escherichia coli* as a heterologous host. *Appl Environ Microbiol* 69: 6698-6702.

Phelps, P.A., Agarwal, S.K., Speitel, G.E., Jr., and Georgiou, G. (1992) *Methylosinus trichosporium* OB3b mutants having constitutive expression of soluble methane monooxygenase in the presence of high levels of copper. *Appl Environ Microbiol* 58: 3701-3708.

Pol, A., Heijmans, K., Harhangi, H.R., Tedesco, D., Jetten, M.S.M., and Op den Camp, H.J.M. (2007) Methanotrophy below pH 1 by a new Verrucomicrobia species. *Nature* 450: 874-878.

Poret-Peterson, A.T., Graham, J.E., Gulledge, J., and Klotz, M.G. (2008) Transcription of nitrification genes by the methane-oxidizing bacterium, *Methylococcus capsulatus* strain Bath. ISME J 2: 1213-1220.

Prior, S.D., and Dalton, H. (1985) The effect of copper ions on membrane content and methane monooxygenase activity in methanol-grown cells of *Methylococcus capsulatus* (Bath). J Gen Microbiol 131: 155-163.

Ratledge, C., and Dover, L.G. (2000) Iron metabolism in pathogenic bacteria. *Ann Rev Microbiol* 54: 881-941.

Reshetnikov, A.S., Mustakhimov, I.I., Khmelenina, V.N., and Trotsenko, Y.A. (2005) Cloning, purification, and characterization of diaminobutyrate acetyltransferase from the halotolerant methanotroph *Methylomicrobium alcaliphilum* 20Z. *Biochem-Moscow* 70: 878-883.

Rittman, B.E. (1982) The effect of shear stress on biofilm loss rate. *Biotechnol Bioeng* 24: 501-506.

Rodhe, H. (1990) A comparison of the contribution of various gases to the greenhouse effect. *Science* 248: 1217-1219.

Rosenzweig, A.C., Frederick, C.A., Lippard, S.J., Nordlund, P., and auml (1993) Crystal structure of a bacterial non-haem iron hydroxylase that catalyses the biological oxidation of methane. *Nature* 366: 537-543.

Rosenzweig, A.C., Nordlund, P., Takahara, P.M., Frederick, C.A., and Lippard, S.J. (1995) Geometry of the soluble methane monooxygenase catalytic diiron center in two oxidation states. *Chem Biol* 2: 409-418.

Rozen, S. and Skaletsky, H. (2000) Primer3 on the WWW for general users and for biologist programmers. In Bioinformatics Methods and Protocols: Methods in Molecular Biology. Krawetz, S., Misener, S. (eds). Totowa, NJ, USA: Humana Press, pp 365-386.

Schwarzer, D., Finking, R., and Marahiel, M.A. (2003) Nonribosomal peptides: from genes to products. *Nat Prod Rep* 20: 275-287.

Schwyn, B. and Neilands, J.B. (1987) Universal chemical assay for the detection and determination of siderophores. *Anal Biochem* 160: 47-56.

Scott, C.S., and Chiu, W.A. (2006) Trichloroethylene cancer epidemiology: a consideration of select issues. *Environ Health Perspect* 114: 1471-1478.

Semrau, J.D., Chistoserdov, A., Lebron, J., Costello, A., Davagnino, J., Kenna, E. et al. (1995) Particulate methane monooxygenase genes in methanotrophs. *J Bacteriol* 177: 3071-3079.

Semrau, J.D., DiSpirito, A.A., and Murrell, J.C. (2008) Life in the extreme: thermoacidophilic methanotrophy. *Trends Microbiol* 16: 190-193.

Semrau, J.D., DiSpirito, A.A., and Yoon, S. (2010) Methanotrophs and copper. FEMS Microbiol Rev, DOI: 10.1111/j.1574-6976.2010.00212.x

Shen, B., Du, L., Sanchez, C., Edwards, D.J., Chen, M., and Murrell, J.M. (2001) The biosynthetic gene cluster for the anticancer drug bleomycin from *Streptomyces verticillus* ATCC15003 as a model for hybrid peptide–polyketide natural product biosynthesis. *J Ind Microbiol Biotechnol* 27: 378-385.

Shen, B., Du, L., Sanchez, C., Edwards, D.J., Chen, M., and Murrell, J.M. (2002) Cloning and characterization of the bleomycin biosynthetic gene cluster from *Streptomyces verticillus* ATCC150031. *J Nat Prod* 65: 422-431.

Shenker, M., Chen, Y., and Hadar, Y. (1995) Rapid method for accurate determination of colorless siderophores and synthetic chelates. *Soil Sci Soc Am J* 59: 1612-1618.

Sipkema, E.M., de Koning, W., Ganzeveld, K.J., Janssen, D.B., and Beenackers, A.A.C.M. (1998) Experimental pulse technique for the study of microbial kinetics in continuous culture. *J Biotechnol* 64: 159-176.

Song, J., and Kinney, K.A. (2001) Effect of directional switching frequency on toluene degradation in a vapor-phase bioreactor. *Appl Microbiol Biotechnol* 56: 108-113.

Sorokin, D.Y., Jones, B.E., and Kuenen, J.G. (2000) An obligate methylotrophic, methane-oxidizing *Methylomicrobium* species from a highly alkaline environment. *Extremophiles* 4: 145-155.

Stachelhaus, T., Mootz, H.D., and Marahiel, M.A. (1999) The specificity-conferring code of adenylation domains in nonribosomal peptide synthetases. *Chem Biol* 6: 493-505.

Stafford, G.P., Scanlan, J., McDonald, I.R., and Murrell, J.C. (2003) rpoN, mmoR and mmoG, genes involved in regulating the expression of soluble methane monooxygenase in *Methylosinus trichosporium* OB3b. *Microbiology* 149: 1771-1784.

Stainthorpe, A.C., Murrell, J.C., Salmond, G.P.C., Dalton, H., and Lees, V. (1989) Molecular analysis of methane monooxygenase from *Methylococcus capsulatus* (Bath). *Arch Microbiol* 152: 154-159.

Stanley, S.H., Prior, S.D., Leak, D.J., and Dalton, H. (1983) Copper stress underlies the fundamental change in intracellular location of methane mono-oxygenase in methane-oxidizing organisms - studies in batch and continuous cultures. *Biotechnol Lett* 5: 487-492.

Staunton, J., and Weissman, K.J. (2001) Polyketide biosynthesis: a millennium review. *Nat Prod Rep* 18: 380-416.

Stolyar, S., Costello, A.M., Peeples, T.L., and Lidstrom, M.E. (1999) Role of multiple gene copies in particulate methane monooxygenase activity in the methane-oxidizing bacterium *Methylococcus capsulatus* Bath. *Microbiology* 145: 1235-1244.

Stralis-Pavese, N., Sessitsch, A., Weilharter, A., Reichenauer, T., Riesing, J., Csontos, J. et al. (2004) Optimization of diagnostic microarray for application in analysing landfill methanotroph communities under different plant covers. *Environ Microbiol* 6: 347-363.

Sundh, I., Mikkelä, C., Nilsson, M., and Svensson, B.H. (1995) Potential aerobic methane oxidation in a sphagnum-dominated peatland-controlling factors and relation to methane emission. *Soil Biol Biochem* 27: 829-837.

Tamura K, Dudley J, Nei M & Kumar S (2007) MEGA4: molecular evolutionary genetics analysis (MEGA) software version 4.0. *Mol Biol Evol* 24: 1596–1599.

Tellez, C.M., Gaus, K.P., Graham, D.W., Arnold, R.G., and Guzman, R.Z. (1998) Isolation of copper biochelates from *Methylosinus trichosporium* OB3b and soluble methane monooxygenase mutants. *Appl Environ Microbiol* 64: 1115-1122.

Theisen, A.R., Ali, M.H., Radajewski, S., Dumont, M.G., Dunfield, P.F., McDonald, I.R. et al (2005) Regulation of methane oxidation in the facultative methanotroph *Methylocella silvestris* BL2. Mol Microbiol 58: 682-692.

Trotsenko, Y.A., and Khmelenina, V.N. (2002) Biology of extremophilic and extremotolerant methanotrophs. *Arch Microbiol* 177: 123-131.

Tse, G., Orbey, H., and Sandler, S.I. (1992) Infinite dilution activity coefficients and Henry's law coefficients of some priority water pollutants determined by a relative gas chromatographic method. *Environ Sci Technol* 26: 2017-2022.

Tsien, H.C., Brusseau, G.A., Hanson, R.S., and Waclett, L.P. (1989) Biodegradation of trichloroethylene by *Methylosinus trichosporium* OB3b. *Appl Environ Microbiol* 55: 3155-3161.

van Bodegom, P., Stams, F., Mollema, L., Boeke, S., and Leffelaar, P. (2001) Methane oxidation and the competition for oxygen in the rice rhizosphere. *Appl Environ Microbiol* 67: 3586-3597.

van Groenestijn, J.W., and Kraakman, N.J.R. (2005) Recent developments in biological waste gas purification in Europe. *Chem Eng J* 113: 85-91.

van Hylckama Vlieg, J.E.T, de Koning, W., and Janssen, D.B (1996) Transformation kinetics of chlorinated ethenes by *Methylosinus trichosporium* OB3b and detection of unstable epoxides by on-line gas chromatography. *Appl Environ Microbiol* 62: 3304-3312.

van Hylckama Vlieg, J.E.T., De Koning, W., and Janssen, D.B. (1997) Effect of chlorinated ethene conversion on viability and activity of *Methylosinus trichosporium* OB3b. *Appl Environ Microbiol* 63: 4961-4964.

van Hylckama Vlieg, J.E.T., and Janssen, D.B. (2001) Formation and detoxification of reactive intermediates in the metabolism of chlorinated ethenes. *J Biotechnol* 85: 81-102.

Verce, M.F., Ulrich, R.L., and Freedman, D.L. (2000) Characterization of an isolate that uses vinyl chloride as a growth substrate under aerobic conditions. *Appl Environ Microbiol* 66: 3535-3542.

Wahlen, M. (1993) The global methane cycle. *Ann Rev Earth Planet Sci* 21: 407.

Waki, M., Yokoyama, H., Ogino, A., Suzuki, K., and Tanaka, Y. (2008) Nitrogen removal from purified swine wastewater using biogas by semi-partitioned reactor. *Bioresour Technol* 99: 5335-5340.

Walsh, C.T., and Nolan, E.M. (2008) Morphing peptide backbones into heterocycles. *Proc Nat Acad Sci USA* 105: 5655-5656.

Walters, K.J., Gassner, G.T., Lippard, S.J., and Wagner, G. (1999) Structure of the soluble methane monooxygenase regulatory protein B. *Proc Nat Acad Sci USA* 96: 7877-7882.

Wandersman, C.C., and Delepelaire, P. (2004) Bacterial iron sources: from siderophores to hemophores. *Ann Rev Microbiol* 58: 611-647.

Ward, N., Larsen, O., Sakwa, J., Bruseth, L., Khouri, H., Durkin, A.S. et al. (2004) Genomic insights into methanotrophy: The complete genome sequence of *Methylococcus capsulatus* (Bath). *Plos Biol* 2: 1616-1628.

Wartiainen, I., Hestnes, A.G., McDonald, I.R., and Svenning, M.M. (2006) *Methylobacter tundripaludum* sp. nov., a methane-oxidizing bacterium from Arctic wetland soil on the Svalbard islands, Norway (78° N). *Int J Syst Evol Microbiol* 56: 109-113.

Westrick, J.J., Mello, J.W., and Thomas, R.F. (1984) The groundwater supply survey. *J Am Water Works Assoc* 76: 52-59.

Whittenbury, R., Phillips, K.C., and Wilkinson, J.F. (1970) Enrichment, isolation and some properties of methane-utilizing bacteria. *J Gen Microbiol* 61: 205-218.

Wiedemeier, T.H., Rifai, H.S., Wilson, J.T., and Newell, C. (1999) *Natural Attenuation of Fuels and Chlorinated Solvents in the Subsurface*: John Wiley & Sons, Inc., New York.

Yu, S.S.-F., Chen, K.H.-C., Tseng, M.Y.-H., Wang, Y.-S., Tseng, C.-F., Chen, Y.-J. et al. (2003) Production of high-quality particulate methane monooxygenase in high yields from *Methylococcus capsulatus* (Bath) with a hollow-fiber membrane bioreactor. *J Bacteriol* 185: 5915-5924.

Zahn, J.A., and DiSpirito, A.A. (1996) Membrane-associated methane monooxygenase from *Methylococcus capsulatus* (Bath). *J Bacteriol* 178: 1018-1029.

Zamble, D.B., McClure, C.P., Penner-Hahn, J.E., and Walsh, C.T. (2000) The McbB component of microcin B17 synthetase is a zinc metalloprotein *Biochemistry* 39: 16190-16199.